Formulations for Analysis of Probe-Fed Printed Antennas in SuperNEC

Mmamolatelo E. Mathekga

A dissertation submitted to the Faculty of Engineering and the Built Environment, University of the Witwatersrand, Johannesburg, in fulfilment of the requirements for the degree of Master of Science in Engineering.

Johannesburg, 2008

Declaration

I declare that this dissertation is my own, unaided work, except where otherwise acknowledged. It is being submitted for the degree of Master of Science in Engineering in the University of the Witwatersrand, Johannesburg. It has not been submitted before for any degree or examination in any other university.

Signed this _____ day of _____ 20___

_____
Mmamolatelo E. Mathekga

Dedicated to my mother - Ms. N.T. Mathekga

Abstract

Formulations for analysis of printed antenna structures are derived and compared, to determine one to implemented in SuperNEC based on the efficiency of its numerical solution in terms of memory usage and solution time. SuperNEC is a software application for computing the response of electromagnetic structures to electromagnetic fields. SuperNEC cannot be used for simulation of printed antenna structures. This is because the formulation that is implemented in SuperNEC does not account for the effect of the substrates that the radiating elements of the antenna structure are printed on, and it is also not intended for antenna structures whose radiating elements are surfaces. Two MoM (Method of Moments) formulations and a FEM (Finite Element Method)-MoM formulation are presented, together with different models for the antenna feed. The FEM-MoM formulation is selected for implementation in SuperNEC because it is argued that it is likely to be more memory efficient when compared to the MoM formulations, and also that less time is required to fill the matrices resulting from the numerical solution of the formulation. The formulation is implemented in a stand alone software application, which will be integrated into SuperNEC. Numerical results that are computed using the software application are presented to illustrate correct implementation of the formulation. The results are compared to: an exact solution, results from another publication, and results computed using a different formulation. Good agreement is obtained in each case.

Acknowledgements

I would like to extend my acknowledgements to my family particularly my mother. Your constant support - financial or otherwise - is really appreciated and it is what kept me going. Thank you and God bless.

I would also like to thank Prof. A.R. Clark for the discussions, advice and trust. But more importantly I would like to say thank you for letting me do it my way.

I also like to thank the people at Poynting for their help.

And, Heather Fraser. The Electromagnetics Laboratory would have been a dull place without you.

Preface

This dissertation is presented to the University of the Witwatersrand, Johannesburg for the degree of Master of Science in Engineering.

The dissertation is entitled *Formulations for Analysis of Probe-Fed Printed Antennas in SuperNEC*. The derivation of three formulations that can be used for analysis of probe-fed printed antennas are presented, with various models for the antenna feed. One of the formulations is chosen for implementation in SuperNEC based on the efficiency of its numerical solution in terms of memory usage and solution time. The chosen formulation is implemented as a stand alone software application, which will be integrated into SuperNEC and numerical results that were computed using the software application are presented.

This document complies with the university's *paper model format*. The paper contains the main results of the research. The appendices present in detail the work conducted during the research.

Appendix A presents:

- Detailed derivation of the three formulations, which can be used for the analysis of probe-fed printed antenna structures.
- Discussion on the choice of the formulation of the formulation to be implemented in SuperNEC.

Appendix B presents the numerical results computed using the software application, which implements the FEM-MoM formulation.

Appendix C presents the application of MoM for reducing the MoM formulation part of the FEM-MoM formulation into a matrix equation.

Appendix D presents the application of FEM for reducing the FEM formulation part of the FEM-MoM formulation into a matrix equation.

Appendix E presents the procedure for solving the matrix equations, which were derived in appendices B and C.

Appendix F is the user manual of the software application that was developed to implement the FEM-MoM formulation.

Contents

List of Figures

List of Tables

Part 1

Paper: Formulations for Analysis of Probe-Fed Printed Antennas in SuperNEC

Formulations for Analysis of Probe-Fed Printed Antennas in SuperNEC

Mmamolatelo E. Mathekga

Abstract—**Formulations for analysis of printed antenna structures are derived and compared, to determine one to implemented in SuperNEC based on the efficiency of its numerical solution in terms of memory usage and solution time. SuperNEC is a software application for computing the response of electromagnetic structures to electromagnetic fields. SuperNEC cannot be used for simulation of printed antenna structures. This is because the formulation that is implemented in SuperNEC does not account for the effect of the substrates that the radiating elements of the antenna structure are printed on, and it is also not intended for antenna structures whose radiating elements are surfaces. Two MoM (Method of Moments) formulations and a FEM (Finite Element Method)-MoM formulation are presented, together with different models for the antenna feed. The FEM-MoM formulation is selected for implementation in SuperNEC because it is argued that it is likely to be more memory efficient when compared to the MoM formulations, and also that less time is required to fill the matrices resulting from the numerical solution of the formulation. The formulation is implemented in a stand alone software application, which will be integrated into SuperNEC. Input impedance computed using the software application, for a probe-fed printed antenna are presented and compared with results from a previous publication and good agreement is obtained.**

Index Terms—**FEM, Formulation, MoM, Printed Antenna, Probe Feed**

I. INTRODUCTION

THE use of higher frequencies for communication and the need for miniaturisation, has made printed antennas the antennas of choice. Printed antennas are antennas that are made from a conducting strips bonded to a substrate as shown figure 1. The substrate and the conducting strips may be shaped as necessary to meet the antenna design requirements. The probe-feed is one of the methods that are used for feeding these types of antennas, particularly when using a coaxial cable to connect the antenna to the electronic device that it is used with. It consists of a conducting wire (usually the inner wire of a coaxial cable), which goes through a hole on one of the conducting strips and connects to the other conducting surface on the opposite side of the substrate. Fields from the cable enter the antenna through the hole on one of the conducting surfaces. Details of the co-axial feed can be seen in figure 1.

These antennas are popular because of their many advantages. Some of the advantages are: low production costs, ability to conform to surfaces, and they do not have protruding parts and are not susceptible to breakage like wire antennas.

Simulation forms an integral part of design. This is because designs have become so complex that creating a prototype is not feasible until the design can be confirmed to some extent. Thus, the need arises for more accurate simulation software to minimise development time and cost, since an accurate simulation means a more accurate first prototype.

SuperNEC is software application for computing the response of electromagnetic structures to electromagnetic fields. It is a C++ implementation of the formulation of NEC-2 (Numerical Electromagnetics Code) [1] used for treating wire structures with a hybrid MoM (Method of Moments) - UTD (Unified Theory of Diffraction) solver. However, SuperNEC cannot be used for simulation of probe-fed printed antenna structures with dielectric substrates. The reason for this is that: the formulation implemented in SuperNEC is meant for conducting wires radiating in free-space or in the presence of other conducting structures [1].

SuperNEC is also unsuitable for analysis of probe-fed printed antenna structures such as the one in figure 1. The reason for this is that conducting strips of printed antennas are surfaces and not wires. Therefore, simulation of these types of antennas in SuperNEC, ignoring the fact that the effect of the substrate is not taken into account; is performed by representing the conducting strips as a wire grid.

The practice of modeling conducting surfaces as wire grids has been used successfully by Richmond in [2] and satisfactory results have been obtained for monostatic RCS (Radar Cross-Section) of conducting plates and bodies of revolution. Guidelines for creating wire grids that can be used for modeling conducting surfaces in NEC-2 are presented in [1] and [3]. The wire grid model of a conducting surface is found to be accurate for far field parameters but, its validity for near field parameters cannot be confirmed [1].

The fact that accurate solutions have been obtained cannot be denied. However, the formulation is not intended for modeling conducting surfaces. Therefore, accurate results cannot be guaranteed, especially when one considers that refining the wire grid does not necessarily result in a more accurate solution as would be expected [4, Chapter 5]. This is because of the thin-wire approximations that are made in the derivation of the formulation. Therefore, a different formulation is required for analysis of printed antennas in SuperNEC.

Analysis of printed antennas has been performed using MoM and FEM (Finite Element Method) [5], [6], [7], [8], [9], [10] and different formulations have been used with both numerical techniques. The subject of this paper is the:

- Selection of MoM and FEM formulations for use in SuperNEC.
- Derivation of the selected formulations with different source models for the feed.
- Selection of one of the formulations for implementation in SuperNEC based on the efficiency of its numerical solution in terms of memory usage and solution time.
- Presentation of the results computed using the selected formulation.

The presentation in this paper is structured as follows. The different formulations that can be used for analysis of probe-fed printed antennas are presented and the ones that may be used in SuperNEC are chosen in section II. Then, the derivation of the selected formulation and models for the feed are presented in sections III, IV, and V. The choice for the formulation that will be implemented in
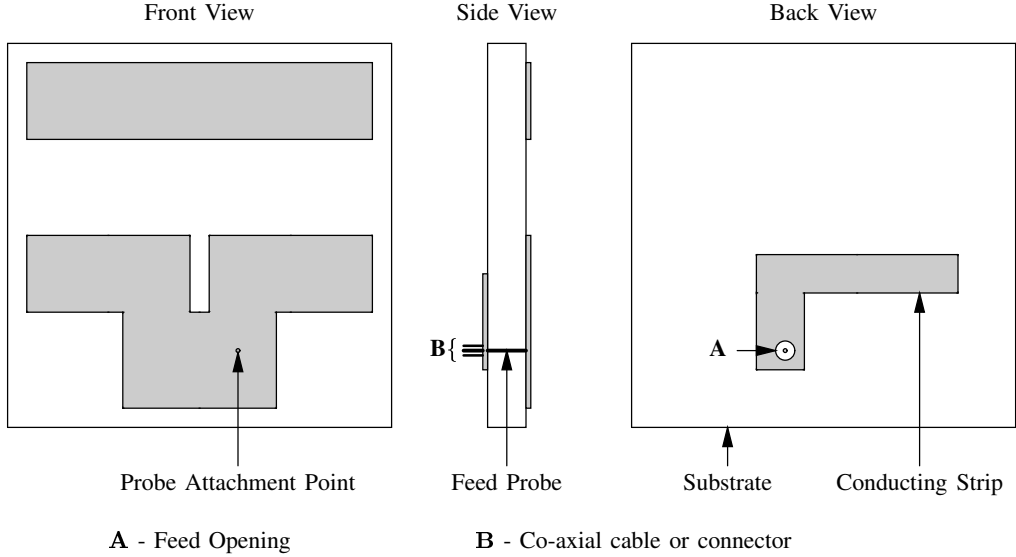
Fig. 1. Example probe fed printed antenna.

SuperNEC is presented in section VI together with the details of the numerical solution of the formulation and results computed using the formulation.

II. FORMULATIONS

A MoM analysis of probe-fed printed antennas involves the computation of the electric and/or magnetic current density that are substituted for the material objects that the antenna is made of, using equivalent principles. There are two approaches that are adopted for deriving formulations for the MoM analysis of printed antennas. They are:

- Representing the conducting strips of the antenna by equivalent currents, and accounting for the effect of the substrate in the Green's function [6].
- Representing both the substrate and conducting strips of the antenna structure by equivalent currents [7], [8].

The first approach is not considered because Green's functions that are used, are derived assuming that the substrate is infinite [4]. As a results, they do not fully account for all the effects of the substrate on the performance of the antenna. These Green's functions have been used successfully for the analysis of printed antenna structures [5], [6], but it remains that the formulation is not intended for antenna structures with finite substrates and will not provide information on the effects of a finite substrate and accuracy cannot be guaranteed under all conditions.

Therefore, only MoM formulations where the both the substrate and conducting strips are represented by equivalent currents are considered. There are two such formulations that are considered, where the equivalent currents for the substrate are defined using either the volume or surface equivalence principle.

FEM analysis of printed antennas is performed by computing the electric field everywhere, imposing the boundary conditions on the conducting strips of the antenna and feed region. However, the electric field can only be computed over a finite volume region (V) because of computational considerations [11]. Solution of the electric field within V requires specification of the fields on the enclosing boundary (S) to simulate the effect of infinite space. There are numerous approaches that are adopted for generating the required boundary conditions [11], [12]. The exact method is to use FEM together with MoM, where the FEM and MoM formulations form

coupled equations, which may be used for computing the electric field within V and the fields on S. This formulation is known in the literature as the Finite Element - Boundary Integral (FE-BI) method [11].

Therefore, two MoM formulations and the FEM and MoM formulations for the FE-BI method are chosen for derivation. The formulation for the FE-BI method is called the FEM-MoM formulation in this paper.

III. MoM FORMULATIONS

The subject of this section is the derivation of two sets of equations, which may be used for the analysis of probe-fed printed antennas using MoM.

Consider a situation where an arbitrary field source produces fields in free-space. When an antenna structure is introduced into the environment; some of the fields from the field source are scattered by the antenna structure. The scattered fields are the fields that are reflected from the antenna surface in order to satisfy field boundary conditions on the surface of the antenna. The scattered fields add to the fields produced by the field source to give the total field everywhere in the environment as:

$$\mathbf{E}^{\text{total}} = \mathbf{E}^{\text{antenna}} + \mathbf{E}^{\text{source}} \tag{1}$$

$$\mathbf{H}^{\text{total}} = \mathbf{H}^{\text{antenna}} + \mathbf{H}^{\text{source}} \tag{2}$$

Assume that the conducting surfaces and the substrate of the antenna structure are removed and each replaced by equivalent current densities, which are defined such that the sum of the fields that they radiate is equal to the scattered fields. Using the superposition principle [13]: the fields scattered by the antenna structure are equal to the sum of the fields that are radiated by the current densities used for representing the conducting surfaces and substrate individually. Therefore:

$$\mathbf{E}^{\text{antenna}} = \mathbf{E}^{\text{subs}} + \mathbf{E}^{\text{cond}} \tag{3}$$

$$\mathbf{H}^{\text{antenna}} = \mathbf{H}^{\text{subs}} + \mathbf{H}^{\text{cond}} \tag{4}$$

Where: $\mathbf{E}^{\text{subs}}$ and $\mathbf{H}^{\text{subs}}$ are the electric and magnetic fields that are scattered by the dielectric substrate respectively, and $\mathbf{E}^{\text{cond}}$ and $\mathbf{H}^{\text{cond}}$ are the electric and magnetic fields that are scattered by the conducting surface respectively.

A. Field Scattered by Conducting Surfaces

Using the surface equivalence principle with the field conditions inside and on the boundary of the finite volume conductor, which is assumed to be perfectly conducting: the conductor is represented by equivalent electric current density on a closed fictitious surface, which encloses the conductor and is chosen equal to the surface of the conductor. Given that fields inside the conductor are equal to zero: the conductor is removed and region inside the fictitious surface is filled with free-space material.

This reduces the problem to an electric current density on the fictitious surface radiating in free-space. The electric current density is defined as:

$$\mathbf{J}_{\text{eq}}^{\text{cond}} = \hat{n} \times \mathbf{H}^{\text{total}} \tag{5}$$

Where: $\hat{n}$ is the outward pointed unit normal on the surface of the conductor, and $\mathbf{H}^{\text{total}}$ is the magnetic field in free-space. Using the notation from [11]: the fields that are scattered by the conductor are given by:

$$\mathbf{E}^{\text{cond}} = -Z_0 \mathcal{L}(\mathbf{J}_{\text{eq}}^{\text{cond}}) \tag{6}$$

$$\mathbf{H}^{\text{cond}} = -\mathcal{K}(\mathbf{J}_{\text{eq}}^{\text{cond}}) \tag{7}$$

$\mathcal{L}$ and $\mathcal{K}$ are operators, which are defined as:

$$\mathcal{L}(\mathbf{X}) = jk_0 \iint_S \mathbf{X}(\mathbf{r}')G(\mathbf{r},\mathbf{r}')\mathrm{d}s' + \frac{j}{k_0^2}\iint_S \nabla' \cdot \mathbf{X}(\mathbf{r}')\nabla G(\mathbf{r},\mathbf{r}')\mathrm{d}s' \tag{8}$$

And:

$$\mathcal{K}(\mathbf{X}) = \iint_S \mathbf{X}(\mathbf{r}') \times \nabla G(\mathbf{r},\mathbf{r}')\mathrm{d}s' \tag{9}$$

Where:

- $G(\mathbf{r},\mathbf{r}') = e^{-jk|\mathbf{r}-\mathbf{r}'|}/4\pi|\mathbf{r}-\mathbf{r}'|$, is the free-space Green's function
- $Z_0 = \sqrt{\mu_0/\epsilon_0}$ is the wave impedance of free-space.
- $k = 2\pi/\lambda$ is the wavenumber.
- S is the surface over which $\mathbf{X}$ is defined.
- $\mathbf{r}$ and $\mathbf{r}'$ are the position vectors everywhere in the environment and on S respectively.

The above derivation may also be applied for computing the fields that are scattered by a real conductor. Fields in a real conductor are confined to a thin layer on the surface at high frequencies. The conductivity value of conductors are large enough that the tangential electric field can be assumed to be negligible.

B. Fields Scattered by Substrate

Fields that are scattered by the substrate are computed using the volume and surface equivalence principles.

1) Using the Volume Equivalence Principle: The substrate is replaced by equivalent electric and magnetic current densities, which are defined as [11]:

$$\mathbf{J}_{\text{eq}}^{\text{subs}}(\mathbf{r}) = j\omega(\epsilon - \epsilon_0)\mathbf{E}^{\text{total}}(\mathbf{r}) \tag{10}$$

$$\mathbf{M}_{\text{eq}}^{\text{subs}}(\mathbf{r}) = j\omega(\mu - \mu_0)\mathbf{H}^{\text{total}}(\mathbf{r}) \tag{11}$$

Where: ϵ and μ are the permittivity and permeability of the substrate material respectively. Antenna substrates are not magnetic materials and $\mu = \mu_0$. Therefore, the the equivalent volume magnetic current density is zero. The fields that are scattered by the substrate are given by [11]:

$$\mathbf{E}^{\text{subs}}(\mathbf{r}) = -jkZ_0 \iiint_{V_{\text{subs}}} \mathbf{J}_{\text{eq}}^{\text{subs}}(\mathbf{r}')G(\mathbf{r},\mathbf{r}')\mathrm{d}v' - \frac{jk}{Z_0}\iiint_{V_{\text{subs}}} \nabla' \cdot \mathbf{J}_{\text{eq}}^{\text{subs}}(\mathbf{r}')\nabla G(\mathbf{r},\mathbf{r}')\mathrm{d}v' \tag{12}$$
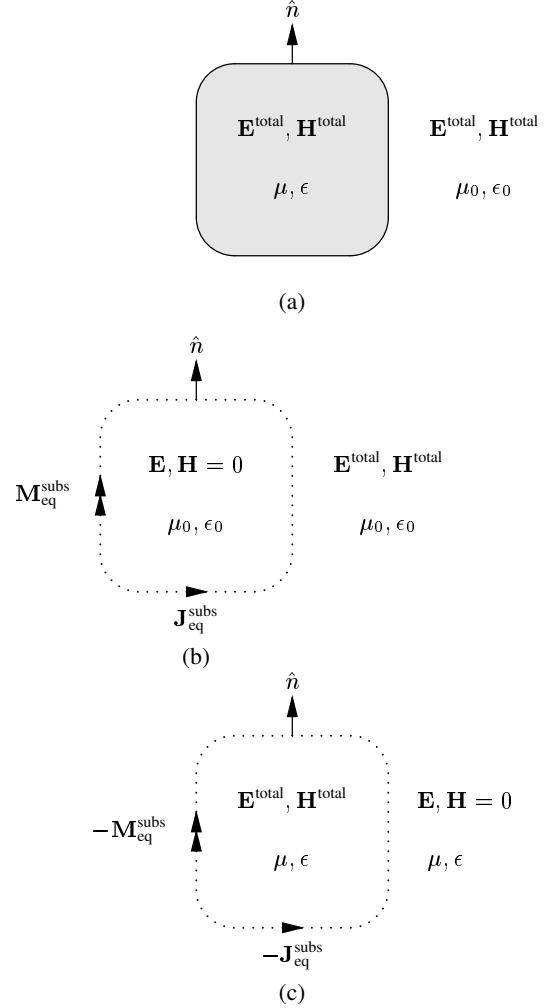
Fig. 2. Substrate (a) with outer (b) and inner (c) equivalent problems.

And:

$$\mathbf{H}^{\text{subs}}(\mathbf{r}) = -\iiint_{V_{\text{subs}}} \mathbf{J}_{\text{eq}}^{\text{subs}}(\mathbf{r}') \times \nabla G(\mathbf{r},\mathbf{r}')\mathrm{d}v' \tag{13}$$

Where: V_{subs} is the region occupied by the substrate, and $\mathbf{r}'$ is an arbitrary position vector in V_{subs}.

The above formulation may be applied when the substrate is both homogeneous and inhomogeneous. When the substrate is inhomogeneous; the different regions of the substrate with different electromagnetic properties are represented by different volume equivalent electric current densities, which are defined by equation (10); substituting values of ϵ as necessary.

2) Using the Surface Equivalence Principle: Using Love's equivalence principle [14]: the fields that are scattered by the substrate and those inside the substrate are computed using the problems (b) and (c) in figure 2 respectively. Both problems involve equivalent electric and magnetic current densities on a fictitious surface (dotted lines), which is selected equal to the surface of the substrate.

The current densities in the two problems are equal in magnitudes but are in opposite direction, as indicated in figure 2. Their magnitudes are equal because of the continuity of tangential fields at the free-space dielectric boundary.

Only the problem in figure 2 (b) is required for computation of the scattered fields. The problem in figure 2 (c) is included to provide an additional boundary condition that is required for computation of the equivalent current densities.

$\mathbf{J}_{\text{eq}}^{\text{subs}}$ and $\mathbf{M}_{\text{eq}}^{\text{subs}}$ are given by [14]:

$$\mathbf{J}_{\text{eq}}^{\text{subs}} = \hat{n} \times \mathbf{H}_{\text{total}} \qquad (14)$$

$$\mathbf{M}_{\text{eq}}^{\text{subs}} = -\hat{n} \times \mathbf{E}_{\text{total}} \qquad (15)$$

And, the scattered fields are given by:

$$\mathbf{E}^{\text{subs}}(\mathbf{r}) = -Z_0 \mathcal{L}(\mathbf{J}_{\text{eq}}^{\text{subs}}) + \mathcal{K}(\mathbf{M}_{\text{eq}}^{\text{subs}}) \qquad (16)$$

$$\mathbf{H}^{\text{subs}}(\mathbf{r}) = -\frac{1}{Z_0}\mathcal{L}(\mathbf{M}_{\text{eq}}^{\text{subs}}) - \mathcal{K}(\mathbf{J}_{\text{eq}}^{\text{subs}}) \qquad (17)$$

The field inside the substrate are given by:

$$\mathbf{E}^{\text{subs}}(\mathbf{r}) = Z \mathcal{L}(\mathbf{J}_{\text{eq}}^{\text{subs}}) - \mathcal{K}(\mathbf{M}_{\text{eq}}^{\text{subs}}) \qquad (18)$$

$$\mathbf{H}^{\text{subs}}(\mathbf{r}) = \frac{1}{Z}\mathcal{L}(\mathbf{M}_{\text{eq}}^{\text{subs}}) + \mathcal{K}(\mathbf{J}_{\text{eq}}^{\text{subs}}) \qquad (19)$$

Where $Z = \sqrt{\mu/\epsilon}$.

The above formulation can only applied when the dielectric substrate is homogenous.

C. Integral Equations

It is concluded from the previous sections that:

- Two equations are required for solution of $\mathbf{J}^{\text{cond}}$ and $\mathbf{J}_{\text{eq}}^{\text{subs}}$ when using the volume equivalence principle for computation of the field scattered by the substrate,
- And, three equations are required for solution of: $\mathbf{J}^{\text{cond}}$, $\mathbf{J}_{\text{eq}}^{\text{subs}}$, and $\mathbf{M}_{\text{eq}}^{\text{subs}}$ when using the surface equivalence principle for computation of the field scattered by the substrate.

The required equations are derived by imposing the field boundary conditions.

The first boundary condition, which is common when using the volume or surface equivalence principles is the electric field boundary condition on the conducting surfaces of the antenna structure. This boundary condition is imposed using the following equation:

$$\hat{n} \times \mathbf{E}^{\text{total}} = 0 \qquad (20)$$

$$-\hat{n} \times \mathbf{E}^{\text{source}} = \hat{n} \times \mathbf{E}^{\text{cond}} + \hat{n} \times \mathbf{E}^{\text{subs}} \qquad (21)$$

Where: $\hat{n}$ is the unit normal on the conducting surfaces of the antenna structure (S_{cond}), $\mathbf{E}^{\text{cond}}$ is given by equation (6), and $\mathbf{E}^{\text{subs}}$ is given by equation (12) when using the volume equivalence principle for computation of fields scattered by the substrate, or equation (16) otherwise.

Equation (21) may be used on open conducting surfaces even though $\mathbf{E}^{\text{cond}}$ is formulated for a closed conducting surface [15]. An open conducting surfaces is an infinitesimally thin surfaces with defined boundaries and is used for representing conducting plates or strip of zero thickness. It is considered as the limiting case when the thickness of the closed surface approaches zero, in which case the equivalent electric current density ($\mathbf{J}^{\text{cond}}$) is the sum of the current on the top and bottom surfaces of the closed surface [15]. Therefore, the equations presented in section III-A may also be used for computing the fields scattered by the conducting strips of the antenna.

The additional equations that are required are derived in the following sections.

1) Using the Volume Equivalence Principle: The additional equation that is required is derived using the definition of the volume equivalent electric current density (i.e. equation (10)), and is given by:

$$-j\frac{\mathbf{J}_{eq}(\mathbf{r})}{\omega(\epsilon - \epsilon_0)} = \mathbf{E}^{\text{source}} + \mathbf{E}^{\text{cond}} + \mathbf{E}^{\text{subs}} \qquad (22)$$

Where: $\mathbf{E}^{\text{subs}}$ is given by equation (12), and $\mathbf{E}^{\text{cond}}$ is given by equation (6).

2) Using the Surface Equivalence Principle: The two additional equations that are required for solution of the current densities are derived by imposing the boundary condition on the fictitious boundary for both equivalent problems in figure 2. This is achieved using either the definition of the equivalent electric or magnetic current densities in either case. However, equations that result from such a derivation do not give unique solutions for frequencies that correspond to the resonant frequencies of the cavity formed by the fictitious surface [11].

This problem is avoided by using the CFIE (Combined Field Integral Equation) for imposing field boundary conditions. The CFIE is defined as:

$$\alpha\text{EFIE} + Z_0(1 - \alpha)\hat{n} \times \text{MFIE}$$

Where:

- α is a dimensionless number between zero and one.
- Z_0 is the intrinsic impedance.
- EFIE (Electric Field Integral Equation) and MFIE (Magnetic Field Integral Equation) are the equations, which results from using the definitions of the equivalent magnetic and electric current densities respectively.

α is chosen as 0.5 for this application in-line with the argument in [11, p. 465] that choosing α as such, results in the optimum combination of the EIFE and MFIE.

The EFIE and MFIE for the problem in figure 2 (b) are derived using equations (14) and (15) respectively, and are given by:

$$-\mathbf{M}_{\text{eq}}^{\text{subs}} = \hat{n} \times \mathbf{E}^{\text{cond}} + \hat{n} \times \mathbf{E}^{\text{subs}} + \hat{n} \times \mathbf{E}^{\text{source}} \qquad (23)$$

$$\mathbf{J}_{\text{eq}}^{\text{subs}} = \hat{n} \times \mathbf{H}^{\text{cond}} + \hat{n} \times \mathbf{H}^{\text{subs}} + \hat{n} \times \mathbf{H}^{\text{source}} \qquad (24)$$

Where $\mathbf{r}$ and $\hat{n}$ are the position vector and unit normal on the surface of the substrate. The required CFIE is given by:

$$\hat{n} \times \mathbf{E}^{\text{source}} - Z\hat{n} \times \hat{n} \times \mathbf{H}^{\text{source}} = -Z\hat{n} \times \mathbf{J}_{\text{eq}}^{\text{subs}} - \mathbf{M}_{\text{eq}}^{\text{subs}} +$$
$$Z\hat{n} \times \hat{n} \times \mathbf{H}^{\text{cond}} - \hat{n} \times \mathbf{E}^{\text{cond}} + \qquad (25)$$
$$Z\hat{n} \times \hat{n} \times \mathbf{H}^{\text{subs}} - \hat{n} \times \mathbf{E}^{\text{subs}}$$

Where: $\mathbf{E}^{\text{cond}}$ and $\mathbf{H}^{\text{cond}}$ given by equations (6) and (7) respectively, and $\mathbf{E}^{\text{subs}}$ and $\mathbf{H}^{\text{subs}}$ are given by equations (16) and (17) respectively.

The CFIE for the problem in figure 2 (c) is derived following a similar procedure, but the equivalent current densities are equal to those for the problem in figure 2 (b) multiplied by minus one. The problem in figure in figure 2 (c) only involves equivalent current densities radiating in an infinite homogeneous medium, therefore:

$$\mathbf{E}^{\text{total}} = \mathbf{E}^{\text{subs}} \qquad (26)$$

$$\mathbf{H}^{\text{total}} = \mathbf{H}^{\text{subs}} \qquad (27)$$

$\mathbf{E}^{\text{subs}}$ and $\mathbf{H}^{\text{subs}}$ are given by equations (18) and (19) respectively. The resulting CFIE is given by:

$$\hat{n} \times \mathbf{E}^{\text{subs}} + Z\hat{n} \times \hat{n} \times \mathbf{H}^{\text{subs}} = \mathbf{M}_{\text{eq}}^{\text{subs}} + Z\hat{n} \times \mathbf{J}_{\text{eq}}^{\text{subs}} \qquad (28)$$

IV. FEM-MoM FORMULATION

V from section II is selected as the region occupied by the antenna structure and is enclosed by a fictitious surface (S), which does not touch the conducting surfaces of the antenna structure.

Solution of the electric field within V requires specification of the fields on S to simulate the effect of infinite space, and the fields on S are not known. Since the interest is only on the electric field inside S, the problem is reduced to an equivalent problem using Love's equivalence principle. This is done by setting the fields outside S to zero. Doing this requires introduction of equivalent current densities

on S to satisfy the field boundary conditions. The equivalent current densities are therefore, given by:

$$\mathbf{J}_{\text{eq}} = -\hat{n} \times \mathbf{H} \tag{29}$$

$$\mathbf{M}_{\text{eq}} = \hat{n} \times \mathbf{E} \tag{30}$$

Where: $\hat{n}$ is the outward pointing normal on S, $\mathbf{E}$ and $\mathbf{H}$ are the fields within V on S. Either $\mathbf{J}_{\text{eq}}$ or $\mathbf{M}_{\text{eq}}$ may be used as the required boundary condition on S, but since the electric field is being computed it is easier to use $\mathbf{J}_{\text{eq}}$ as the boundary condition. However, $\mathbf{J}_{\text{eq}}$ and $\mathbf{M}_{\text{eq}}$ are not known. Since $\mathbf{M}_{\text{eq}}$ is related to $\mathbf{E}$: there are two unknowns (i.e. $\mathbf{J}_{\text{eq}}$ and $\mathbf{E}$). The formulation for the FEM analysis gives a relation between $\mathbf{J}_{\text{eq}}$ and $\mathbf{E}$. Therefore, an additional equation is required for solution of $\mathbf{J}_{\text{eq}}$ and $\mathbf{E}$.

The additional equation is derived using a problem that is equivalent to the antenna problem outside S. This problem is derived using Love's equivalence principle by setting the field inside S equal to zero, which means that the antenna can be removed and the region inside S filled with free-space material, resulting in a problem similar to the one shown in figure 2 (b), where: S is represented by the dotted line. This is easily analysed using MoM as is done in section III-B.

A. FEM Formulation

The boundary value problem for the FEM problem described above is given by:

$$\begin{cases} \nabla \times \left(\frac{1}{\mu}\nabla \times \mathbf{E}\right) - \omega\epsilon\mathbf{E} & = -j\omega\mathbf{J} + \frac{\nabla \times \mathbf{M}}{\mu} & \text{in } V \\ \hat{n} \times \mathbf{E} & = 0 & \text{on } S_{\text{cond}} \\ \hat{n} \times \nabla \times \mathbf{E} & = j\omega\mu\mathbf{J}_{\text{eq}} & \text{on } S \end{cases}$$

Where S_{cond} is the surface of conducting strips within V. Using the Rayleigh-Ritz method: the required variational principle is given by [13, p. 159]:

$$\begin{aligned} F(\mathbf{E}) =& \frac{1}{2}\iiint_V \left(\frac{1}{\mu_r}(\nabla \times \mathbf{E}) \cdot (\nabla \times \mathbf{E}) - k_0^2\epsilon_r\mathbf{E} \cdot \mathbf{E}\right) \mathrm{d}V \\ &+ \iiint_V \mathbf{E} \cdot \left(j\omega\mathbf{J} + \frac{\nabla \times \mathbf{M}}{\mu}\right) \mathrm{d}V \\ &+ jk_0Z_0\iint_S (\mathbf{E} \cdot \mathbf{J}_{\text{eq}})\,\mathrm{d}S \end{aligned} \tag{31}$$

This equation gives the relation between $\mathbf{E}$ within V and $\mathbf{J}_{\text{eq}}$ on S. The tangential field on the conducting strips of the antenna are imposed as a Dirichlet boundary condition.

B. MoM Formulation

The formulation for the problem involving the region outside V is derived following the procedure described in section III-C2, and is given by:

$$\mathbf{M}_{\text{eq}} + Z_0\mathbf{J}_{\text{eq}} + \hat{n} \times \mathbf{E} + Z\hat{n} \times \hat{n} \times \mathbf{H} = 0 \tag{32}$$

V. FEED MODEL

The antenna is fed by an ideal voltage source applied between the inner and outer conductors of the probe feed at the feed opening (see figure 1). This source voltage creates electric and magnetic fields inside the feed opening and the field mode can be assumed to be TEM for most practical purposes [16](see figure 3 (b)).

Numerous approaches for modeling the feed have been proposed in the literature [13], [14], [11]. The common approach is to specify the field across the feed opening. Two methods that are used for specifying the fields across the feed opening are [14, p. 722-726]: the magnetic frill generator, and the delta-gap model. The other less
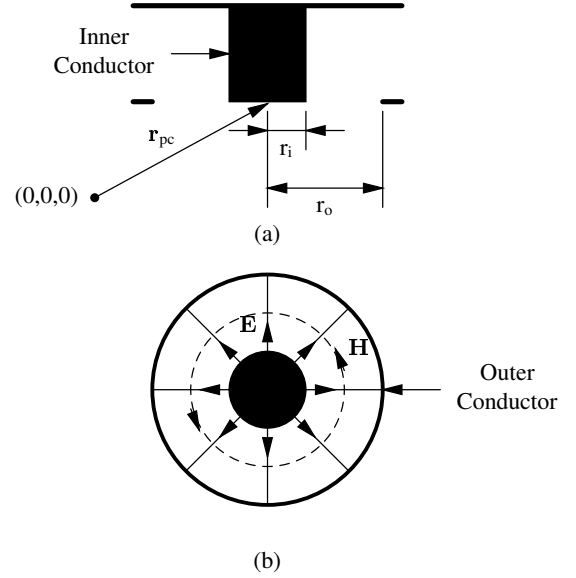
Fig. 3. Cross-section of a probe-fed printed antenna without substrate (a) and the feed opening (b).

common approach is to specify the current distribution on the inner conductor (see figure 3). This approach has been used successfully with FEM formulations [17] and is discussed here for use with the FEM-MoM formulation only.

A. Magnetic Frill Generator

A ring of infinitesimally thin, circumferentially directed equivalent magnetic current density is placed across the feed opening with this model. This equivalent magnetic current density is defined as [18]:

$$\mathbf{M}_{\text{eq}}^{\text{source}} = -2\hat{n} \times \mathbf{E}^{\text{aperture}} \tag{33}$$

Where: $\mathbf{E}^{\text{aperture}}$ is the electric field across the feed opening, and $\hat{n}$ is the normal at the feed opening, which points away from the coaxial cable. Given that TEM mode fields are assumed in the feed opening, $\mathbf{E}^{\text{aperture}}$ is given by [14]:

$$\mathbf{E}^{\text{aperture}}(\mathbf{r}) = \begin{cases} \dfrac{V_{\text{app}}}{2|\mathbf{r} - \mathbf{r}_{\text{pc}}|\ln(r_o/r_i)} & \mathbf{r} \in S_{\text{aperture}} \\ 0 & \text{otherwise} \end{cases} \tag{34}$$

Where: V_{app} is the voltage across the inner and outer conductors at the feed opening, S_{aperture} is the feed opening region, and the definitions of $\mathbf{r}_{\text{pc}}$, r_o, and r_i can be seen in figure 3.

The magnetic current density in equation (33) is defined using the surface equivalence principle in conjunction with image theory [18], assuming that the feed opening exists on an infinite PEC ground plane. Therefore, this source model is appropriate for cases where the feed opening exist on a conducting strip that is large enough for the infinite PEC ground plane approximation to be valid, and is not near the edges of the conducting strip.

1) Use with the MoM Formulation: This feed is incorporated into the MoM formulation using fields radiated by the magnetic frill current as $\mathbf{E}^{\text{source}}$ and $\mathbf{H}^{\text{source}}$, i.e. [14]:

$$\mathbf{E}^{\text{source}}(\mathbf{r}) = \mathcal{K}(\mathbf{M}_{\text{eq}}^{\text{source}}) \tag{35}$$

$$\mathbf{H}^{\text{source}}(\mathbf{r}) = -Z_0\mathcal{L}(\mathbf{M}_{\text{eq}}^{\text{source}}) \tag{36}$$

The feed opening and inner conductor are treated as part of the conducting strips, and the zero tangential electric field boundary condition is applied on their surfaces.

2) Use with the FEM Formulation: The feed model is incorporated into the FEM formulation by substituting the magnetic current density of equation (33) in the FEM formulation (equation (31)), and the inner conductor is treated as part of S_{cond} and the tangential electric field component is set to zero on its surface.

B. Delta Gap Model

With the delta gap model: the electric field across the coaxial aperture is assumed to be constant such that:

$$\mathbf{E}^{\mathrm{aperture}}(\mathbf{r}) = \frac{V_{\mathrm{app}}}{(\mathbf{r}_o - \mathbf{r}_i)}\hat{r} \tag{37}$$

$$\mathbf{H}^{\mathrm{aperture}}(\mathbf{r}) = \frac{|\mathbf{E}^{\mathrm{aperture}}|}{Z}\hat{\theta} \tag{38}$$

This model is accurate for cases where $\mathrm{r}_o - \mathrm{r}_i$ is small compared to the wavelength for a constant field distribution to be assumed across the feed opening.

1) Use with the MoM Formulation: This source model is also incorporated into the MoM formulations via the $\mathbf{E}^{\mathrm{source}}$ term. Using the above equations, the source electric and magnetic fields are given as:

$$\mathbf{E}^{\mathrm{source}}(\mathbf{r}) = \begin{cases} \mathbf{E}^{\mathrm{aperture}}(\mathbf{r}) & \mathbf{r} \in \mathrm{s}_{\mathrm{aperture}} \\ 0 & \mathrm{otherwise} \end{cases} \tag{39}$$

And:

$$\mathbf{H}^{\mathrm{source}}(\mathbf{r}) = \begin{cases} \frac{|\mathbf{E}^{\mathrm{aperture}}|}{Z}\hat{\theta} & \mathbf{r} \in \mathrm{s}_{\mathrm{aperture}} \\ 0 & \mathrm{otherwise} \end{cases} \tag{40}$$

The feed opening and inner conductor are treated as part of the conducting strips, and the zero tangential electric field boundary condition is applied on their surfaces.

2) Use with the FEM Formulation: The feed voltage is incorporated into the FEM formulation as a Dirichlet boundary condition, and the inner conductor is treated as a part of the conducting strips.

C. Probe Feed Model

The inner conductor (see figure 3) of the antenna feed is replaced by an infinitesimally thin current filament whose length equals that of the inner conductor. A constant electric current density ($\mathbf{J}$) is assumed throughout the length of the current filament. The feed opening is treated as part of the conducting strip that it exist on.

Assuming a z directed inner conductor: the electric current density in equation (31) is given by [13]:

$$\mathbf{J}(\mathbf{r}) = \mathrm{I}\delta(x - x_s)\delta(y - y_s)\hat{z} \tag{41}$$

Where: I is the magnitude of the current on the probe-feed, and x_s and y_s are the x and y components of the center of the inner conductor of the probe-feed. This feed model is incorporated into the FEM formulation by substituting the electric current density of equation (41) into equation (31). The feed opening is treated as a part of the conducting surfaces.

This source model gives accurate results for antennas with thin dielectric substrates and for instances where the diameter of the inner conductor can be ignored [11]. When the diameter of the inner conductor cannot be ignored the strip model [19] may be used; where the inner conductor is represented by two current filaments placed as shown in figure 4. w in figure 4 is given by:

$$w = 4r_{\mathrm{ic}} \tag{42}$$

Where r_{ic} is the radius of the inner conductor of the coaxial cable.

Axis through center of inner conductor
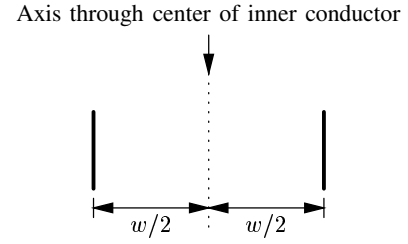
Fig. 4. Positions of the current filaments (solid black lines) using the strip model.

VI. Choice of Formulation

The formulations presented in this paper have been used successfully for analysis of printed antennas in [5], [6], [7], [8], [9], [10]. All the formulations are expected to be equally accurate given that no simplifying assumptions are made during their derivations, except with feed models, which are used with all the formulations. Therefore, criterion for the formulation to be implemented in SuperNEC is based on the efficiency of its numerical solution in terms of memory usage and solution time.

The memory required for a numerical solution of the formulation is for storage of the matrices that are generated during the numerical solution process, and for solution of the resulting matrix equations. The memory required for solution of the resulting matrix equations depends on the matrix solver that is used and is not used as a selection criterion.

The amount of memory required to store a matrix, which results from a FEM formulation is less than αNM, where: α is the largest number of entries per row or column (typically less than 20), N number of unknowns, and M is the amount of memory that is required to store a matrix entry. The memory that is required for storing a matrix, which results from a MoM formulation is $N^2 M$.

Printed antennas analysed using FEM results in more unknowns than an equivalent problem analysed using MoM, because: the free-space region around the antenna has to be discretised as well, and FEM meshes require finer discretisations to reduce the dispersion error [4]. Therefore, matrices resulting from the FEM formulations are larger than the MoM matrices of an equivalent problem. However, given that the memory required for storing a matrix that results from a FEM formulation is proportional to N and that for storing a matrix for a MoM formulation is proportional to N^2; the memory required for storing a FEM matrix is likely to be less than that required to store a MoM matrix for an equivalent antenna problem and will scale favourably with an increasing number of unknowns. This can be seen by considering that the memory required for a FEM problem with 60000 unknowns is equivalent to that required for a MoM problem with 949 unknowns ($\alpha = 15$).

Given the above and the fact that: the MoM formulation using the surface equivalence principle requires 9 full populated matrices, that using the volume equivalence principle requires 4 fully populated matrices, and that for the FEM-MoM formulation requires 4 matrices; 2 fully populated and 2 sparse; the FEM-MoM formulation is expected to be more memory efficient when compared to the other formulations for an equivalent printed antenna problem.

The solution time for the numerical solution of the formulations depends on the time it takes to fill the matrices that are generated during the solution process and time required to solve for the unknowns. The time it takes to solve the matrices depends on the matrix solver used and is not used as a selection criterion. The time required to generate the entries for the matrices of the FEM-MoM formulation is expected to be less than that required to generate the

matrices for the other formulations, for an equivalent problem. This is due to the fact that:

- It requires considerably less time to compute an entry for the FEM formulation than it does for a MoM formulation. Matrix entries for a MoM implementation require the evaluation of two integrals: the testing integral and the integral in the formulation equations. In addition to that, additional terms are introduced if the integrand is singular over the integration domain [11]. Matrix entries for the FEM formulation only require one integration and are less complicated than those for the MoM formulations.
- The integral terms for the MoM formulation are more complicated than those of the FEM formulations.

Therefore, the FEM-MoM formulation is chosen for implementation in SuperNEC. Matrices resulting from the FEM formulation can be solved efficiently both in terms of memory usage and solution time using an iterative solver and the pre-conditioner proposed in [20].

A. Numerical Implementation

The formulation presented in section IV was implemented using the probe feed model for the antenna feed in a stand alone software application, which will be incorporated in SuperNEC.

The finite volume region for the FEM analysis is divided into tetrahedrons and Whitney elements [11] are used for expanding the electric field within the tetrahedrons. The enclosing surface of the volume region is divided into triangles, which are the faces of the outer tetrahedrons and RWG basis functions [21] are used for representing both the equivalent electric and magnetic current densities. The MoM formulation is tested using $RWG + \hat{n} \times RWG$ for the EFIE part of the formulation and $\hat{n} \times RWG$ for the MFIE part of the formulation.

The matrices resulting from the numerical solutions of the FEM and MoM formulations are solved using the outward looking approach [11, p. 470-471].

B. Numerical Results

The application was used for computing the input impedance of the structure in figure 5 to verify the implementation. This structure has previously been analysed in [22] using a hybrid FEM-MoM formulation, which is different from the one implemented here. Their formulation uses the FEM for treatment of the substrate as is done using the surface and volume equivalence principles.

The probe feed model is also used for the results in [22]. The reactance and magnitude of the computed impedance are shown compared to those of [22] in figures 6 and 7 respectively. Satisfactory agreement is obtained in each case. The phase shift above 1100 MHz is due to the discretisation errors [4]. A coarse mesh of the structure was used to limit the number of unknowns because a direct solver was used for solution of the matrix equations resulting from the numerical solution of the formulation. The results may be improved by using a finer discretisation.

This is seen in figure 8, which shows the reactance of the antenna computed using a coarse and a fine meshes. The results for the fine mesh are those in figure 6, and the fine mesh is obtained by increasing the tetrahedron density around the source region of the course mesh. It can clearly be seen that refining the mesh improves the results.

The results from [22] were compared with measured results and compared well.
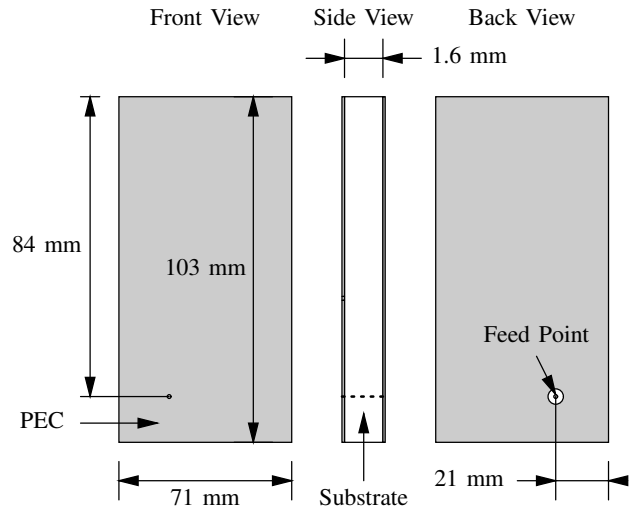
Fig. 5. Geometry of patch antenna with dimensions.
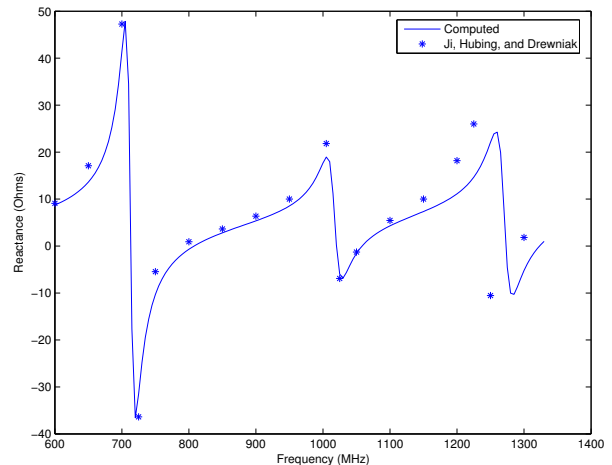
Fig. 6. Reactance of patch antenna as a function of frequency.

VII. Conclusion

Potential formulations for simulation of probe-fed printed antennas in SuperNEC are identified, and their derivations are presented together with different models for the feed. The identified techniques are: two MoM formulation using the surface and volume equivalence principles for deriving the current density that is used for representing the dielectric substrate, and a FEM-MoM formulation using both FEM and MoM for analysis, where the MoM formulation part is introduced to help evaluate the boundary conditions.

The FEM-MoM formulation is chosen for implementation in SuperNEC because it is argued that its numerical solution is likely to be more memory efficient when compared to the other formulations and less time will be required for filling the matrices, which result during the numerical solution process.

The formulation is then implemented using the probe-feed model in a stand alone software application, which will be integrated into SuperNEC. Numerical solution details of the formulation are also presented. Impedance results computed for a probe-fed printed antenna structure are presented and compared to results from a previous publication, and satisfactory agreement is obtained.
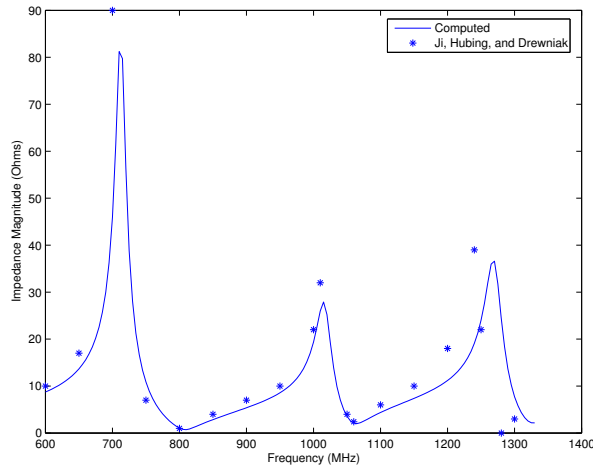
Fig. 7.   Impedance magnitude as a function of frequency.
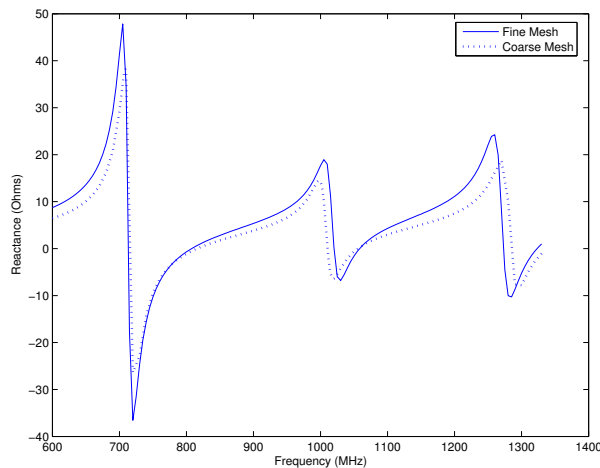
Fig. 8.   Reactance of patch antennas as a function of frequency for a fine and coarse meshes.

REFERENCES

[1] G. Burke and A. Pogio. "Numerical Electromagnetics Code (NEC) - Method of Moments. Part 1: Program Description-Theory." Tech. Rep. Report UCID 18834, Lawrence Livermore National Laboratory, 01 1981.

[2] J. H. Richmond. "A Wire-Grid Model for Scattering by Conducting Bodies." *IEEE Transactions on Antennas and Propagation*, vol. 14, no. 06, pp. 782–786, 11 1966.

[3] C. Trueman and S. Kubina. "Fields of Complex Surfaces Using Wire Grid Modelling." *IEEE Transactions on Magnetics*, vol. 27, no. 05, pp. 4262–4267, 09 1987.

[4] D. B. Davidson. *Computational Electromagnetics for RF and Microwave Engineering*. Cambridge, first ed., 2005.

[5] J. Mosig and F. Gardiol. "General Integral Equation Formulation for Microstrip Antennas and Scatterers." *Proceedings of the IEE*, vol. 132, pp. 424–432, 12 1985.

[6] P. Katehi and N. Alexopoulos. "On the Effect of Substrate Thickness and Permittivity on Printed Circuit Dipole Properties." *IEEE Transactions on Antennas and Propagation*, vol. 31, pp. 34 – 39, 01 1983.

[7] B. Salman and A. McCowen. "The CFIE Technique Applied to Finite-Size Planar and Non-Planar Microstrip Antenna." pp. 338–341. IEE, 04 1996.

[8] T. K. Sarkar, S. M. Rao, and A. R. Djordjević. "Electromagnetic Scattering and Radiation from Finite Microstrip Structures." *IEEE Transactions on Microwave Theory and Techniques*, vol. 38, no. 11, pp. 1568–1575, 11 1990.

[9] M. W. Ali, T. H. Hubing, and J. L. Drewniak. "A Hybrid FEM/MOM Technique for Electromagnetic Scattering and Radiation from Dielectric Objects with Attached Wires." *IEEE Transactions on Electromagnetic Compatibility*, vol. 39, no. 04, pp. 304–314, 11 1997.

[10] S. Makarov, S. Kulkarni, A. Marut, and L. Kempel. "Method of Moments Solution for a Printed Patch/Slot Antenna on Thin Finite Dielectric Substrate Using the Volum Integral Equation." *IEEE Transactions on Antennas and Propagation*, vol. 54, no. 04, pp. 1174–1184, 04 2006.

[11] J. Jin. *The Finite Element Method in Electromagnetics*. New York: John Wiley and Sons, Inc., second ed., 2002.

[12] M. M. Botha and J.-M. Jin. "On the Variational Formulation of Hybrid Finite Element-Boundary Integral Techniques for Electromagnetic Analysis." *IEEE Transactions on Antennas and Propagation*, vol. 52, no. 11, pp. 3037–3047, 11 2004.

[13] L. K. J.L. Volakis, A. Chatterjee. *Finite Element Method for Electromagnetics: Antennas, Microwave Circuits, and Scattering Applications*. New York: IEEE Press, first ed., 2001.

[14] C. A. Balanis. *Advanced Engineering Electromagnetics*. John Wiley and Sons, first ed., 1989.

[15] E. Newman and D. Pozar. "General Integral Equation Formulation for Microstrip Antennas and Scatters." *IEE Proceedings*, vol. 132, no. 12, pp. 424–432, 7 1985.

[16] J. Gong and J. L. Volakis. "An Efficient and Accurate Model of a Coax Cable Feeding Structures for FEM Simulations." *IEEE Transactions on Antennas and Propagation*, vol. 43, no. 12, pp. 1474–1478, 12 1995.

[17] J.-M. Jin and J. L. Volakis. "A Hybrid Finite Element Method for Scattering and Radiation by Microstrip Patch Antennas and Arrays Residing in a Cavity." *IEEE Transactions on Antennas and Propagation*, vol. 39, no. 11, pp. 1598–1604, 11 1991.

[18] L. L. Tsai. "A Numerical Solution for the Near and Far Fields of an Annular Ring of Magnetic Current." *IEEE Transactions on Antennas and Propagation*, vol. 20, no. 05, pp. 569–576, 09 1972.

[19] H. Wang, Y. Jin, and T. H. Hubing. "Finite-Element of Coaxial Cable Feeds and Vias in Power-Bus Structure." *IEEE Transactions on Electromagnetic Compatibility*, vol. 40, no. 04, pp. 569–574, 11 2002.

[20] J. Lui and J.-M. Jin. "A Highly Effective Preconditioner for Solving the Finite Element-Boundary Integral Matrix Equation of 3-D Scattering." *IEEE Transactions on Antennas and Propagation*, vol. 50, no. 9, pp. 1212–1221, 9 2002.

[21] S. Rao, D. Wilton, and A. Glisson. "Electromagnetic Scattering by Surfaces of Arbitrary Shape." *IEEE Transactions on Antennas and Propagation*, , no. 30, pp. 409–418, 05 1982.

[22] Y. Ji, T. Hubing, and J. Drewniak. "Finite Element Modelling of Patch Antenna and Cavity Sources." In *IEEE International Symposium on Electromagnetic Compatibility, 2000*, vol. 2, pp. 811–814. 08 2000. ISBN: 0-7803-5677-2.

I hate this thing

Part 2

Appendices

Appendix A

Derivation of the Formulations for Radiation of Probe-Fed Printed Antennas

A.1 Introduction

Printed antennas are antennas that are made from a conducting strips bonded to a substrate as shown figure A.1. The substrate and the conducting strips may be shaped as necessary to meet the antenna design requirements. The probe-feed is one of the methods that are used for feeding these types of antennas, particularly when using a coaxial cable to connect the antenna to the electronic device that it is used with. It consists of a conducting wire (usually the inner wire of a coaxial cable), which goes through a hole on one of the conducting strip and connects to the other conducting strip on the opposite side of the substrate. Fields from the cable enter the antenna through the hole on one of the conducting strips.

Front View   Side View   Back View

Probe Attachment Point   Feed Probe   Substrate   Conducting Strip

A - Feed Opening   **B** - Co-axial cable or connector
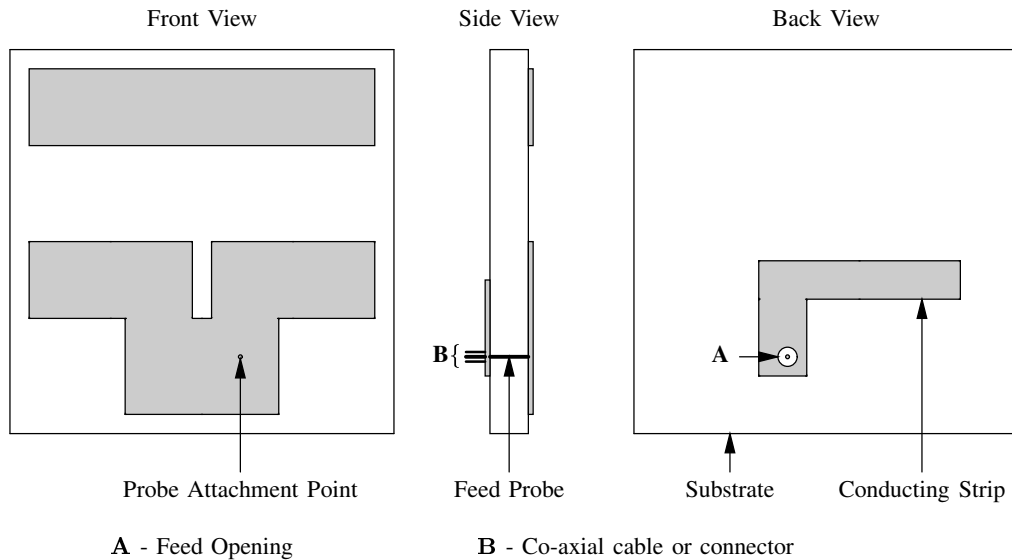
Figure A.1: Example probe fed printed antenna.

The subject of this appendix is: the derivation of three formulations that may be used for analysis of probe-fed printed antenna structures together with models for the feed, and selection of one the formulations for implementation in SuperNEC. The three formulations that are presented are: two MoM (Method of Moments) formulations using the volume and surface equivalence principles, and a FEM (Finite Element Method)-MoM formulation. SuperNEC is software application for computing the response of electromagnetic structures to electromagnetic fields. It is a C++ implementation of the formulation of NEC-2 (Numerical Electromagnetics Code) [1] used for treating wire structures with a hybrid MoM-UTD(Unified Theory of Diffraction) solver.

The presentation is structured as follows. The derivation of the MoM formulations is presented in section A.2, and that for the FEM-MoM formulation is presented in section A.3. The different models for the feed are presented in section A.4. Choice of the formulation that will be implemented in SuperNEC is presented in section A.5.

A.2 MoM Formulations

A MoM formulation is integral equations that may be used for the analysis of the probe-fed printed antenna when using MoM. Integral equations in CEM (Computational Electromagnetics) relate the current densities to fields (electric and magnetic) that they produce: where the current densities are part of the integrand. The analysis of the probe-fed printed antennas using integral equation model involves computing current densities to satisfy field boundary conditions.

Consider a situation where a field source produces fields in an environment (e.g. free-space). When an antenna structure is introduced in the environment; some of the fields that are produced by the field source are scattered from the antenna. The scattered fields are the fields that are reflected at the antenna surface in order to satisfy field boundary conditions on the surface of the antenna. These fields add to the fields that are produced by the field source to give the total fields everywhere in the environments as:

$$\mathbf{E}^{\text{total}}(\mathbf{r}) = \mathbf{E}^{\text{antenna}}(\mathbf{r}) + \mathbf{E}^{\text{source}}(\mathbf{r}) \tag{A.1}$$

$$\mathbf{H}^{\text{total}}(\mathbf{r}) = \mathbf{H}^{\text{antenna}}(\mathbf{r}) + \mathbf{H}^{\text{source}}(\mathbf{r}) \tag{A.2}$$

Assume that the conducting strips and the substrate of the antenna structure are removed and each replaced by current densities, which are defined such that the sum of the fields they radiate is equal to the scattered fields. Using the superposition principle [2]: the fields scattered by the antenna structure are equal to the sum of the fields that are radiated by the current densities used for representing the conducting strips and substrate individually. Therefore:

$$\mathbf{E}^{\text{antenna}}(\mathbf{r}) = \mathbf{E}^{\text{subs}}(\mathbf{r}) + \mathbf{E}^{\text{cond}}(\mathbf{r}) \tag{A.3}$$

$$\mathbf{H}^{\text{antenna}}(\mathbf{r}) = \mathbf{H}^{\text{subs}}(\mathbf{r}) + \mathbf{H}^{\text{cond}}(\mathbf{r}) \tag{A.4}$$

The total field intensities in equations (A.1) and (A.2) become:

$$\mathbf{E}^{\text{total}} = \mathbf{E}^{\text{cond}}(\mathbf{r}) + \mathbf{E}^{\text{subs}}(\mathbf{r}) + \mathbf{E}^{\text{source}}(\mathbf{r}) \tag{A.5}$$

$$\mathbf{H}^{\text{total}} = \mathbf{H}^{\text{cond}}(\mathbf{r}) + \mathbf{H}^{\text{subs}}(\mathbf{r}) + \mathbf{H}^{\text{source}}(\mathbf{r}) \tag{A.6}$$

A.2.1 Fields Scattered by the Conducting Surface

The conducting strips of the substrate are reffered to as conducting surfaces in this section. Fields that are scattered from the conducting surface are computed using the surface equivalence principle.

By the surface equivalence principle: fields inside or outside an arbitrary closed fictitious surface may be computed using equivalent electric and magnetic current densities on the fictitous surface, where [3], [4]:

- The equivalent current densities are defined using field boundary conditions at the enclosing surface as:

$$\mathbf{J}_{\text{eq}}(\mathbf{r}) = \hat{n} \times (\mathbf{H}^{\text{outside}}(\mathbf{r}) - \mathbf{H}^{\text{inside}}(\mathbf{r})) \tag{A.7}$$

$$\mathbf{M}_{\text{eq}}(\mathbf{r}) = \hat{n} \times (\mathbf{E}^{\text{inside}}(\mathbf{r}) - \mathbf{E}^{\text{outside}}(\mathbf{r})) \tag{A.8}$$

Where: $(\mathbf{E}^{\text{inside}}, \mathbf{H}^{\text{inside}})$ and $(\mathbf{E}^{\text{outside}}, \mathbf{H}^{\text{outside}})$ are the fields inside and outside the fictitious surface respectively, and $\hat{n}$ is the outward directed unit normal on the fictitious surface, and $\mathbf{r}$ is the position vector on the fictitious surface.
- The fields inside the fictitious surface may be made anything when using the equivalent current densities for computing the fields outside the fictitious surface and vice versa.
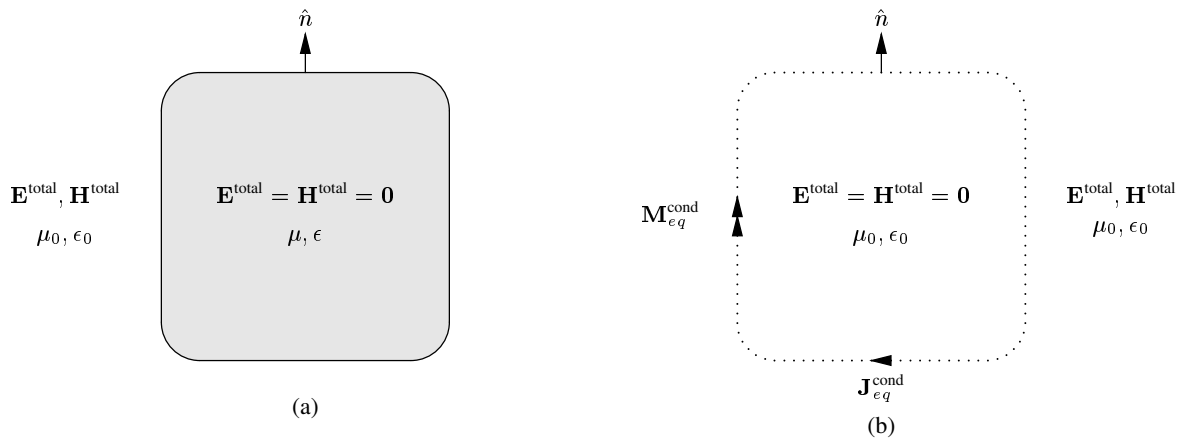
Figure A.2: PEC Conductor (a) and equivalent problem (b).

Using the second point above: the fields inside the fictitious surface are usually chosen equal to zero if the region of interest is that outside the fictitious surface and vice versa. This results in a form of the surface equivalence principle known as *Love's equivalence principle*. Setting the field as zero outside the region of interest is done so that the composition of the region can be modified without affecting the fields [4].

Fields scattered by a finite volume conductor, which is assumed to be perfectly conducting (i.e. a PEC [1](perfect electrical conductor)) are computed using the surface equivalence principle as follows. The conductor is replaced by equivalent electric and magnetic current densities on a fictitious surface, which encloses the conductor and is chosen equal to surface of the conductor as shown in figure A.2 (b). Given that the fields inside a conductor are equal to zero [4]: the conductor is removed and the region inside the fictitious surface is filled with free-space material. This means that the equivalent current densities radiate in free-space and the free-space Green's function may be used for computation of the radiated fields.

The fields on the surface a conductor are governed by the following boundary conditions [5]:

- Tangential electric field is zero everywhere on the surface.
- Normal magnetic field is zero everywhere on the surface.

Therefore, equivalent current densities in figure A.2 (b) are given by [4]:

$$\mathbf{J}_{eq}^{cond} = \hat{n} \times \mathbf{H}^{total} \tag{A.9}$$

$$\mathbf{M}_{eq}^{cond} = \mathbf{0} \tag{A.10}$$

And the fields that are scattered by the conductor are given by [4]:

$$\mathbf{E}^{conductor}(\mathbf{r}) = -jkZ_0 \iint_{s_{cond}} \left(\mathbf{J}_{eq}^{cond}(\mathbf{r}')G(\mathbf{r},\mathbf{r}') + \frac{1}{k^2}\nabla' \cdot \mathbf{J}_{eq}^{cond}(\mathbf{r}')\nabla G(\mathbf{r},\mathbf{r}') \right) ds' \tag{A.11}$$

$$\mathbf{H}^{conductor}(\mathbf{r}) = -\iint_{s_{cond}} \mathbf{J}_{eq}^{cond}(\mathbf{r}') \times \nabla G(\mathbf{r},\mathbf{r}')ds' \tag{A.12}$$

Where:

- $\mathbf{J}_{eq}^{cond}$ is the equivalent electric current density on the surface of the conductor.
- $G(\mathbf{r},\mathbf{r})$ is the free-space Green's function, which is given by:

$$G(\mathbf{r},\mathbf{r}') = \frac{e^{-jk|\mathbf{r}-\mathbf{r}'|}}{4\pi|\mathbf{r}-\mathbf{r}'|} \tag{A.13}$$

- $\mathbf{r}'$ and $\mathbf{r}$ are the position vectors on the surface of the conductor and everywhere in the environment respectively.
- $k = 2\pi/\lambda$, is the propagation constant.

[1]A PEC is a conductor with an infinite value of conductivity.

- $Z_0 = \sqrt{\frac{\mu_0}{\epsilon_0}}$, is the characteristic impedance of the environment.
- μ_0 is the permeability of the environment.
- ϵ_0 is the permittivity of the environment.
- $\omega = 2\pi f$, where f is the frequency in Hz.

The derivation above may also be used for computing the fields that are scattered by a real conductor[2] even though a PEC was assumed during the derivation. This is because fields in a conductor are confined to a thin layer on the surface at high frequencies, and the conductivity values of conductors are large enough for the tangential field on the surface of the conductor to can be assumed negligible. Therefore, the boundary conditions for a PEC are satisfied approximately in a real conductor.

A.2.2 Fields Scattered by the Substrate

Fields scattered by the substrate are computed using the volume and surface equivalence principles. The details for computing the scattered fields using both principles are presented in the following sections.

A.2.2.1 Using the Volume Equivalence Principle

The substrate is removed and replaced by the equivalent volume electric and magnetic current densities, which are defined by [6]:

$$\mathbf{J}_{eq}^{subs}(\mathbf{r}) = j\omega(\epsilon - \epsilon_0)\mathbf{E}^{total}(\mathbf{r}) \tag{A.14}$$

$$\mathbf{M}_{eq}^{subs}(\mathbf{r}) = j\omega(\mu - \mu_0)\mathbf{H}^{total}(\mathbf{r}) \tag{A.15}$$

Where:

- $\mathbf{r}$ is an arbitrary position vector in V_{subs}, which is the region occupied by the antenna substrate.
- ϵ and μ are the permittivity and permeability of the substrate material respectively.

Given that antenna substrates are non-magnetic material $\mu = \mu_0$, and the volume equivalent magnetic current density is zero.

The scattered fields are given by [6]:

$$\mathbf{E}^{substrate}(\mathbf{r}) = -jkZ \iiint_{V_{subs}} \left(\mathbf{J}_{eq}^{subs}(\mathbf{r}')G(\mathbf{r}, \mathbf{r}') + \frac{1}{k^2}\nabla' \cdot \mathbf{J}_{eq}^{subs}(\mathbf{r}')\nabla G(\mathbf{r}, \mathbf{r}') \right) dv' \tag{A.16}$$

$$\mathbf{H}^{substrate}(\mathbf{r}) = - \iiint_{V} \mathbf{J}_{eq}^{subs}(\mathbf{r}') \times \nabla G(\mathbf{r}, \mathbf{r}') dv' \tag{A.17}$$

Where: $\mathbf{r}'$ is arbitrary position vector in V_{subs}, and $\mathbf{r}$ is an arbitrary position vector in the environment including V_{subs}.

A.2.2.2 Using the Surface Equivalence Principle

Using Love's equivalence principle: fields that are scattered by the substrate and those inside the substrate are computed using the equivalent problems that are shown in figure A.3 (b) and figure A.3 (c) respectively. The dotted lines in figure A.3 represent the fictitious surface with equivalent current densities, and it is chosen equal to the outer surface of the substrate. Using equations (A.7) and (A.8), and the continuity of tangential fields: the equivalent current densities for both problems have equal magnitudes but are in opposite directions, as indicated in figure A.3.

---

[2]A real conductor is used here to refer to a conductor with a finite conductivity value.
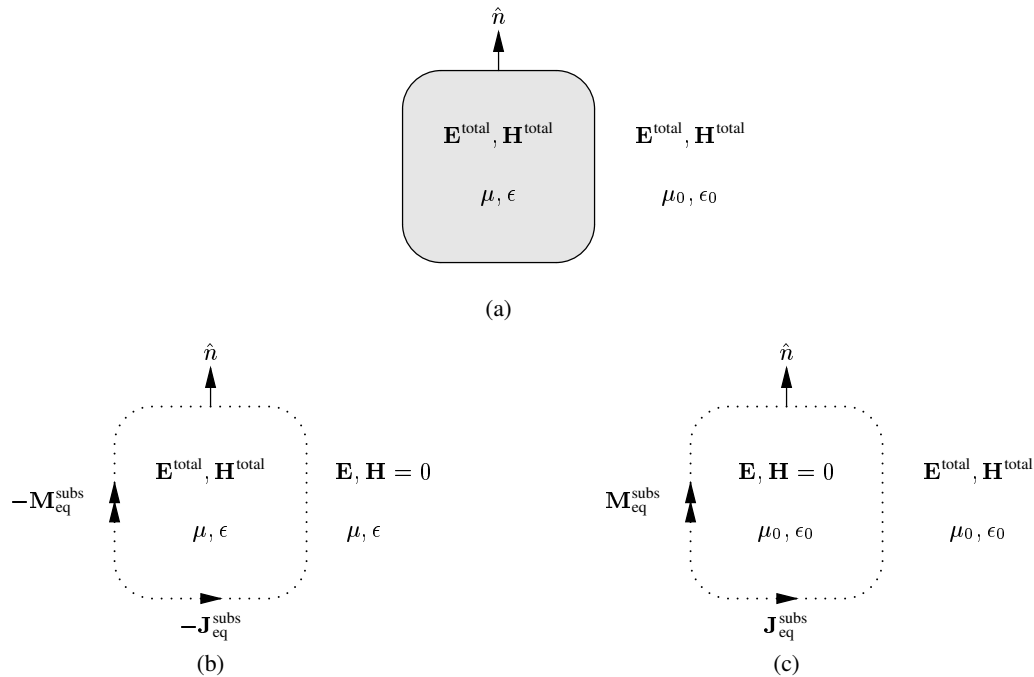
Figure A.3: Substrate (a) with outer (b) and inner (c) equivalent problems.

The equivalent current densities for the problem in figure A.3 (b) are given by:

$$\mathbf{J}_{\text{eq}}^{\text{subs}} = \hat{n} \times \mathbf{H}^{\text{total}} \tag{A.18}$$

$$\mathbf{M}_{\text{eq}}^{\text{subs}} = -\hat{n} \times \mathbf{E}^{\text{total}} \tag{A.19}$$

And, the scattered fields are given by:

$$
\begin{aligned}
\mathbf{E}^{\text{subs}}(\mathbf{r}) = {}& - jkZ_0 \oiint_s \left(\mathbf{J}_{\text{eq}}^{\text{subs}}(\mathbf{r}')G(\mathbf{r},\mathbf{r}') + \frac{1}{k^2}\nabla' \cdot \mathbf{J}_{\text{eq}}^{\text{subs}}(\mathbf{r}')\nabla G(\mathbf{r},\mathbf{r}') \right) \mathrm{d}s' \\
& + \oiint_s \mathbf{M}_{\text{eq}}^{\text{subs}}(\mathbf{r}') \times \nabla G(\mathbf{r},\mathbf{r}')\mathrm{d}s'
\end{aligned} \tag{A.20}
$$

$$
\begin{aligned}
\mathbf{H}^{\text{subs}}(\mathbf{r}) = {}& - j\frac{k}{Z_0} \oiint_s \left(\mathbf{M}_{\text{eq}}^{\text{subs}}(\mathbf{r}')G(\mathbf{r},\mathbf{r}') + \frac{1}{k^2}\nabla' \cdot \mathbf{M}_{\text{eq}}^{\text{subs}}(\mathbf{r}')\nabla G(\mathbf{r},\mathbf{r}') \right) \mathrm{d}s' \\
& - \oiint_s \mathbf{J}_{\text{eq}}^{\text{subs}}(\mathbf{r}') \times \nabla G(\mathbf{r},\mathbf{r}')\mathrm{d}s'
\end{aligned} \tag{A.21}
$$

Where: $\mathbf{r}'$ is the position vector on the fictitious surface, $\mathbf{r}$ is the position vector everywhere in the environment, and $G(\mathbf{r},\mathbf{r}')$ is given by equation (A.13).

Fields inside the substrate are given by:

$$
\begin{aligned}
\mathbf{E}^{\text{subs}}(\mathbf{r}) = {}& jkZ \oiint_s \left(\mathbf{J}_{\text{eq}}^{\text{subs}}(\mathbf{r}')G(\mathbf{r},\mathbf{r}') + \frac{1}{k^2}\nabla' \cdot \mathbf{J}_{\text{eq}}^{\text{subs}}(\mathbf{r}')\nabla G(\mathbf{r},\mathbf{r}') \right) \mathrm{d}s' \\
& - \oiint_s \mathbf{M}_{\text{eq}}^{\text{subs}}(\mathbf{r}') \times \nabla G(\mathbf{r},\mathbf{r}')\mathrm{d}s'
\end{aligned} \tag{A.22}
$$

$$
\begin{aligned}
\mathbf{H}^{\text{subs}}(\mathbf{r}) = {}& j\frac{k}{Z} \oiint_s \left(\mathbf{M}_{\text{eq}}^{\text{subs}}(\mathbf{r}')G(\mathbf{r},\mathbf{r}') + \frac{1}{k^2}\nabla' \cdot \mathbf{M}_{\text{eq}}^{\text{subs}}(\mathbf{r}')\nabla G(\mathbf{r},\mathbf{r}') \right) \mathrm{d}s' \\
& + \oiint_s \mathbf{J}_{\text{eq}}^{\text{subs}}(\mathbf{r}') \times \nabla G(\mathbf{r},\mathbf{r}')\mathrm{d}s'
\end{aligned} \tag{A.23}
$$

Where: $\mathbf{r}'$ is the position vector on the fictitious surface, $\mathbf{r}$ is the position vector everywhere in the environment, and $G(\mathbf{r},\mathbf{r}')$ is given by equation (A.13) with $k = \omega\sqrt{\mu\epsilon}$.

A.2.3 Integral Equations

It is concluded from the previous sections that:

$$\mathbf{E}^{\text{total}} = \mathbf{E}^{\text{cond}}(\mathbf{J}_{\text{eq}}^{\text{cond}}) + \mathbf{E}^{\text{subs}}(\mathbf{J}_{\text{eq}}^{\text{subs}}) + \mathbf{E}^{\text{source}} \tag{A.24}$$

$$\mathbf{H}^{\text{total}} = \mathbf{H}^{\text{conductor}}(\mathbf{J}_{\text{eq}}^{\text{cond}}) + \mathbf{H}^{\text{subs}}(\mathbf{J}_{\text{eq}}^{\text{subs}}) + \mathbf{E}^{\text{source}} \tag{A.25}$$

When using the volume equivalence principle for computation of the fields that are scattered by the substrate, and:

$$\mathbf{E}^{\text{total}} = \mathbf{E}^{\text{cond}}(\mathbf{J}_{\text{eq}}^{\text{cond}}) + \mathbf{E}^{\text{subs}}(\mathbf{J}_{\text{eq}}^{\text{subs}}, \mathbf{M}_{\text{eq}}^{\text{subs}}) + \mathbf{E}^{\text{source}} \tag{A.26}$$

$$\mathbf{H}^{\text{total}} = \mathbf{H}^{\text{cond}}(\mathbf{J}_{\text{eq}}^{\text{cond}}) + \mathbf{H}^{\text{subs}}(\mathbf{J}_{\text{eq}}^{\text{subs}}, \mathbf{M}_{\text{eq}}^{\text{subs}}) + \mathbf{E}^{\text{source}} \tag{A.27}$$

When using the surface equivalence principle for computation of the fields that are scattered by the substrate.

Therefore, two equations are required for solution of $\mathbf{J}_{\text{eq}}^{\text{cond}}$ and $\mathbf{J}_{\text{eq}}^{\text{subs}}$ when using the volume equivalence principle and three equations are required for solution of: $\mathbf{J}_{\text{eq}}^{\text{cond}}$, $\mathbf{J}_{\text{eq}}^{\text{subs}}$, and $\mathbf{M}_{\text{eq}}^{\text{subs}}$; when using the surface equivalence principle. The required equations are derived by imposing field boundary conditions.

The first boundary condition, which is common when using the volume and surface equivalence principles is the zero tangential electric field on the conducting surfaces of the antenna structure. This boundary condition is imposed using the following equation:

$$0 = \hat{n} \times \mathbf{E}^{\text{total}}(\mathbf{r}) \tag{A.28}$$

$$0 = \hat{n} \times \mathbf{E}^{\text{cond}}(\mathbf{r}) + \hat{n} \times \mathbf{E}^{\text{subs}}(\mathbf{r}) + \hat{n} \times \mathbf{E}^{\text{source}}(\mathbf{r}) \tag{A.29}$$

Where: $\hat{n}$ is the outward pointing unit normal on the surface of the conductor, and $\mathbf{r}$ is the position vector on the surface of the conductor. $\mathbf{E}^{\text{cond}}$ is given by equation (A.11). $\mathbf{E}^{\text{subs}}$ depends on the equivalence principle used for the computing the fields scattered by the substrate: it is given by (A.16) if the volume equivalence principle is used, and equation (A.20) otherwise.

Equation (A.29) may be used on open conducting surfaces even though $\mathbf{E}^{\text{cond}}$ is formulated for a closed conducting surface [7]. An open conducting surfaces is an infinitesimally thin surfaces with defined boundaries and is used for representing conducting plates of zero thickness. It is considered as the limiting case when the thickness of the closed surface approaches zero, in which case the equivalent electric current density ($\mathbf{J}_{\text{eq}}^{\text{cond}}$) is the sum of the current on the top and bottom surfaces of the closed surface [7].

Derivation of the additional integral equations is presented in the following sections.

A.2.3.1 Using the Volume Equivalence Principle

The additional equation that is required is derived using the definition of the volume equivalent electric current density (equation (A.14)).

The definition of the equivalent electric current density is re-written in terms of the total electric as follows:

$$\mathbf{E}^{\text{total}}(\mathbf{r}) = \frac{j}{\omega(\epsilon_0 - \epsilon)}\mathbf{J}_{\text{eq}}^{\text{subs}}(\mathbf{r}) \qquad \mathbf{r} \in V_{\text{sub}} \tag{A.30}$$

Substituting $\mathbf{E}^{\text{total}}$ from equation (A.5) into the above equation gives:

$$\mathbf{E}^{\text{conductor}}(\mathbf{r}) + \mathbf{E}^{\text{substrate}}(\mathbf{r}) + \mathbf{E}^{\text{source}}(\mathbf{r}) = \frac{j}{\omega(\epsilon_0 - \epsilon)}\mathbf{J}_{\text{eq}}(\mathbf{r}) \qquad \mathbf{r} \in V_{\text{sub}} \tag{A.31}$$

$\mathbf{E}^{\text{cond}}$ and $\mathbf{E}^{\text{subs}}$ are given by equations (A.11) and (A.16) respectively.

A.2.3.2 Using the Surface Equivalence Principle

The two additional equations that are required for solution of the current densities are derived by imposing the boundary conditions on the fictitious surface for both the problems in figure A.3 (b) and (c). This is achieved using either the definition of the equivalent electric or magnetic current densities in either case.

However, the equations that results from using the definitions of the equivalent electric and magnetic current densities for both the inner and outer equivalent problems, do not give unique solutions at the frequencies that are equal to the resonant frequencies of the cavity formed by the fictitious surface [6]. This problem is averted by using the CFIE (Combined Field Integral Equations), which is the weighted sum of the EFIE (Electric Field Integral Equation) and MFIE (Magnetic Field Integral Equation) given by [6]:

$$\alpha \text{EFIE} + Z(1 - \alpha)\hat{n} \times \text{MFIE}$$

Where:

- α is a dimensionless number between zero and one.
- Z_0 is the intrinsic impedance.
- EFIE and MFIE are the equations, which results from using the definitions of the equivalent magnetic and electric current densities respectively.

α is chosen as 0.5 for this application in-line with the argument in [6, p. 465] that choosing α as such, results in the optimum combination of the EIFE and MFIE.

The EFIE and MFIE for the problem in figure A.3 (b) are derived using equations (A.18) and (A.19) respectively, and are given by:

$$-\mathbf{M}_{\text{eq}}^{\text{subs}}(\mathbf{r}) = \hat{n} \times \mathbf{E}^{\text{cond}}(\mathbf{r}) + \hat{n} \times \mathbf{E}^{\text{subs}}(\mathbf{r}) + \hat{n} \times \mathbf{E}^{\text{source}}(\mathbf{r}) \tag{A.32}$$

$$\mathbf{J}_{\text{eq}}^{\text{subs}}(\mathbf{r}) = \hat{n} \times \mathbf{H}^{\text{cond}}(\mathbf{r}) + \hat{n} \times \mathbf{H}^{\text{subs}}(\mathbf{r}) + \hat{n} \times \mathbf{H}^{\text{source}}(\mathbf{r}) \tag{A.33}$$

Where $\mathbf{r}$ and $\hat{n}$ are the position vector and unit normal on the surface of the substrate. The required CFIE is given by:

$$\hat{n} \times \mathbf{E}^{\text{source}}(\mathbf{r}) - Z\hat{n} \times \hat{n} \times \mathbf{H}^{\text{source}}(\mathbf{r}) = Z\hat{n} \times \hat{n} \times \mathbf{H}^{\text{cond}}(\mathbf{r}) - \hat{n} \times \mathbf{E}^{\text{cond}}(\mathbf{r}) +$$
$$Z\hat{n} \times \hat{n} \times \mathbf{H}^{\text{subs}}(\mathbf{r}) - \hat{n} \times \mathbf{E}^{\text{subs}}(\mathbf{r}) - \tag{A.34}$$
$$\mathbf{M}_{\text{eq}}^{\text{subs}}(\mathbf{r}) - Z\hat{n} \times \mathbf{J}_{\text{eq}}^{\text{subs}}(\mathbf{r}) \qquad \mathbf{r} \in S_{\text{sub}}$$

Where: $\mathbf{E}^{\text{cond}}(\mathbf{r})$ and $\mathbf{H}^{\text{cond}}(\mathbf{r})$ given by equations (A.11) and (A.12) respectively, and $\mathbf{E}^{\text{subs}}(\mathbf{r})$ and $\mathbf{H}^{\text{subs}}(\mathbf{r})$ given by equations (A.20) and (A.21) respectively.

The CFIE for the problem in figure A.3 (c) is derived following a similar procedure, but the equivalent current densities of the inner equivalent problem are equal to those of the problem in figure A.3 (b) multiplied by minus one. The problem in figure A.3 (c) only involves equivalent current densities radiating in an infinite homogeneous medium, therefore:

$$\mathbf{E}^{\text{total}} = \mathbf{E}^{\text{substrate}} \tag{A.35}$$

$$\mathbf{H}^{\text{total}} = \mathbf{H}^{\text{substrate}} \tag{A.36}$$

$\mathbf{E}^{\text{subs}}$ and $\mathbf{H}^{\text{subs}}$ are given by equations (A.22) and (A.23) respectively. The resulting CFIE is given by:

$$\hat{n} \times \mathbf{E}^{\text{substrate}}(\mathbf{r}) + Z\hat{n} \times \hat{n} \times \mathbf{H}^{\text{substrate}}(\mathbf{r}) = \mathbf{M}_{\text{eq}}^{\text{subs}} + Z\hat{n} \times \mathbf{J}_{\text{eq}}^{\text{subs}} \qquad \mathbf{r} \in S_{\text{sub}} \tag{A.37}$$

A.2.4 Discussion

The MoM formulations are given by:

1) Equations (A.29) and (A.31). These equations may be used for computing $\mathbf{J}_{\text{eq}}^{\text{cond}}$ and $\mathbf{J}_{\text{eq}}^{\text{subs}}$, which may then be used for computing the neccessary antenna parameters.

2) Equations (A.29), (A.34), and (A.37). These equations may be used for computing $\mathbf{J}_{eq}^{cond}$, $\mathbf{J}_{eq}^{subs}$ and $\mathbf{M}_{eq}^{subs}$, which may then be used for computing the neccessary antenna parameters.

Both formulations may be used with printed antennas of arbitrary configuration. However, only the formulation using the volume equivalence principle may be used for the analysis of antennas with inhomogeneous substrates, where: the different regions of the substrate with different electromagnetic properties are represented by different volume equivalent electric current densities, which are defined by equation (A.14); substituting values of ϵ as necessary.

A.3 FEM-MoM Formulation

One of the strong points FEM is the straight forward treatment of complex geometries and material inhomogeneities [8, p. 15]. The probe-fed printed antenna structure is a complex structure, given that it is composed of an arbitrary configuration of: conducting strips, conducting wires, and, a dielectric (which can be inhomogeneous). Therefore, FEM is better suited for the analysis of these structures.

FEM analysis of these structures involves computing the electric field in the region that the structure occupies, imposing the necessary boundary conditions on the conducting regions and feed area. The electric field is computed using the electric field wave equation, which is given by:

$$\nabla \times \left(\frac{1}{\mu}\nabla \times \mathbf{E}\right) - \omega^2\epsilon\mathbf{E} = -j\omega\mathbf{J} + \nabla \times \frac{\mathbf{M}}{\mu} \tag{A.38}$$

Where $\mathbf{J}$ and $\mathbf{M}$ are the impressed electric and magnetic current densities within the substrate of the antenna structure.

The solution of equation (A.38) for the electric field using FEM, can be computed only over a finite volume region (V) and not all space. This is because the FEM solution involves reducing the equation that governs the problem into a matrix equation, and the size of the matrix in the equation is proportional to the volume region. Therefore, V is defined here as the region occupied by the antenna and is enclosed by a fictitious surface (S), which does not touch the conducting surfaces of the antenna structure.

Solution of equation (A.38) within V requires specification of the fields on S to make it seem as if the volume region is infinite and not truncated [2]. Since the interest is only on the electric field inside S, the problem is reduced to a problem that is equivalent to the original problem inside S. This is done using Love's equivalence principle, and the equivalent problem is shown in A.4 (b) with $\mathbf{M}_{eq}$ and $\mathbf{J}_{eq}$ given by:

$$\mathbf{J}_{eq} = \hat{n} \times \mathbf{H} \tag{A.39}$$

$$\mathbf{M}_{eq} = -\hat{n} \times \mathbf{E} \tag{A.40}$$

Either $\mathbf{M}_{eq}$ or $\mathbf{J}_{eq}$ may be used as the required boundary condition on S, but since the electric field is being computed it is easier to use $\mathbf{J}_{eq}$ as a boundary condition since its directly related to the tangential magnetic field on S.

However, $\mathbf{M}_{eq}$ and $\mathbf{J}_{eq}$ are not known. Since $\mathbf{M}_{eq}$ is related to $\mathbf{E}$: there are only two unknowns, i.e. $\mathbf{E}$ or $\mathbf{J}_{eq}$. The formulation for the FEM analysis gives the relation between $\mathbf{E}$ and $\mathbf{J}_{eq}$. Therefore, another equation is required for solution of $\mathbf{E}$ and $\mathbf{J}_{eq}$.

The additional equation is derived using a problem derived using Love's equivalence principle, which is equivalent to the antenna problem outside S. This problem is shown in figure A.4 (c), and it involves equivalent current densities on S radiating in free-space. The analysis of this problem for $\mathbf{M}_{eq}$ and $\mathbf{J}_{eq}$ is performed using MoM as it resembles the problems of section A.2.
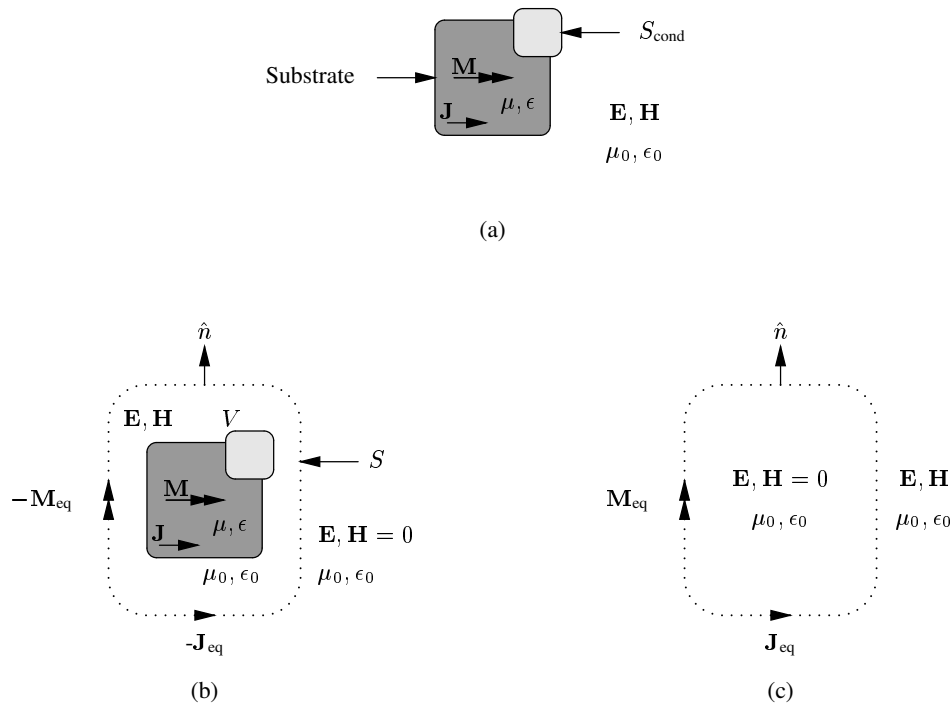
Figure A.4: Arbitrary printed antenna structure (a) with inner (b) and outer (c) equivalent problems.

A.3.1 FEM Formulation

FEM formulation is the equation that is solved using FEM for the electric field. There are two methods that are used for deriving the FEM formulation, namely: the Rayleigh-Ritz and Garlerkin methods. These methods are discussed in detail in [6], [2], [5]. The formulation in this section is derived using the Rayleigh-Ritz method, where the formulation is a *functional* or *variational principle*. This is a function, which is formulated in terms of the electric field and is made stationary by the electric field that satisfies equation (A.38) under given boundary conditions [6], [8].

The generalised variational principle that is presented in [6, Chapter 6] is used as the FEM formulation. It is given by:

$$
\begin{aligned}
F(\boldsymbol{E}) ={}& \frac{1}{2} \iiint_V \left(\frac{1}{\mu_r} (\nabla \times \mathbf{E}) \cdot (\nabla \times \mathbf{E}) - k_0^2 \epsilon_r \mathbf{E} \cdot \mathbf{E} \right) \mathrm{d}V \\
& + \iint_S \left(\frac{\gamma_e}{2} (\hat{n} \times \mathbf{E}) \cdot (\hat{n} \times \mathbf{E}) + \mathbf{E} \cdot \mathbf{U} \right) \mathrm{d}S \\
& + \iiint_V \left(jk_0 Z_0 \mathbf{E} \cdot \mathbf{J} + \mathbf{E} \cdot (\nabla \times \frac{\mathbf{M}}{\mu}) \right) dV
\end{aligned}
\tag{A.41}
$$

Where γ_e and $\mathbf{U}$ are parameters that are related to the boundary conditions. The unknown $\mathbf{J}_{\mathrm{eq}}$ is incorporated into the formulation as follows. The first variation of the equation (A.41) gives the integrand of the surface integral, which equals to zero for:

$$
\frac{1}{\mu_r} \hat{n} \times (\nabla \times \mathbf{E}) + \gamma_e \, \hat{n} \times (\hat{n} \times \mathbf{E}) = \mathbf{U}
\tag{A.42}
$$

Maxwell's electric field curl equation is given by:

$$
\nabla \times \mathbf{E}(\mathbf{r}) = -j\omega\mu\mathbf{H}(\mathbf{r})
\tag{A.43}
$$

The dot product of the unit normal on S with equation (A.43) results in:

$$
\hat{n} \times (\nabla \times \mathbf{E}(\mathbf{r})) = -j\omega\mu\hat{n} \times \mathbf{H}(\mathbf{r})
\tag{A.44}
$$

The above equation is equal to equation (A.42), for:

$$\gamma_e = 0 \tag{A.45}$$

$$\mathbf{U} = -j\omega\mu_0\mathbf{H}(\mathbf{r}) \tag{A.46}$$

Therefore, setting γ_e and $\mathbf{U}$ as above in equation (A.41) results in:

$$
\begin{aligned}
F(\boldsymbol{E}) =& \frac{1}{2}\iiint_V \left[\frac{1}{\mu_r}(\nabla\times\mathbf{E})\cdot(\nabla\times\mathbf{E}) - k_0^2\epsilon_r\mathbf{E}\cdot\mathbf{E} \right]\mathrm{d}V + \\
& \iiint_V \left(jk_0Z_0\mathbf{E}\cdot\mathbf{J} + \mathbf{E}\cdot(\nabla\times\frac{\mathbf{M}}{\mu}) \right)\mathrm{d}V - \\
& jk_0Z_0 \oiint_S \mathbf{E}\cdot(\hat{n}\times\mathbf{H})\mathrm{d}S
\end{aligned}
\tag{A.47}
$$

Which can be written in another form using equation (A.39) and figure A.4, as:

$$
\begin{aligned}
F(\boldsymbol{E}) =& \frac{1}{2}\iiint_V \left[\frac{1}{\mu_r}(\nabla\times\mathbf{E})\cdot(\nabla\times\mathbf{E}) - k_0^2\epsilon_r\mathbf{E}\cdot\mathbf{E} \right]\mathrm{d}V + \\
& \iiint_V \left(jk_0Z_0\mathbf{E}\cdot\mathbf{J} + \mathbf{E}\cdot(\nabla\times\frac{\mathbf{M}}{\mu}) \right)\mathrm{d}V + \\
& jk_0Z_0 \oiint_S \mathbf{E}\cdot\mathbf{J}_{\mathrm{eq}}\mathrm{d}S
\end{aligned}
\tag{A.48}
$$

A.3.2 MoM Formulation

Following section A.2.3.2; a CFIE is also used here as the MoM formulation. The required CFIE is derived using the definitions of the equivalent electric and magnetic current densities, and is given by:

$$\mathbf{M}_{\mathrm{eq}}(\mathbf{r}) - Z_0\hat{n}\times\mathbf{J}_{\mathrm{eq}}(\mathbf{r}) = -\hat{n}\times\mathbf{E}(\mathbf{r}) - \hat{n}\times\hat{n}\times\mathbf{H}(\mathbf{r}) \qquad \mathbf{r}\in S \tag{A.49}$$

$\mathbf{E}$ and $\mathbf{H}$ are the fields that are radiated by the equivalent currents, and they are given by:

$$
\begin{aligned}
\mathbf{E}(\mathbf{r}) =& -jkZ \oiint_s \left(\mathbf{J}_{\mathrm{eq}}(\mathbf{r}')G(\mathbf{r},\mathbf{r}') + \frac{1}{k^2}\nabla'\cdot\mathbf{J}_{\mathrm{eq}}(\mathbf{r}')\nabla G(\mathbf{r},\mathbf{r}') \right)\mathrm{d}s' \\
& + \oiint_s \mathbf{M}_{\mathrm{eq}}(\mathbf{r}')\times\nabla G(\mathbf{r},\mathbf{r}')\mathrm{d}s' \qquad \mathbf{r}'\in S
\end{aligned}
\tag{A.50}
$$

And:

$$
\begin{aligned}
\mathbf{H}(\mathbf{r}) =& -j\frac{k}{Z} \oiint_s \left(\mathbf{M}_{\mathrm{eq}}(\mathbf{r}')G(\mathbf{r},\mathbf{r}') + \frac{1}{k^2}\nabla'\cdot\mathbf{M}_{\mathrm{eq}}(\mathbf{r}')\nabla G(\mathbf{r},\mathbf{r}') \right)\mathrm{d}s' \\
& - \oiint_s \mathbf{J}_{\mathrm{eq}}(\mathbf{r}')\times\nabla G(\mathbf{r},\mathbf{r}')\mathrm{d}s' \qquad \mathbf{r}'\in S
\end{aligned}
\tag{A.51}
$$

A.3.3 Discussion

Equations (A.48) and (A.49) may be used for solution of: $\mathbf{J}_{eq}$ and $\mathbf{M}_{eq}$ on S, and $\mathbf{E}$ within V. $\mathbf{J}_{eq}$ and $\mathbf{M}_{eq}$ may then be used for computing the fields radiated by the antenna everywhere, except inside V.

A.4 Feed Model

The antenna is fed by an ideal voltage source applied between the inner and outer conductors of the probe feed at the feed opening (see figures A.1 and A.5). This source voltage creates electric and magnetic fields inside the feed opening and the field mode can be assumed to be TEM for most practical purposes [9](see figure A.5 (b)).

Numerous approaches have been proposed for modeling this type of feed in the literature [2], [4], [6]. The common approach is to specify the fields in the feed opening. Two popular methods that are used for
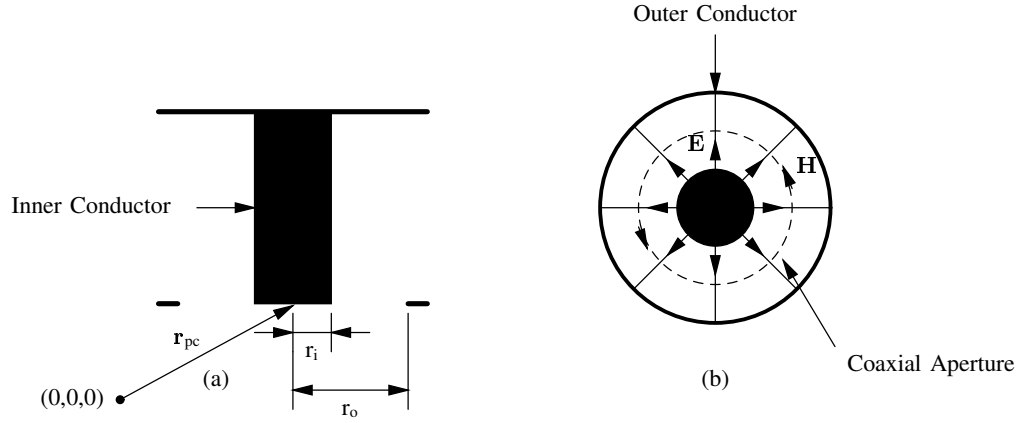
Figure A.5: Cross-section of a probe-fed printed antenna without substrate (a) and the feed opening (b).

specifying the fields across the coaxial aperture are [4, p. 722-726]: the magnetic frill generator, and the delta-gap model. The other less common approach is to specify the current distribution on the inner conductor (see figure A.5) of the feed. This approach has been used successfuly with FEM formulation [10], therefore, it is discussed for use with the FEM formulation only.

A.4.1 Magnetic Frill Generator

A ring of infinitesimaly thin, circumferentially directed equivalent magnetic current density is placed across the feed opening with this model. This equivalent magnetic current density is defined as [11]:

$$\mathbf{M}_{\text{eq}}^{\text{source}} = -2\hat{n} \times \mathbf{E}^{\text{aperture}} \tag{A.52}$$

Where: $\mathbf{E}^{\text{aperture}}$ is the electric field across the feed opening, and $\hat{n}$ is the normal at the feed opening, which points away from the coaxial cable. Given that TEM mode fields are assumed in the feed opening, $\mathbf{E}^{\text{aperture}}$ is given by [4]:

$$\mathbf{E}^{\text{aperture}}(\mathbf{r}) = \begin{cases} \dfrac{V_{\text{app}}}{2|\mathbf{r} - \mathbf{r}_{\text{pc}}|\ln(r_o/r_i)} & \mathbf{r} \in s_{\text{aperture}} \\ 0 & \text{otherwise} \end{cases} \tag{A.53}$$

Where: V_{app} is the voltage across the inner and outer conductors of the coaxial feed at the point where the coaxial cable attaches to the antenna structure, S_{aperture} is the feed opening region, and the definitions of $\mathbf{r}_{\text{pc}}$, r_o, and r_i can be seen in figure A.5.

The magnetic current density in equation (A.52) is defined using the surface equivalence principle in conjunction with image theory [11], assuming that the aperture exists on an infinite PEC ground plane. Therefore, this source model is appropriate for cases where the feed opening exist on a conducting strip that is large enough for the formulation to be valid, and is not near the edges of the conducting strip.

A.4.1.1 Use with the MoM Formulation

This feed is incorporated into the MoM formulation by, using fields radiated by the magnetic frill current as $\mathbf{E}^{\text{source}}$ and $\mathbf{H}^{\text{source}}$, i.e. [4]:

$$\mathbf{E}^{\text{source}}(\mathbf{r}) = \iint_s \mathbf{M}_{\text{eq}}^{\text{source}}(\mathbf{r}') \times \nabla G(\mathbf{r}, \mathbf{r}') \mathrm{d}s' \tag{A.54}$$

$$\mathbf{H}^{\text{source}}(\mathbf{r}) = -j\frac{k}{Z} \oiint_s \left(\mathbf{M}_{\text{eq}}^{\text{source}}(\mathbf{r}') G(\mathbf{r}, \mathbf{r}') + \frac{1}{k^2} \nabla' \cdot \mathbf{M}_{\text{eq}}^{\text{source}}(\mathbf{r}') \nabla G(\mathbf{r}, \mathbf{r}') \right) \mathrm{d}s' \tag{A.55}$$

Where $G(\mathbf{r}, \mathbf{r}')$ is the free-space Green's function. The feed opening and inner conductor are treated as part of the conducting strips, and the zero tangential electric field boundary condition is applied on their surfaces.

A.4.1.2 Use with the FEM Formulation

This feed model is incorporated into the FEM formulation by substituting the magnetic current density of equation (A.52) in the FEM formulation (equation (A.48)), and the inner conductor of the feed is treated as part of S_{cond} and the tangential electric field component is set to zero on its surface.

A.4.2 Delta Gap Model

With the delta gap model: the electric field across the coaxial aperture is assumed to be constant such that:

$$\mathbf{E}^{\text{aperture}}(\mathbf{r}) = \frac{V_{\text{app}}}{(\mathbf{r}_o - \mathbf{r}_i)}\hat{r} \tag{A.56}$$

And:

$$\mathbf{H}^{\text{aperture}}(\mathbf{r}) = \frac{\left|\mathbf{E}^{\text{aperture}}\right|}{Z}\hat{\theta} \tag{A.57}$$

This model is accurate for cases where $\mathbf{r}_o - \mathbf{r}_i$ is small compared to the wavelength (at the frequency of simulation) for a constant field distribution to be assumed across the feed opening.

A.4.2.1 Use with the MoM Formulation

This source model is also incorporated into the MoM formulations via the $\mathbf{E}^{\text{source}}$ and $\mathbf{H}^{\text{source}}$ terms. Using the above equations, the source electric and magnetic fields are given as:

$$\mathbf{E}^{\text{source}}(\mathbf{r}) = \begin{cases} \mathbf{E}^{\text{aperture}}(\mathbf{r}) & \mathbf{r} \in S_{\text{aperture}} \\ 0 & \text{otherwise} \end{cases} \tag{A.58}$$

And:

$$\mathbf{H}^{\text{source}}(\mathbf{r}) = \begin{cases} \dfrac{\left|\mathbf{E}^{\text{aperture}}\right|}{Z}\hat{\theta} & \mathbf{r} \in S_{\text{aperture}} \\ 0 & \text{otherwise} \end{cases} \tag{A.59}$$

The feed opening and inner conductor are treated as part of the conducting strips, and the zero tangential electric field boundary condition is applied on their surfaces.

A.4.2.2 Use with the FEM Formulation

The feed voltage is incorporated into the FEM formulation as a Dirichlet boundary condition and is imposed the same way the zero tangential field boundary condition on S_{cond} is imposed. The inner conductor is treated as a part of S_{cond}.

A.4.3 Probe Feed Model

The inner conductor (see figure A.5 (a)) is replaced by an infinitesimally thin current filament of the same length. A constant electric current density ($\mathbf{J}$) is assumed throughout the length of the current filament. The feed opening is treated as part of the conducting strip that the coaxial cable attaches to.

Assuming a z directed inner conductor; the electric current density in equation (A.47) is given by [2]:

$$\mathbf{J}(\mathbf{r}) = I\delta(x - x_s)\delta(y - y_s)\hat{z} \tag{A.60}$$

Where: I is the magnitude of the current on the probe-feed, and x_s and y_s are the x and y components of the center of the inner conductor. This feed model is incorporated into the FEM formulation by substituting

the electric current density of equation (A.60) into equation (A.47). The feed opening is treated as part of the conducting strips of the antenna structure.

This source model gives accurate results for antennas with thin dielectric substrates and for instances where the diameter of the inner conductor can be ignored [6]. When the diameter of the inner conductor cannot be ignored the strip model [12] may be used; where the inner conductor is represented by two current filaments placed as shown in figure A.6. w in figure A.6 is given by:

$$w = 4r_{ic} \tag{A.61}$$

Where r_{ic} is the radius of the inner conductor of the coaxial cable.

Axis through center of inner conductor
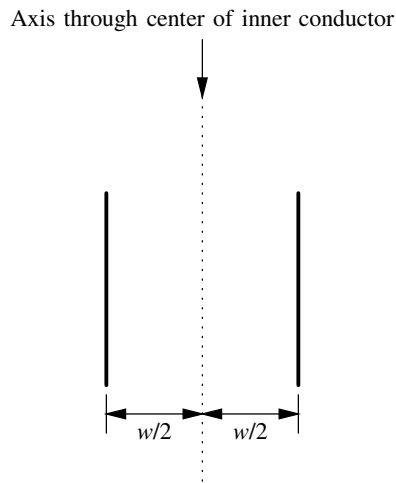
Figure A.6: Positions of the current filaments (solid black lines) using the strip model.

A.5 Choice of Formulation

The formulations presented in this paper have been used successfully for analysis of printed antennas in [13], [14], [15], [16], [17]. All the formulations are expected to be equally accurate given that no simplifying assumptions are made during their derivations, except with feed models, which are used with all the formulations. Therefore, criterion for the formulation to be implemented in SuperNEC is based on the efficiency of its numerical solution in terms of:

- Memory usage
- Solution Time

The formulations presented in the preceding sections are solved for the unknown quantities (i.e. current densities and/or electric field) using FEM and/or MoM. The approach that is adopted with both numerical techniques is to reduce the formulation into a matrix equation, which can be solved using a computer. This is done by expanding the unknown quantities by a sum of weighted basis functions, and the weights become the new unknowns. The weights are determined by reducing each of the formulation equations into a matrix equation involving the sum of a square matrix-column vector product, for each of the unknown quantities in the equation. The resulting matrix equations for each of the formulation equations are then solved together for the unknown weights.

The memory usage criterion above is important because the matrices that are generated during the solution process can be large for problems involving printed antennas. These matrices have to be stored and the solution of the matrix equations also requires memory. The time required to fill and solve the resulting matrices is also important because the antenna structure can only be analysed for the parameter of interest (e.g. input impedance) per frequency using the formulations presented in this appendix and the variation of the impedance might be required for a large frequency band.

The memory requirement and solution time for the numerical solution of the formulations presented in the preceding sections, are compared and the formulation, which requires the least memory and time for solution of the unknown quantities is chosen for implementation in SuperNEC.

A.5.1 Memory Usage

The memory that is required for a numerical solution using FEM and MoM is for storage of the matrices that are generated during the solution process and solution of the resulting matrix equations.

A.5.1.1 Storage of Matrices

The amount of memory required for storage of a matrix that results for a problem with n-unknowns is:

- Less than $\alpha n M$ when using FEM [6, p. 586]. Where: α is the largest number of elements that an unknown variable is associated with, and M is the amount of memory required to store a matrix entry. This is because FEM formulations result in sparse matrices with a large number of matrix entries equal to zero, and only the non-zero entries are stored.
- Equal to $n^2 M$ when using MoM. This is because MoM formulations result in full matrices.

Therefore, MoM implementations require more memory when compared to FEM implementations for a problem with an equal number of unknowns.

Printed antenna problems analysed using FEM generally result in more unknowns than equivalent problem analysed using MoM. This is because the FEM analysis includes the region surrounding the structure while only the structure is considered with MoM. Matrices resulting from a FEM analysis do not necessarily require more memory for storage when compared to the matrices that result from a MoM analysis of the same problem. To give an example: a problem that is analysed using FEM with 60000 unknowns requires the amount of memory, which is less than that required by an equivalent problem analysed using MoM with 949 unknowns; assuming that $\alpha = 15$. It unlikely that an equivalent MoM problem analysed using the formulations presented in this appendix will have the number of unknowns less than 949, based on experience.

Table A.1: Matrices generated for the different formulations.

Formulation	Matrix	Quantity	Size	Sparse/Full
MoM Formulation (*Volume Equivalence Principle*)	$\mathbf{J}_{eq}^{cond}$	2	$N_c \times N_c$	Full
	$\mathbf{J}_{eq}^{subs}$	2	$N_s^V \times N_s^V$	Full
MoM Formulation (*Surface Equivalence Principle*)	$\mathbf{J}_{eq}^{cond}$	3	$N_c \times N_c$	Full
	$\mathbf{J}_{eq}^{subs}$	3	$N_s^S \times N_c$	Full
	$\mathbf{M}_{eq}^{subs}$	3	$N_s^S \times N_s^S$	Full
FEM-MoM Formulation	$\mathbf{J}_{eq}$ (*MoM*)	1	$N_b \times N_b$	Full
	$\mathbf{J}_{eq}$ (*FEM*)	1	$N_b \times N_b$	Sparse
	$\mathbf{M}_{eq}$ (*MoM*)	1	$N_b \times N_b$	Full
	$\mathbf{E}$ (*FEM*)	1	$N_e \times N_e$	Sparse

Table A.1 gives a breakdown of the matrices that are generated for the numerical solution of the different formulations. The variables for the sizes of the matrices are defined as follows:

- N_c is the number of unknowns that are associated with the electric current density on the conducting surface of the structure.
- N_s^S is the number of unknowns that are associated with the equivalent electric and magnetic current densities on the surface of the substrate.

- N_d is the number of unknowns that are associated with the equivalent electric and magnetic current densities on the enclosing surface of the FEM problem domain.
- N_s^V is the number of unknowns that are associated with the equivalent volume electric current density.
- N_e is the number of unknowns that are associated with the electric field within the FEM problem domain.

The variables above, are presented in order of increasing value and their values are proportional to the size of the antenna and the frequency at which the analysis is performed. The exact values of the variables depend on a particular problem, but the following relation holds in general:

- N_c is always smaller than all the variables,
- The values of N_s^S and N_d are comparable.
- N_s^V is considerably larger than N_s^S and N_d.
- N_e is the largest and its value is greater than the sum of all the other variables combined. Its value depends on the structure that is being simulated, but it will most likely not be more than $50*N_s^V$.

Based on table A.1 and the above paragraph: the amount of memory required for storage of the matrices resulting from the FEM-MoM formulation is expected to be less than that required for storage of the resulting matrices from the numerical solutions of the other formulations for an equivalent problem. This is because:

- The numerical solution of the MoM formulation results in 6 matrices, which are comparable to two of the matrices of the FEM-MoM formulation resulting from the MoM formulation part, in size. With regard to the matrices resulting from the FEM formulation part; there are 7 more full matrices compared to two sparse matrices resulting from the FEM formulation: one of the matrices is the same size as the matrices resulting from the MoM formulations, but requires less memory for storage, and the other is appreciably larger than all the matrices, but since its sparse the memory required is less than that required for storage of most of the matrices.
- The memory required by the MoM formulation using the volume equivalence principle is expected to be greater than that required by the FEM-MoM formulation. The two matrices, which result from the MoM formulation part are smaller than those from the MoM formulation using the volume equivalence principle, for the volume equivalent current term. This is because matrices from the MoM formulation part of the FEM-MoM formulation result from the discretisation of the surface, which encloses the FEM problem domain and those from the MoM formulation using surface equivalence principle results from the volume discretisation of the substrate. Even though the size of N_e is larger than that of N_s^V; the amount of memory required to store the matrix for the electric field will be equal or comparable to that for storing the matrix for the volume equivalent current density term for N_e appreciably larger than N_s^V.

The number of unknowns depends on the problem being solved, and it cannot be readily shown that the FEM-MoM formulation will require less memory. However, if one considers that the amount of memory that is required to store a matrix resulting from a FEM formulation increases linearly with the number of unknowns and that resulting from the MoM formulation increases quadratically with the number of unknowns, then it can be appreciated that the FEM-MoM formulation is likely the more memory efficient formulation, since antenna simulation problem generally result in a large number of unknowns.

A.5.1.2 Solution of Matrix Equations

The memory required for solution of the resulting matrix depends on the method used for solving the resulting matrices.

When using direct solvers, the required memory depends on the size of the matrix being solved. The resulting matrix equation for the FEM-MoM formulation will require more memory for solution using a direct solver because of the large number of unknowns associated with a FEM analysis.

When using an iterative solver the amount of memory required for solution of the matrix equation depends on: the size of the matrix (but is considerably less than that required by a direct solver), and the properties of the matrices. The memory required by iterative solvers is for computation of the matrix-vector product. Matrices resulting from the FEM-MoM formulation are sparse, and matrix multiplication with a sparse matrix

is memory efficient. It is shown in [6, p. 470-480] that the matrices resulting from the FEM-MoM formulation can be solved with relatively less memory using iterative solvers.

Therefore, it is not clear which formulation will require more memory for solution of the resulting matrix equations since it depends on the method used for solving the resulting matrix equations.

A.5.2 Solution Time

Solution time for both numerical methods is determined by the time required to fill the required matrices and time required to solve the matrix equations.

A.5.2.1 Matrix Fill Time

The time required to generate a matrix entry for the FEM formulation is appreciably less than that required to generate an entry for the MoM formulation. This is so because:

- The terms for the MoM matrices involves evaluation of two integrals, compared to a single integral with FEM: the two integrals are the testing integral (see appendix C) and integral in the formulation equations.
- The integral terms of the MoM formulation are more complicated than those of the FEM formulations.
- The singularities in the integrands of the MoM formulation, require introduction of additional terms for evaluation [6]. This increase the time it takes to compute a matrix entry.
- Each unknown in a MoM system is coupled with all the other unknowns, resulting in full matrices, and with FEM the unknowns are only related to a few of the elements (15 at most as indicated above). Therefore, fewer terms are evaluated for FEM formulations as compared to MoM formulations.

The time required to fill the matrices for the FEM-MoM formulation is expect to be less than that required to fill the matrices for the other formulations. This is because:

- 4 fully populated matrices have to be filled with the MoM formulation using the volume equivalence principle.
- 9 fully populated matrices have to be filled with the MoM formulation using the surface equivalence principle.
- 2 fully populated and 2 sparse matrices are filled using the FEM-MoM hybrid formulation.

A.5.2.2 Matrix Solution Time

The time required to solve the resulting matrices depends on the matrix solver that is used. The solution time is proportional to the size of the matrix when using a direct solver. The solution time is proportional to the time it take to compute a the matrix-vector product and the number of iterations before convergence. The matrix-vector product depends on the number of elements contained in the matrix, i.e. whether is full or sparse, as the matrix-vector product can be computed efficiently using for a sparse matrix. The number of iterations depends on the condition number of the matrix, which may be improved by using a pre-conditioner [6].

Therefore, more time will be required for solution of the matrices resulting from the FEM-MoM formulation since the size of the matrix resulting from the FEM formulation is large. However, the the matrices resulting from the FEM-MoM formulation may be solved in less time using a pre-conditioner that is developed in [18], which may also be computed efficiently.

Therefore, it is not clear which formulation will require more time for solution of the resulting matrix equations since it depends on the method used for solving the resulting matrix equations.

A.5.3 Discussion

The FEM-MoM formulation is chosen for implementation in SuperNEC because it is likely to be more memory efficent when compared to the other formulations given that the matrices resulting from the FEM formulation part are sparse and the amount of memory required for storage increases linearly with the number of unknowns, and the time required to fill the matrices resulting from the formulation is less than that for the other formulations. The memory and time required for solution of the resulting matrices depend on the matrix solver that is used and are therefore not used as a selection criterion.

A.6 Conclusion

The derivation of two MoM formulations and a FEM-MoM formulation for analysis of probe-fed printed antennas have been presented together with different models for representing the antenna feed. The formulations are then compared on the basis of memory usage and time required for solution of the unknown parameters.

The FEM-MoM formulation is selected for implementation in SuperNEC. It is argued that its numerical solution using FEM and MoM will be more memory efficient and that is will require less time to fill the matrices generated for the formulation when compared to the two MoM formulations. The memory and time required for solution of the resulting matrix equations is not used as a criterion because it depends on the matrix solver that is used.

References

[1] G. Burke and A. Pogio. "Numerical Electromagnetics Code (NEC) - Method of Moments. Part 1: Program Description-Theory." Tech. Rep. Report UCID 18834, Lawrence Livermore National Laboratory, 01 1981.

[2] L. K. J.L. Volakis, A. Chatterjee. *Finite Element Method for Electromagnetics: Antennas, Microwave Circuits, and Scattering Applications*. New York: IEEE Press, first ed., 2001.

[3] K. Chen. "A Mathematical Formulation of the Equivalent Principle." *IEEE Transactions on Microwave Theory and Techniques*, vol. 37, no. 10, pp. 1576–1581, 10 1989.

[4] C. A. Balanis. *Advanced Engineering Electromagnetics*. John Wiley and Sons, first ed., 1989.

[5] P. P. Silvester and G. Pelosi. *Finite Element for Wave Electromagnetics*. IEEE Press, first ed., 1994.

[6] J. Jin. *The Finite Element Method in Electromagnetics*. New York: John Wiley and Sons, Inc., second ed., 2002.

[7] E. Newman and D. Pozar. "General Integral Equation Formulation for Microstrip Antennas and Scatters." *IEE Proceedings*, vol. 132, no. 12, pp. 424–432, 7 1985.

[8] D. B. Davidson. *Computational Electromagnetics for RF and Microwave Engineering*. Cambridge, first ed., 2005.

[9] J. Gong and J. L. Volakis. "An Efficient and Accurate Model of a Coax Cable Feeding Structures for FEM Simulations." *IEEE Transactions on Antennas and Propagation*, vol. 43, no. 12, pp. 1474–1478, 12 1995.

[10] J.-M. Jin and J. L. Volakis. "A Hybrid Finite Element Method for Scattering and Radiation by Microstrip Patch Antennas and Arrays Residing in a Cavity." *IEEE Transactions on Antennas and Propagation*, vol. 39, no. 11, pp. 1598–1604, 11 1991.

[11] L. L. Tsai. "A Numerical Solution for the Near and Far Fields of an Annular Ring of Magnetic Current." *IEEE Transactions on Antennas and Propagation*, vol. 20, no. 05, pp. 569–576, 09 1972.

[12] H. Wang, Y. Jin, and T. H. Hubing. "Finite-Element of Coaxial Cable Feeds and Vias in Power-Bus Structure." *IEEE Transactions on Electromagnetic Compatibility*, vol. 40, no. 04, pp. 569–574, 11 2002.

[13] P. Katehi and N. Alexopoulos. "On the Effect of Substrate Thickness and Permittivity on Printed Circuit Dipole Properties." *IEEE Transactions on Antennas and Propagation*, vol. 31, pp. 34 – 39, 01 1983.

[14] B. Salman and A. McCowen. "The CFIE Technique Applied to Finite-Size Planar and Non-Planar Microstrip Antenna." pp. 338–341. IEE, 04 1996.

[15] T. K. Sarkar, S. M. Rao, and A. R. Djordjević. "Electromagnetic Scattering and Radiation from Finite Microstrip Structures." *IEEE Transactions on Microwave Theory and Techniques*, vol. 38, no. 11, pp. 1568–1575, 11 1990.

[16] M. W. Ali, T. H. Hubing, and J. L. Drewniak. "A Hybrid FEM/MOM Technique for Electromagnetic Scattering and Radiation from Dielectric Objects with Attached Wires." *IEEE Transactions on Electromagnetic Compatibility*, vol. 39, no. 04, pp. 304–314, 11 1997.

[17] S. Makarov, S. Kulkarni, A. Marut, and L. Kempel. "Method of Moments Solution for a Printed Patch/Slot Antenna on Thin Finite Dielectric Substrate Using the Volum Integral Equation." *IEEE Transactions on Antennas and Propagation*, vol. 54, no. 04, pp. 1174–1184, 04 2006.

[18] J. Lui and J.-M. Jin. "A Highly Effective Preconditioner for Solving the Finite Element-Boundary Integral Matrix Equation of 3-D Scattering." *IEEE Transactions on Antennas and Propagation*, vol. 50, no. 9, pp. 1212–1221, 9 2002.

Appendix B

Numerical Results

B.1 Introduction

The FEM (Finite Element MEthod)-MoM (Method of Moments) formulation presented in section A.3 of appendix A is implemented in a software application using the probe feed model. The software application is developed as a stand alone executable, which will be integrated into SuperNEC. The software was developed using C++ with certain modules created using Matlab. It can be used for analysis of probe-fed printed antennas using the probe-feed model (see section A.4.3 of appendix A). Details of the software application may be obtained in appendix F.

Structures that are analysed using the software application are represented as a connection of tetrahedrons for three dimensional objects and a connection triangles for are two dimensional objects. These connections of triangles and tetrahedrons are called meshes, and are discussed in more detail in appendix F. The size of the triangles or tetrahedrons in the mesh depends on the frequency at which the structure is being analysed. The rule of thumb for the sizes of the triangles or tetrahedrons is that [1, p. 5]: the triangles must be constructed such that there are 100 segments per square wavelengths, and the tetrahedrons must be constructed such that there are 1000 segments per cubic wavelength. The segments in the preceding statements are the line segments, which connects the different corners of the triangle or tetrahedron. The above are just guidelines and better results are obtained using more segments per square or cubic wavelength.

Numerical results computed using the software application for the radar cross section of a PEC (perfect electrical conductor) sphere and the input impedance of a probe-fed printed antenna are presented to illustrate correct implementation of the formulation. The presentation is structured as follows. The results for the radar cross section of a sphere are presented in section B.2, and those for the input impedance of a probe-fed printed antenna are presented in section B.3.

B.2 Radar Cross Section of PEC Sphere

Computed results for the monostatic and bistatic radar cross sections of a PEC sphere are presented. Results for the monostatic rcs (radar cross section) are computed using the MoM formulation part of the FEM-MoM formulation, and those for the bistatic rcs are computed using the FEM-MoM formulation. The results computed using the MoM formulation are compared to the Mie-series solution, and those computed using the FEM-MoM formulation are compared to those computed using the MoM formulation for a similar problem.

The MoM formulation part of the formulation is used for analysis of a PEC sphere by setting the M_{eq} contribution to zero, which according to section A.2.1 of appendix A, is equivalent to setting the tangential component of the electric field equal to zero.

B.2.1 Monostatic Radar Cross Section

The configuration for this example is shown in figure B.1, where a PEC sphere of radius 0.1 m is excited by a -z-directed plane wave with a y directed linearly polarised electric field vector. The rcs is computed for the following frequency range: 100 MHz to 3050 MHz.
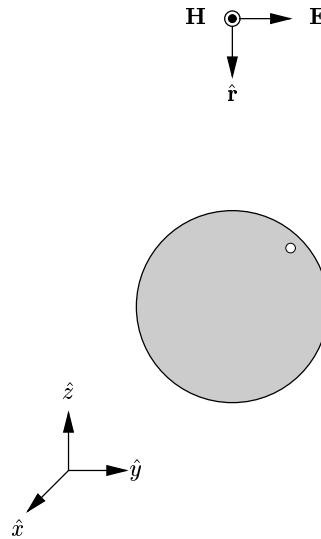
Figure B.1: PEC sphere illuminated by plane wave.

The computed rcs is shown together with the Mie-series solution in figure B.2. It can be seen in the figure that the computed rcs compares well with the Mie-series solution. The difference at higher frequencies starting at around 2 GHz is due to interpolation errors. The mesh used for representing the structure is not fine enough for the frequencies above 2 GHz. This may be improved by using finer mesh, i.e. increasing the number of segments per square wavelength.

B.2.2 Bistatic Radar Cross Section

A sphere covered by a dielectric coat is used with the FEM-MoM formulation, where the electromagnetic properties of the dielectric coat are similar to those of free-space. The thickness of the coat is selected such that only a single layer of tetrahedrons represents the coat in the mesh. The MoM solution was computed using a the same problem configuration as in section B.2.1 with a different radius sphere.

The problem configuration of the coated sphere is shown in figure B.3. The excitation plane wave is a -z directed plane wave with a y directed linearly polarised plane wave. The rcs is computed at $\phi = 0^0$ and $0^0 \leq \theta \leq 180^0$.

The computed results are shown in figure B.4. It can be seen that there is excellent agreement between results obtained using the MoM and FEM-MoM formulations.

B.3 Printed Antenna Impedance

In this section the results for computation of the input impedance of a probe-fed patch antenna in figure B.5 are presented. The input impedance is computed for the following frequency range: 600 MHz to 1300 MHz.
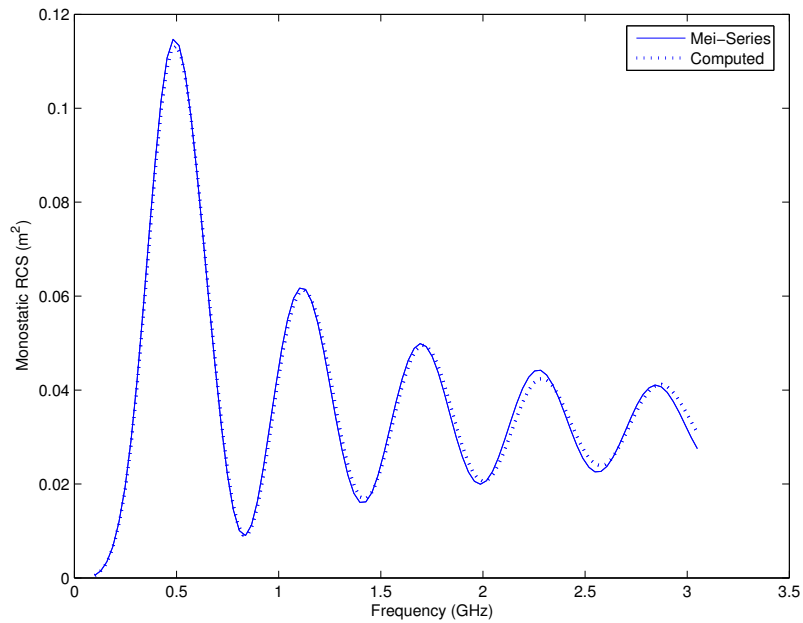
Figure B.2: Monostatic RCS of a PEC sphere.

R1 = 436.7 mm

R2 = 336.7 mm
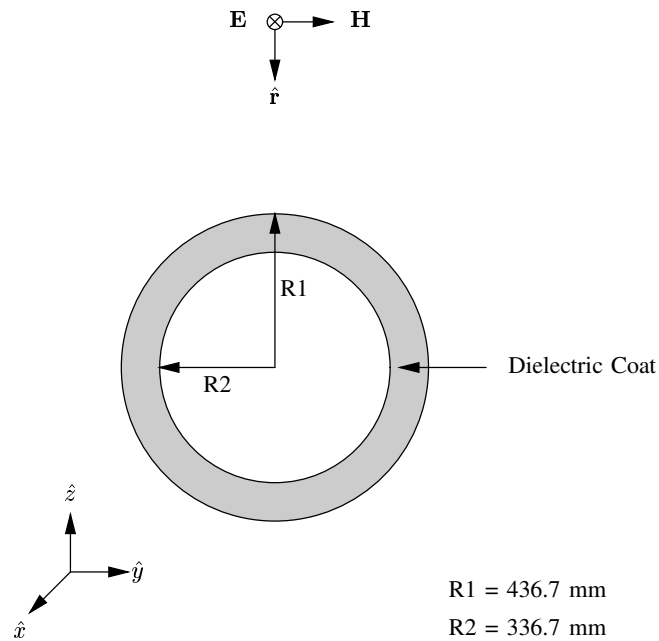
Figure B.3: Coated PEC sphere illuminated by a plane wave.

The computed input reactance and magnitude of the input impedance are shown compared with the results from [2]. Results from [2] are computed using a hybrid FEM-MoM formulation where the FEM formulation is used for the analysis of the substrate and MoM for conducting outside the substrate [3]. Their results compare successfully with measurement, and they were computed using a similar feed model.

The phase shift at around 1250 MHz is due to discretisation errors. A coarse mesh is used to limit the number of unknown because a direct solver is used for solution of the resulting matrices. The results may be
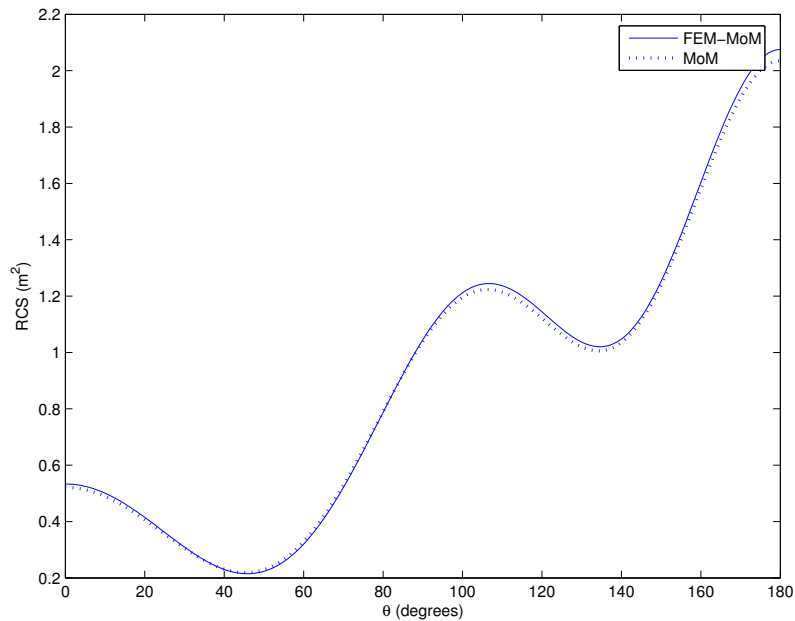
Figure B.4: Bistatic RCS of PEC sphere of radius 0.3367 m for $\phi = 0^0$ and $0^0 \leq \theta 180^0$.
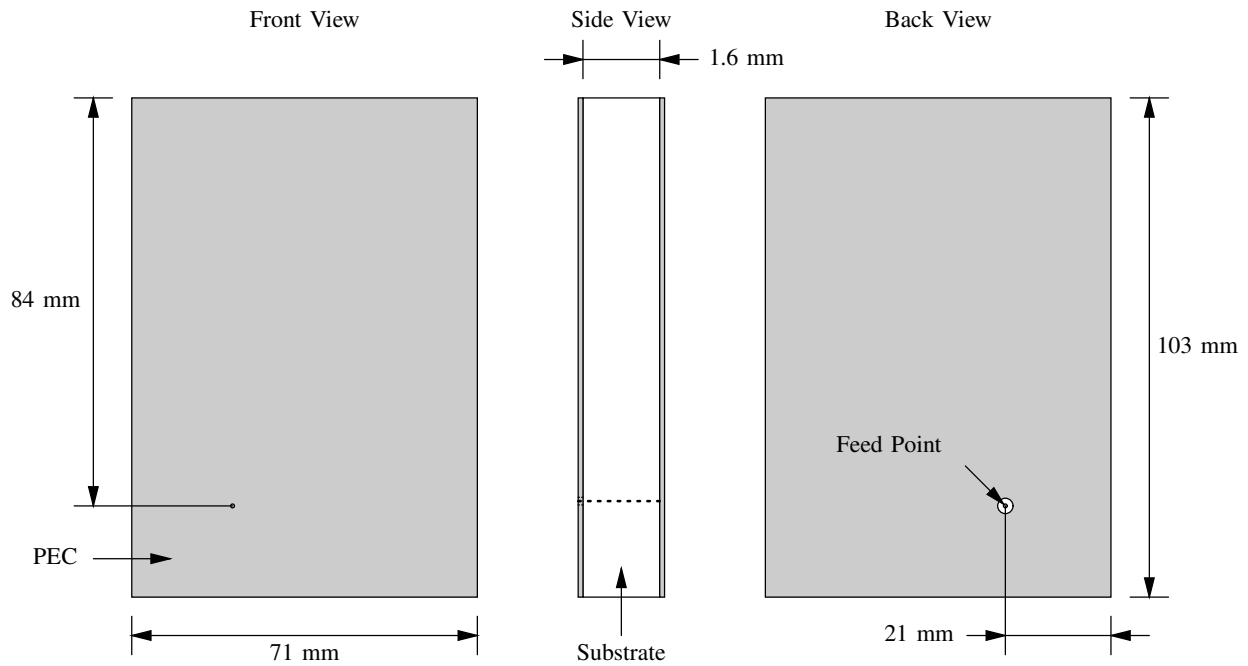
Figure B.5: Geometry of patch antenna structure with dimensions.

improved using a finer discretisation. Improvement of the results with increasing mesh density may be seen in figure B.8, where the reactance values computed with a coarse and fine mesh are compared. The results for the fine mesh are those in figure B.6. The fine mesh is the coarse mesh with an increased tetrahedron density around the feed region. It can be seen that the results improved when a finer mesh was used, as expected [1, Chp. 1].
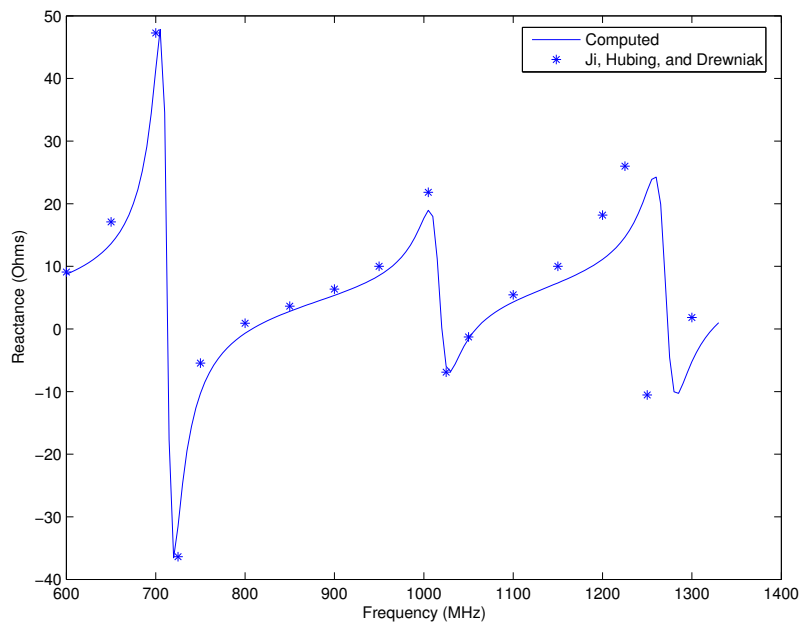
Figure B.6: Reactance of the patch antenna as a function of frequency.
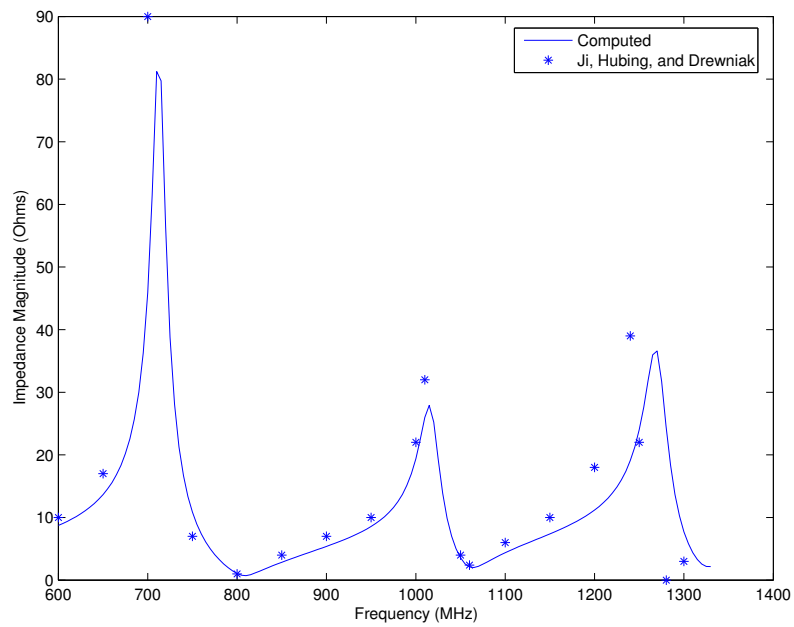
Figure B.7: Impedance magnitude as a function of frequency.
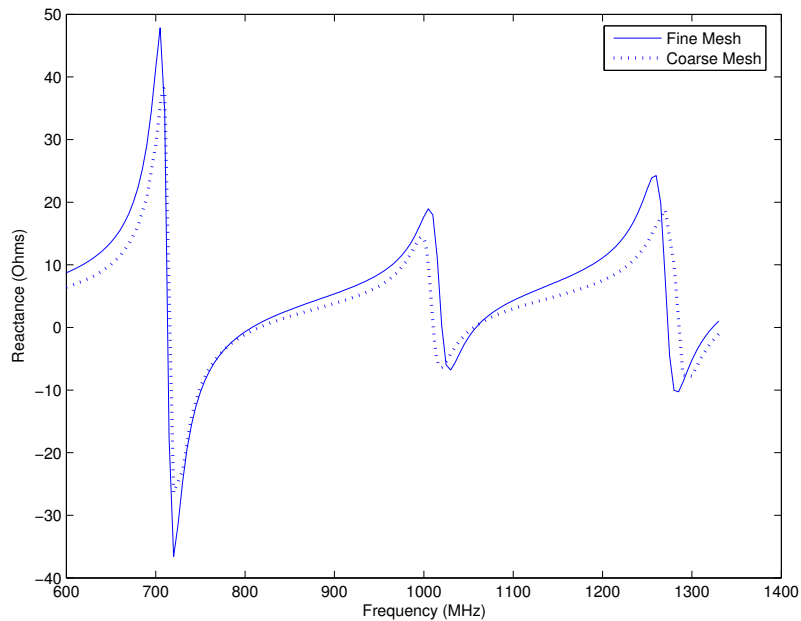
Figure B.8: Results for a coarse and fine mesh of the antenna structure.

B.4 Conclusion

Numerical results computed using the software application for the radar cross section of a PEC (perfect electrical conductor) sphere and the input impedance of a probe-fed printed antenna are presented. Results for the monostatic and bistatic rcs of a sphere, computed using the MoM and FEM-MoM formulations respectively are shown and compared to the Mie-series solution and MoM formulation respectively. Results for the input impedance are shown compared to result from a previous publication.

Excellent agreement is obtained for all the radar cross sections results. The input impedance results compared well with the results from a previous publication but there was a notable phase shift at high frequencies, which is believed to be due to interpolation errors and could be improved using a mesh with more segments per cubic wavelengths.

References

[1] D. B. Davidson. *Computational Electromagnetics for RF and Microwave Engineering*. Cambridge, first ed., 2005.

[2] Y. Ji, T. Hubing, and J. Drewniak. "Finite Element Modelling of Patch Antenna and Cavity Sources." In *IEEE International Symposium on Electromagnetic Compatibility, 2000*, vol. 2, pp. 811–814. 08 2000. ISBN: 0-7803-5677-2.

[3] M. W. Ali, T. H. Hubing, and J. L. Drewniak. "A Hybrid FEM/MOM Technique for Electromagnetic Scattering and Radiation from Dielectric Objects with Attached Wires." *IEEE Transactions on Electromagnetic Compatibility*, vol. 39, no. 04, pp. 304–314, 11 1997.

Appendix C

Reduction of MoM Formulation into a Matrix Equation

C.1 Introduction

MoM (Method of Moments) is a numerical technique for solving boundary-value problems [1]. The boundary-value problem is solved using MoM by reducing the equation that governs it, into a matrix equation that can be solved using a computer [1], [2]. The boundary-value problems that are solved in CEM (Computational Electromagetics) using MoM; are represented as integral equations. These integral equations relate the electric and/or magnetic currents to the electric and/or magnetic fields that they produce.

The reduction of the MoM formulation part of the FEM (Finite Element Method)-MoM formulation used for the analysis of probe-fed printed antennas, to a matrix equation is presented. Derivation of the FEM-MoM formulation is presented in section A.3 of appendix A. The analysis is performed by firstly reducing the problem into two coupled problem, using the surface equivalence principle. The antenna structure is enclosed within a fictitious surface, which does not touch conducting strips of the structure. Then the following problems are defined, using the surface equivalence principle:

1) The first problem involves the region enclosed by the fictitious surface defined above with equivalent electric and magnetic current densities on the fictitious surface and fields set to zero everywhere outside the fictitious surface. Analysis of this problem for the electric field inside volume region is performed using FEM, where the FEM formulation relates the electric field within the volume region and the equivalent electric current density on the fictitious surface.
2) The second problem involves the region outside the fictitious surface also with equivalent electric and magnetic current densities on a fictitious surface, fields everywhere inside the fictitious surface set to zero and the region inside the fictitious replaced by free-space material. Analysis of this problem is performed using MoM, where the MoM formulation gives a relation between equivalent electric and magnetic current densities.

The equivalent current densities in the two problems above are defined using the field boundary conditions, where it is found that the magnitudes of the corresponding current densities are equal but the current densities are in opposite directions. Therefore, the FEM and MoM formulations form two coupled equations, which are used for solution of the electric field inside the fictitious surface and the equivalent electric current density on the fictitious surface. The equivalent magnetic current density on the fictitious surface is obtained from the electric field within the region enclosed by the fictitious surface.

The presentation is structured as follows. The MoM formulation, which is derived in appendix A is presented. Then, an overview of the MoM procedure for solution of the boundary value problems is presented. This is followed by the implementation of the procedure that is discussed in the overview, in the following sections. Lastly the evaluation of the matrix element equations is discussed in detail.

C.2 MoM Formulation

The derivation of the integral equation model (i.e. MoM formulation) for the FEM-MoM formulation is discussed in section A.3.2 of appendix A, and it is given as:

$$
\begin{aligned}
\hat{n} \times \mathbf{E}^{\mathrm{inci}}(\mathbf{r}) - Z\hat{n} \times \hat{n} \times \mathbf{H}^{\mathrm{inci}}(\mathbf{r}) =& Z\hat{n} \times \hat{n} \times \mathcal{K}(\mathbf{J}_{eq}) + Z\hat{n} \times \mathcal{P}(\mathbf{J}_{eq}) - \\
& \hat{n} \times \hat{n} \times \mathcal{P}(\mathbf{M}_{eq}) - \hat{n} \times \mathcal{K}(\mathbf{M}_{eq}) - \\
& \mathbf{M}_{\mathrm{eq}}(\mathbf{r}) - Z\hat{n} \times \mathbf{J}_{\mathrm{eq}}(\mathbf{r})
\end{aligned}
\tag{C.1}
$$

Using the notation from [1] where, $\mathcal{P}$ and $\mathcal{K}$ are defined as:

$$
\mathcal{P}(\mathbf{X}) \quad = \quad jk \oiint_S \left(\mathbf{X}G(\mathbf{r},\mathbf{r}') + \frac{1}{k^2}\nabla' \cdot \mathbf{X}\nabla G(\mathbf{r},\mathbf{r}') \right) \mathrm{d}s'
\tag{C.2}
$$

$$
\mathcal{K}(\mathbf{X}) \quad = \quad \oiint_S \mathbf{X} \times \nabla G(\mathbf{r},\mathbf{r}') \mathrm{d}s'
\tag{C.3}
$$

Where: S is the surface, which encloses the FEM problem domain, r' is the position vector on S, r is the position vector for an arbitrary point in the environment, and $\mathbf{E}^{\mathrm{inci}}$ and $\mathbf{H}^{\mathrm{inci}}$ are the electric and magnetic fields of a plane wave. The plane wave is introduced here because it used extensively for testing the implementation of the formulation. $\mathbf{E}^{\mathrm{inci}}$ and $\mathbf{H}^{\mathrm{inci}}$ are given by:

$$
\mathbf{E}^{\mathrm{inci}} = \mathbf{e}e^{-jk(\hat{p}\cdot\mathbf{r})}
\tag{C.4}
$$

$$
\mathbf{H}^{\mathrm{inci}} = \frac{\hat{p} \times \mathbf{E}^{\mathrm{inci}}}{Z}
\tag{C.5}
$$

Where: $\mathbf{e}$ is the polarisation vector of the electric field for the plane wave, and $\hat{p}$ is the propagation direction.

Equation (C.1) can also be written as:

$$
\begin{aligned}
\hat{n} \times \mathbf{E}^{\mathrm{inci}}(\mathbf{r}) - Z\hat{n} \times \hat{n} \times \mathbf{H}^{\mathrm{inci}}(\mathbf{r}) =& Z\hat{n} \times \hat{n} \times \widetilde{\mathcal{K}}(\mathbf{J}_{eq}) + Z\hat{n} \times \mathcal{P}(\mathbf{J}_{eq}) - \\
& \hat{n} \times \hat{n} \times \mathcal{P}(\mathbf{M}_{eq}) - \hat{n} \times \widetilde{\mathcal{K}}(\mathbf{M}_{eq}) - \\
& \frac{1}{2}\mathbf{M}_{\mathrm{eq}}(\mathbf{r}) - \frac{Z}{2}\hat{n} \times \mathbf{J}_{\mathrm{eq}}(\mathbf{r})
\end{aligned}
\tag{C.6}
$$

Where: $\widetilde{\mathcal{K}}$ is the principal value integral. It is the integral that is defined by $\mathcal{K}$, with the singular point ($\mathbf{r} = \mathbf{r}'$) removed [1, p. 464-465],i.e.:

$$
\widetilde{\mathcal{K}}(\mathbf{X}) = \lim_{e \to 0} \iint_{s-s_e} \mathbf{X} \times \nabla G(\mathbf{r},\mathbf{r}') \mathrm{d}s'
\tag{C.7}
$$

Where: s_e is circular disk centered at $\mathbf{r}$ with radius e.

Equation (C.6) gives the relation between the equivalent electric and magnetic current densities, which are not known. The MoM solution procedure is applied in the following section to reduce the equation into a matrix equation.

C.3 Overview of the Method of Moments

MoM procedure for solving integral equations is presented in [2] and chapter 14 of [1], and most of the details presented in this overview are adopted from [1].

Given a boundary value problem, which is represented by following equation:

$$
\mathcal{L}(f) = g
\tag{C.8}
$$

Where: $\mathcal{L}$ is an integral operator, g is known, f is an unknown function to be determined, and the problem domain is denoted by Ω. The solution of the above equation for f is obtained using MoM as follows.

The unknown function is expanded as a sum of weighted basis functions, i.e.:

$$
f = \sum_{n}^{N} a_n f_n
\tag{C.9}
$$

Where: a_n is the nth weight, f_n is the nth basis function, and N the number of basis functions used for representing f. f_n is known and its choice is dictated by: the problem boundary conditions, and the properties of the operator [2]. a_n is unknown and its definition depends on the choice of f_n. Approximation of f as is done in equation (C.9) is to reduce the problem to that of determining numbers instead of a function whose form can be anything.

Substituting equation (C.9) into equation (C.8) results in an equation with N unknowns, i.e.:

$$\sum_{n=1}^{N} a_n \mathcal{L}(f_n) = g \tag{C.10}$$

It is a well known fact that: N conditions or equations are required in order to obtain a unique solution for an equation with N unknowns. Therefore, N equations are required for solution of a_n values. The required equations are generated by taking the inner product of equation (C.10) with a N functions w_m, which are in the range of the operator ($\mathcal{L}$); i.e.:

$$\sum_{m}^{N} \sum_{n}^{N} \langle w_m, \mathcal{L}(f_n) \rangle = \sum_{m}^{N} \langle w_m, g \rangle \tag{C.11}$$

Where $\langle h, r \rangle$ is the inner product between h and r over an arbitrary domain S. w_m are called testing or weighting functions [1]. Equation (C.11) is then written in matrix form as follows:

$$[Z]\{I\} = \{V\} \tag{C.12}$$

Where: Z is a square matrix, I and V are column vectors. These variables are given by:

$$Z_{mn} = \langle w_m, \mathcal{L}f_n \rangle \tag{C.13}$$
$$V_m = \langle w_m, g \rangle \tag{C.14}$$
$$I_n = a_n \tag{C.15}$$

If Z is not singular, the unknown weights can be determined by inverting Z and multiplying it with V, i.e.:

$$\{I\} = [Z]^{-1}\{V\} \tag{C.16}$$

Then the solution of equation (C.8) is calculated using equation (C.9).

Following the above presentation and [1, Chapter 14]; the steps that are involved in reducing an MoM formulation into a matrix equations are:

- Selection of the basis and testing functions.
- Formulation of the matrix equation by taking the inner product of the formulation with the set of testing functions.

C.4 Basis and Testing Functions

The choice of the basis functions for representing the unknown electric and magnetic current densities is presented together with the choice of testing function used for the discretisation of the integral equation.

C.4.1 Basis Functions

The unknown electric and magnetic current densities of equation (C.6) are approximated using sub-domain basis functions. Sub-domain basis functions are basis function that are defined only over a part of the problem domain and their use requires that the problem domain be divided into simpler geometric shapes [1]. Therefore, the surface that supports the current distributions is divided into triangles. Triangles are used for this purpose because of their ability to conform to any boundary [3].

The RWG (Rao-Wilton-Glisson) function is used as the basis function for both electric and magnetic current densities. This function is used in the CEM (computational electromagnetics) community for representing
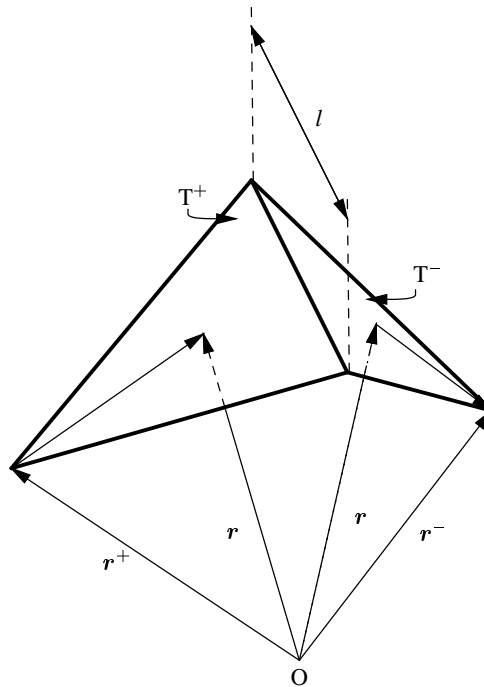
Figure C.1: Triangles with parameters related to the definition of the RWG basis function [3].

current distributions over triangular domains. It is named after: S.M. Rao, D.R. Wilton, and A.W. Glisson, who introduced it in 1982 [4]. It is defined with reference to figure C.1 as [3]:

$$\mathbf{f}_n(\mathbf{r}) = \begin{cases} \dfrac{l_n}{2A_n^+}(\mathbf{r} - \mathbf{r}_n^+), & \mathbf{r} \in T_n^+ \\ \dfrac{l_n}{2A_n^-}(\mathbf{r} - \mathbf{r}_n^-), & \mathbf{r} \in T_n^- \\ \mathbf{0}, & \text{otherwise} \end{cases} \tag{C.17}$$

Where:

- A_n^+ and A_n^-, are the areas of triangles T^+ and T^- respectively.
- $\mathbf{r}_n^+$ and $\mathbf{r}_n^-$, are the vectors from the origin of the reference coordinate system to the nodes in triangles T^+ and T^- that are opposite the shared edges.
- $\mathbf{r}$ is vector from the origin of the reference coordinate system to an arbitrary point on either T^+ or T^-.
- The subscript n is a variable used to identify the shared edge.

The RWG function is defined with reference to an edge that is shared by two triangles. Therefore, only those edges of the triangle that are shared with another triangle will have an associated RWG basis function. It guarantees continuity of the normal component of the current density on the shared edge [3]. The weights (a_n) are defined as the magnitude of the normal component of the current density on the edge that the function is defined relative to.

Another property of the RWG function, which makes it particularly suited for use with the FEM-MoM formulation, is that it is related to the basis functions that are used for approximating the electric field in a triangular domain (see section D.5 of appendix D). The relation is given by [1], [4]:

$$\mathbf{RWG} = \hat{n} \times \mathbf{NED} \tag{C.18}$$

Where: $\mathbf{NED}$ denotes the basis functions that are used for representing electric and magnetic field over triangular domain in FEM. The relation of equation (C.18), agrees with the definition of the equivalent electric and magnetic current densities, which are given by:

$$\mathbf{J}_{eq}(\mathbf{r}) = \hat{n} \times \mathbf{H}(\mathbf{r}) \tag{C.19}$$

$$\mathbf{M}_{eq}(\mathbf{r}) = -\hat{n} \times \mathbf{E}(\mathbf{r}) \tag{C.20}$$

Where: $\mathbf{r}$ is the position vector on the fictitious surface of the equivalent problem that is formulated using MoM. The weights when using **NED** for representing the electric and magnetic fields over triangular domains are also defined relative to the triangle edges. Therefore, the relations in equations (C.19) and (C.20) are enforced by equating the weights.

C.4.2 Testing Functions

Two different sets of basis functions are used for discretising the integral equation of equation (C.6). Equation (C.6) is called a CFIE (Combined Field Integral Equation), which is defined as [5]:

$$\alpha\text{EFIE} + Z(1 - \alpha)\hat{n} \times \text{MFIE}$$

Where: EFIE and MFIE are the acronyms for Electric Field Integral Equation and Magnetic Field Integral Equation respectively, and α is a number between one and zero. The value of α is chosen equal to 0.5 in the CFIE of equation (C.6). This choice is in-line with the argument in [1, p. 465] that choosing $\alpha = 0.5$ results in the optimum combination of the EFIE and MFIE.

The testing functions are chosen as the RWG $+ \hat{n} \times$ RWG for the EFIE part of the integral equation and $\hat{n} \times \mathbf{RWG}$ for the MFIE part. The EFIE part of the CFIE in equation (C.6) on the right hand side of the equal sign is given by the: second, fourth, and fifth terms, and the remaining terms belong to the MFIE. This choice is shown to give the most accurate results in [6].

C.5 Formulation of System Matrices

The matrix equation required for solution of equation (C.6) is of the form:

$$[Z^{\mathbf{M}_{\text{eq}}}]\{I^{\mathbf{M}_{\text{eq}}}\} + [Z^{\mathbf{J}_{\text{eq}}}]\{I^{\mathbf{J}_{\text{eq}}}\} = \{V\} \tag{C.21}$$

If the RWG basis function is denoted by $\mathbf{f}$, then equation (C.6) is written as:

$$\hat{n} \times \mathbf{E}^{\text{inci}}(\mathbf{r}) - Z\hat{n} \times \hat{n} \times \mathbf{H}^{\text{inci}}(\mathbf{r}) =$$
$$\sum_{e=1}^{N_e}\sum_{n}^{N} I_n^{\mathbf{J}_{\text{eq}}} Z\left(\hat{n} \times \hat{n} \times \widetilde{\mathcal{K}}(\mathbf{f}_n) + \hat{n} \times \mathcal{P}(\mathbf{f}_n) - \frac{1}{2}\hat{n} \times \mathbf{f}_n(\mathbf{r})\right) -$$
$$\sum_{e=1}^{N_e}\sum_{n}^{N} I_n^{\mathbf{M}_{\text{eq}}}\left(\hat{n} \times \hat{n} \times \mathcal{P}(\mathbf{f}_n) + \hat{n} \times \widetilde{\mathcal{K}}(\mathbf{f}_n) + \frac{1}{2}\mathbf{f}_n(\mathbf{r})\right) \qquad \text{for edge } n \text{ in } S_e \tag{C.22}$$

Where: S_e is e^{th} triangle, which supports the RWG functions, and N_e is the total number of triangles that the enclosing boundary of the FEM problem region is divided into. $Z^{\mathbf{M}_{\text{eq}}}$, $Z^{\mathbf{J}_{\text{eq}}}$, and V are given by the following equation, using the testing functions from the previous section.

$$Z_{mn}^{\mathbf{J}_{\text{eq}}} = \sum_{e}^{N_e}\sum_{m}^{N}\sum_{n}^{N} Z\left(\langle\hat{n} \times \mathbf{f}_m, \hat{n} \times \hat{n} \times \widetilde{\mathcal{K}}(\mathbf{f}_n) - \frac{1}{2}\hat{n} \times \mathbf{f}_n\rangle + \right.$$
$$\left. \langle\mathbf{f}_m + \hat{n} \times \mathbf{f}_m, \hat{n} \times \mathcal{P}(\mathbf{f}_n)\rangle\right) \tag{C.23}$$

$$Z_{mn}^{\mathbf{M}_{\text{eq}}} = \sum_{e}^{N_e}\sum_{m}^{N}\sum_{n}^{N}\left(\langle\mathbf{f}_m + \hat{n} \times \mathbf{f}_m, \hat{n} \times \widetilde{\mathcal{K}}(\mathbf{f}_n) + \hat{n} \times \frac{1}{2}\mathbf{f}_n\rangle + \right.$$
$$\left. \langle\hat{n} \times \mathbf{f}_m, \hat{n} \times \hat{n} \times \mathcal{P}(\mathbf{f}_n)\rangle\right) \tag{C.24}$$

$$V_m = \sum_{e}^{N_e}\sum_{m}^{N}\left(\langle\mathbf{f}_m + \hat{n} \times \mathbf{f}_m, \hat{n} \times \mathbf{E}^{\text{inci}}\rangle - \langle\hat{n} \times \mathbf{f}_m, Z\hat{n} \times \hat{n} \times \mathbf{H}^{\text{inci}}\rangle\right) \tag{C.25}$$

The equations above are valid for edges m and n within triangle e. The inner product is defined as:

$$\langle\mathbf{h}, \mathbf{c}\rangle = \iint_S \mathbf{h}^* \cdot \mathbf{c}\,dS \tag{C.26}$$

Where: $\mathbf{h}$ and $\mathbf{c}$ are arbitrary vector variables, * denotes complex conjugation, and S is the domain where the inner product is evaluated.

The element of $Z_{mn}^{\mathbf{M}_{eq}}$, $Z_{mn}^{\mathbf{J}_{eq}}$, and V_m require the evaluation of the following integrals with the testing functions equal to $\mathbf{f}$ and $\hat{n} \times \mathbf{f}$:

$$I1_{mn} = \iint_{s_m} \mathbf{t}_m(\mathbf{r}) \cdot \iint_{s_n} \nabla G(\mathbf{r}, \mathbf{r}') \nabla'_s \cdot \mathbf{f}_n(\mathbf{r}') \mathrm{d}s'_n \mathrm{d}s_m \tag{C.27}$$

$$I2_{mn} = \iint_{s_m} \mathbf{t}_m(\mathbf{r}) \cdot \iint_{s_n} G(\mathbf{r}, \mathbf{r}') \mathbf{f}_n(\mathbf{r}') \mathrm{d}s'_n \mathrm{d}s_m \tag{C.28}$$

$$I3_{mn} = \iint_{s_m} \mathbf{t}_m(\mathbf{r}) \cdot \iint_{s_n} \nabla G(\mathbf{r}, \mathbf{r}') \times \mathbf{f}_n(\mathbf{r}') \mathrm{d}s'_n \mathrm{d}s_m \tag{C.29}$$

$$I4_m(\mathbf{C}) = \iint_{s_m} \mathbf{t}_m(\mathbf{r}) \cdot \mathbf{C}(\mathbf{r}) \mathrm{d}s'_n \mathrm{d}s_m \tag{C.30}$$

$$I5_m = \iint_{s_m} \mathbf{t}_m(\mathbf{r}) \cdot \iint_{s_n} \mathbf{f}(\mathbf{r}') \mathrm{d}s'_n \mathrm{d}s_m \tag{C.31}$$

Where:

- $\mathbf{t}_m$ denotes the testing functions.
- $\mathbf{f}_n$ denotes the RWG basis functions which is used for representing the magnetic and electric current densities.
- s_m is the triangular domain, which $\mathbf{t}_m$.
- s_n is the triangular domain, which $\mathbf{f}_n$.
- $\mathbf{C}$ is a place holder for either $\mathbf{E}^{\mathrm{inc}}$ or $\mathbf{H}^{\mathrm{inc}}$.

The above integrals are performed over a triangular domains, because the RWG basis functions are non-zero only within two triangular domains (see equation (C.17)).

$Z_{mn}^{\mathbf{M}_{eq}}$, $Z_{mn}^{\mathbf{J}_{eq}}$, and V_m are then given by:

$$Z_{mn}^{\mathbf{J}_{eq}} = \sum_{n}^{N} \sum_{m}^{N} Z \left(jk(I2_{mn}^{\mathrm{RWG}} - I2_{mn}^{\mathrm{nRWG}}) + \frac{j}{k}(I1_{mn}^{\mathrm{RWG}} - I1_{mn}^{\mathrm{nRWG}}) - \frac{1}{2} I5_{mn}^{\mathrm{RWG}} - I3_{mn}^{n\,RWG} \right) \tag{C.32}$$

$$Z_{mn}^{\mathbf{M}_{eq}} = \sum_{n}^{N} \sum_{m}^{N} \left(\frac{1}{2}(I5_{mn}^{\mathrm{nRWG}} - I5_{mn}^{\mathrm{RWG}}) + (I3_{mn}^{\mathrm{nRWG}} - I3_{mn}^{\mathrm{RWG}}) + \frac{j}{k} I1_{mn}^{\mathrm{nRWG}} + jk I2_{mn}^{\mathrm{nRWG}} \right) \tag{C.33}$$

$$V_{mn} = \sum_{m=1}^{N} I4_m^{\mathrm{RWG}}(\mathbf{E}^i) + I4_m^{\mathrm{nRWG}}(\mathbf{E}^{\mathrm{inc}}) + Z I4_m^{\mathrm{RWG}}(\mathbf{H}^{\mathrm{inc}}) \tag{C.34}$$

C.6 Evaluation of the Integrals

The integrals of equations (C.27), (C.28), (C.29), (C.30), and (C.31); are evaluated numerically. This is because there is no known analytical solution for the integrals of equations (C.27), (C.28), and (C.29). Integrals of equations (C.30) and (C.31) can be integrated analytically but are integrated numerically as well.

The integrands of the inner integrals of equations (C.27), (C.28), and (C.29); are singular. The singularity results from the Green's function (i.e. $G(\mathbf{r}, \mathbf{r}')$) when the source and observation points are equal (i.e. $\mathbf{r} = \mathbf{r}'$). This occurs when the triangles where $\mathbf{f}_n$ is defined is same as the one where $\mathbf{t}_n$ is defined, i.e., $s_m = s_n$. Numerical integration methods do not give accurate results when the integration domain contains a singularity [5], or when the integrand is nearly singular, which occurs when s_m and s_n are near each other. For the two conditions just described, the inner integrals are performed by replacing the Green's function with the following:

$$G(\mathbf{r}, \mathbf{r}') = \left(G(\mathbf{r}, \mathbf{r}') - \frac{1}{4\pi|\mathbf{r} - \mathbf{r}'|} + \frac{k^2}{8\pi}|\mathbf{r} - \mathbf{r}'| \right) + \frac{1}{4\pi|\mathbf{r} - \mathbf{r}'|} - \frac{k^2}{8\pi}|\mathbf{r} - \mathbf{r}'| \tag{C.35}$$

The term in parenthesis, in equation (C.35) is the Green's function minus two terms. Subtraction of the two terms from the Green's function results in a function, which is not singular and has a continuous derivative

when $\mathbf{r} = \mathbf{r}'$ [5]. Therefore, the inner integrals involving the term in parenthesis are evaluated numerically. The fourth term in equation (C.35) is singular and the inner integrals, which involve it, are evaluated analytically. The fifth term is not singular, but the inner integrals, which involve it are also evaluated analytically since their integrals are known.

The evaluation of integrals I1, I2, and I3 for singular and nearly singular conditions is discussed in the following sections.

C.6.1 Evaluation of I1

I1 has a singularity of order $1/|\mathbf{r} - \mathbf{r}'|^2$. This is caused by the gradient operation on the Green's function.

C.6.1.1 Testing with RWG Function

When $\mathbf{t}_m = \mathbf{f}_m$ equation (C.27) becomes:

$$\text{I1}_{mn}^{\text{RWG}} = \iint_{s_m} \mathbf{f}_m(\mathbf{r}) \cdot \nabla \iint_{s_n} G(\mathbf{r}, \mathbf{r}') \nabla'_s \cdot \mathbf{f}_n(\mathbf{r}') \mathrm{d}s' \mathrm{d}s \tag{C.36}$$

Where: $\mathbf{r}'$ and $\mathbf{r}$ are the position vectors on s_n and s_m respectively. The order of the singularity is reduced to $1/|\mathbf{r} - \mathbf{r}'|$ by moving the gradient operator from the Green's function and onto the testing function [3]. This is done as follows [3].

Using the following vector identity:

$$\nabla \cdot (a\mathbf{b}) = a\nabla \cdot \mathbf{b} + \mathbf{b} \cdot \nabla a \tag{C.37}$$

With:

$$a = \iint_{s_n} G(\mathbf{r}, \mathbf{r}') \nabla'_s \cdot \mathbf{f}_n(\mathbf{r}') \mathrm{d}s' \tag{C.38}$$

$$\mathbf{b} = \mathbf{f}_m(\mathbf{r}) \tag{C.39}$$

Equation (C.36), becomes:

$$\text{I1}_{mn}^{\text{RWG}} = \iint_{s_m} \nabla \cdot \left(\mathbf{f}_m(\mathbf{r}) \iint_{s_n} G(\mathbf{r}, \mathbf{r}') \nabla'_s \cdot \mathbf{f}_n(\mathbf{r}') \mathrm{d}s' \right) \mathrm{d}s - \\ \iint_{s_m} \nabla \cdot \mathbf{f}_m(\mathbf{r}) \cdot \iint_{s_n} G(\mathbf{r}, \mathbf{r}') \nabla'_s \cdot \mathbf{f}_n(\mathbf{r}') \mathrm{d}s' \mathrm{d}s \tag{C.40}$$

The gradient operator is then decomposed into the surface and normal gradient operators, i.e.:

$$\nabla = \nabla_s + \nabla_n \tag{C.41}$$

The meanings of the surface and normal gradient operators can be inferred from the following, equations:

$$\nabla_n \phi = (\nabla \phi \cdot \hat{n}) \hat{n} \tag{C.42}$$

$$\nabla_s \phi = \nabla \phi - \nabla_n \phi \tag{C.43}$$

Where: ϕ is an arbitrary scalar variable. Equation (C.40) then becomes:

$$\text{I1}_{mn}^{\text{RWG}} = \iint_{s_m} \nabla_s \cdot \left(\mathbf{f}_m(\mathbf{r}) \iint_{s_n} G(\mathbf{r}, \mathbf{r}') \nabla'_s \cdot \mathbf{f}_n(\mathbf{r}') \mathrm{d}s' \right) \mathrm{d}s - \\ \iint_{s_m} \nabla_s \cdot \mathbf{f}_m(\mathbf{r}) \cdot \iint_{s_n} G(\mathbf{r}, \mathbf{r}') \nabla'_s \cdot \mathbf{f}_n(\mathbf{r}') \mathrm{d}s' \mathrm{d}s \tag{C.44}$$

This is because: $\mathbf{f}_m$ and $\mathbf{f}_n$ do not have components normal on s_m and s_n respectively, i.e.:

$$\nabla_n \cdot \mathbf{f}_m = \nabla_n \cdot \mathbf{f}_n = 0 \tag{C.45}$$

Using the surface divergence theorem, i.e. [1]:

$$\iint_s \nabla_s \cdot \mathbf{g} \mathrm{d}s = \oint_C \hat{m} \cdot \mathbf{g} \mathrm{d}C \tag{C.46}$$

Where: $\hat{m}$ is the outward directed unit normal to the contour C. Equation (C.44), then becomes:

$$I1_{mn}^{\text{RWG}} = \oint_C \hat{m} \cdot \mathbf{f}_m(\mathbf{r}) \iint_{s_n} G(\mathbf{r},\mathbf{r}')\nabla'_s \cdot \mathbf{f}_n(\mathbf{r}')\,ds'\,dC - $$
$$\iint_{s_m} \nabla_s \cdot \mathbf{f}_m(\mathbf{r}) \cdot \iint_{s_n} G(\mathbf{r},\mathbf{r}')\nabla'_s \cdot \mathbf{f}_n(\mathbf{r}')\,ds'\,ds \tag{C.47}$$

Since contour C is a triangle, $\hat{m}$ is defined by:

$$\hat{m} = \sum_{i=1}^{3} \hat{m}_i \tag{C.48}$$

Where: $\hat{m}_i$ is the unit normal to side i of the triangle. The RWG function has a normal component only on the edge that it is associated with (see section C.4.1) and is parallel to the other edges. Therefore:

$$\sum_i^3 \hat{m}_i \cdot \mathbf{f}_m(\mathbf{r}') = \hat{m}_{i'} \cdot \mathbf{f}_m(\mathbf{r}') \tag{C.49}$$

Where: i' is the index of the edge of the triangle that the RWG function is associated with. Substituting (C.49) in equation (C.47) results in:

$$I1_{mn}^{\text{RWG}} = \int_C \hat{m}_{i'} \cdot \mathbf{f}_m\mathbf{r}) \iint_{s_n} G(\mathbf{r},\mathbf{r}')\nabla'_s \cdot \mathbf{f}_n\mathbf{r}')\,ds'\,dC - $$
$$\iint_{s_m} \nabla_s \cdot \mathbf{f}_m(\mathbf{r}) \cdot \iint_{s_n} G(\mathbf{r},\mathbf{r}')\nabla'_s \cdot \mathbf{f}_n\mathbf{r}')\,ds'\,ds \tag{C.50}$$

Replacing $\mathbf{f}_m(\mathbf{r})$ with the definition of the RWG function (equation (C.17)) gives:

$$I1_{mn}^{\text{RWG}} = \frac{l_m}{A_m^+} \int_{C+} \hat{m}_{i'} \cdot (\mathbf{r} - \mathbf{p}^+) \iint_{s_n} G(\mathbf{r},\mathbf{r}')\nabla'_s \cdot \mathbf{f}_n(\mathbf{r}')\,ds'\,dC - $$
$$\frac{l_m}{A_m^-} \int_{C-} \hat{m}_{i'} \cdot (\mathbf{p}^- - \mathbf{r}) \iint_{s_n} G(\mathbf{r},\mathbf{r}')\nabla'_s \cdot \mathbf{f}_n(\mathbf{r}')\,ds'\,dC + \tag{C.51}$$
$$\iint_{s_m} \nabla_s \cdot \mathbf{f}_m(\mathbf{r}) \cdot \iint_{s_n} G(\mathbf{r},\mathbf{r}')\nabla'_s \cdot \mathbf{f}_n\mathbf{r}')\,ds'\,ds$$

Where, it can be noticed that:

$$\frac{l_m}{2A_m^+}\hat{m}_{i'} \cdot (\mathbf{r} - \mathbf{p}^+) = \frac{l_m}{2A_m^-}\hat{m}_{i'} \cdot (\mathbf{p}^- - \mathbf{r}) = 1 \tag{C.52}$$

This is because the area of a triangle is equal to the length of side 1 (one of the sides of the triangle) multiplied by perpendicular distance from the node opposite side 1 to a point on side 1. The perpendicular distance is equal to $\hat{m}_{i'} \cdot (\mathbf{r} - \mathbf{p}^+)$ and $\hat{m}_{i'} \cdot (\mathbf{r} - \mathbf{p}^-)$ in the negative and positive triangles respectively; in-line with the definition of the RWG function. $\mathbf{p}^-$ and $\mathbf{p}^+$ that are opposite the shared edge in the negative and positive triangles respectively. As a results, the first two terms in equation (C.51) cancel and the equation reduces to:

$$I1_{mn}^{\text{RWG}} = -\iint_{s_m} \nabla_s \cdot \mathbf{f}_m(\mathbf{r}) \cdot \iint_{s_n} G(\mathbf{r},\mathbf{r}')\nabla'_s \cdot \mathbf{f}_n(\mathbf{r}')\,ds'\,ds \tag{C.53}$$

$$= -\frac{l_m l_n}{A_m A_n} \iint_{s_m} \iint_{s_n} G(\mathbf{r},\mathbf{r}')\,ds'\,ds \tag{C.54}$$

At this stage, the Green's function is substituted with that of equation (C.35), and the result of the substitution is:

$$I1_{mn}^{\text{RWG}} = -\frac{l_m l_n}{A_m A_n} \iint_{s_m} \iint_{s_n} \left(\frac{e^{-jk|\mathbf{r}-\mathbf{r}'|}}{4\pi|\mathbf{r}-\mathbf{r}'|} - \frac{1}{4\pi|\mathbf{r}-\mathbf{r}'|} + \frac{k^2}{8\pi}|\mathbf{r}-\mathbf{r}'| \right) ds'\,ds$$
$$-\frac{l_m l_n}{4\pi A_m A_n} \iint_{s_m} \iint_{s_n} \frac{1}{|\mathbf{r}-\mathbf{r}'|} ds'\,ds + \frac{l_m l_n k^2}{8\pi A_m A_n} \iint_{s_m} \iint_{s_n} |\mathbf{r}-\mathbf{r}'|\,ds'\,ds \tag{C.55}$$

The inner integrals of the second and third integrals in equation (C.53), are given by [5]:

$$\iint_{s_n} \frac{1}{|\mathbf{r}-\mathbf{r}'|}\,ds' = \sum_{i=1}^{3} \left(t_i^0 I_i^{-1} - |N_{\text{obs}}|\beta_i \right) \tag{C.56}$$

$$\iint_{s_n} |\mathbf{r}-\mathbf{r}'|\,ds' = \frac{N_{\text{obs}}^2}{3} \iint_{s_n} \frac{1}{|\mathbf{r}-\mathbf{r}'|}\,ds' + \frac{1}{3}\sum_{i=1}^{3} t_i^0 I_i^1 \tag{C.57}$$
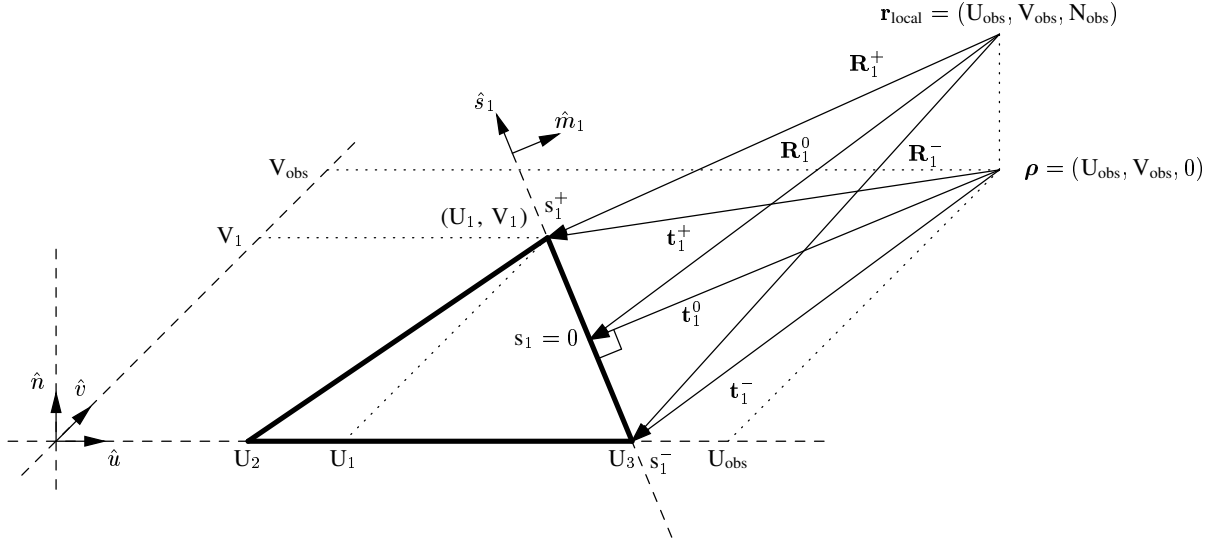
Figure C.2: Triangular domain with definition of variables used for evaluation of the integrals.

Where:

$$I_i^n = \frac{1}{n+1}\left(s_i^+(R_i^+)^n - s_i^-(R_i^-)^n + nR_i^{0\,2}I_i^{n-2}\right) \qquad n = 1, 3, 5, \ldots \tag{C.58}$$

$$\beta_i = \arctan\left(\frac{t_i^0 s_i^+}{(R_i^0)^2 + |N_{\text{obs}}|R_i^+}\right) - \arctan\left(\frac{t_i^0 s_i^-}{(R_i^0)^2 + |N_{\text{obs}}|R_i^-}\right) \tag{C.59}$$

$$I_i^{-1} = \ln\left(\frac{R_i^+ + s_i^+}{R_i^- + s_i^-}\right) \tag{C.60}$$

The variables used in the equations above are defined in figure C.2.

C.6.1.2 Testing with $\hat{n} \times$RWG Function

When $\mathbf{t}_m = \hat{n} \times \mathbf{f}_m$ equation (C.27) becomes:

$$\text{II}_{mn}^{\text{nRWG}} = \iint_{s_m} \hat{n} \times \mathbf{f}_m(\mathbf{r}) \cdot \nabla \iint_{s_n} G(\mathbf{r}, \mathbf{r}')\nabla_s' \cdot \mathbf{f}_n(\mathbf{r}')\,\mathrm{d}s'\,\mathrm{d}s \tag{C.61}$$

Firstly the order of the singularity is reduced. The procedure for doing this is discussed in [5] and is repeated here in a more detailed manner. Using equation (C.37), with:

$$a = \iint_{s_n} G(\mathbf{r}, \mathbf{r}')\nabla_s' \cdot \mathbf{f}_m(\mathbf{r}')\,\mathrm{d}s'\,\mathrm{d}s \tag{C.62}$$

$$\mathbf{b} = \hat{n} \times \mathbf{f}_m(\mathbf{r}) \tag{C.63}$$

Equation (C.61), becomes:

$$\text{II}_{mn}^{\text{nRWG}} = \iint_{s_m} \nabla_s \cdot \left(\hat{n} \times \mathbf{f}_m(\mathbf{r}) \iint_{s_n} G(\mathbf{r}, \mathbf{r}')\nabla_s' \cdot \mathbf{f}_n(\mathbf{r}')\,\mathrm{d}s'\right)\mathrm{d}s -$$
$$\iint_{s_n} \nabla_s \cdot (\hat{n} \times \mathbf{f}_m(\mathbf{r})) \iint_{s_n} G(\mathbf{r}, \mathbf{r}')\nabla_s' \cdot \mathbf{f}_n(\mathbf{r}')\,\mathrm{d}s'\,\mathrm{d}s \tag{C.64}$$

However:

$$\nabla_s \cdot (\hat{n} \times \mathbf{f}_m(\mathbf{r})) = (\nabla_s \times \hat{n}) \cdot \mathbf{f}_m(\mathbf{r}) - \hat{n} \cdot (\nabla_s' \times \mathbf{f}(\mathbf{r})) = 0 \tag{C.65}$$

This is because:

$$\nabla_s \times \mathbf{f}_m(\mathbf{r}) = 0 \tag{C.66}$$

Therefore:

$$\text{II}_{mn}^{\text{nRWG}} = \iint_{s_m} \nabla_s \cdot \left(\hat{n} \times \mathbf{f}_m(\mathbf{r}) \iint_{s_n} G(\mathbf{r}, \mathbf{r}')\nabla_s' \cdot \mathbf{f}_n(\mathbf{r}')\,\mathrm{d}s'\right)\mathrm{d}s \tag{C.67}$$

And, using the surface divergence theorem (equation (C.46)):

$$I1_{mn}^{nRWG} = \int_{\partial s_m} \hat{m}(\mathbf{r}) \cdot \left(\hat{n} \times \mathbf{f}_m(\mathbf{r}) \iint_{s_n} G(\mathbf{r},\mathbf{r}')\nabla'_s \cdot \mathbf{f}_n(\mathbf{r}')\mathrm{d}s' \right) \mathrm{d}l \tag{C.68}$$

$$= \nabla'_s \cdot \mathbf{f}_n(\mathbf{r}') \int_{\partial s_m} \hat{m}(\mathbf{r}) \cdot \left(\hat{n} \times \mathbf{f}_m(\mathbf{r}) \iint_{s_n} G(\mathbf{r},\mathbf{r}')\mathrm{d}s' \right) \mathrm{d}l \tag{C.69}$$

$$= \frac{l_m l_n}{2 A_n A_m} \sum_{i=1}^{3} \int_{\partial s_m} \hat{m}_i(\mathbf{r}) \cdot \left(\hat{n} \times (\mathbf{r} - \mathbf{p}) \iint_{s_n} G(\mathbf{r},\mathbf{r}')\mathrm{d}s' \right) \mathrm{d}l \tag{C.70}$$

It is assumed in equation (C.70), that the outer surface integral is performed over the positive testing triangle. The inner integral of equation (C.70) is similar to that of equation (C.53) and is evaluated using a similar procedure.

C.6.2 Evaluation of I2

The singularity of I2 is of order $1/|\mathbf{r} - \mathbf{r}'|$ and is not simplified further like I1. Since no further simplification are made the integral is treated the same when testing with RWG and $\hat{n} \times$ RWG functions.

Substituting the definition of $G(\mathbf{r},\mathbf{r}')$ in equation (C.35), into equation (C.28) results in:

$$I2_{mn} = \iint_{s_m} \mathbf{t}_m(\mathbf{r}) \cdot \iint_{s_n} \mathbf{f}_n(\mathbf{r}') \left(\frac{e^{-jk|\mathbf{r}-\mathbf{r}'|}}{4\pi|\mathbf{r}-\mathbf{r}'|} - \frac{1}{4\pi|\mathbf{r}-\mathbf{r}'|} + \frac{k^2}{8\pi}|\mathbf{r}-\mathbf{r}'| \right) \mathrm{d}s'_n \mathrm{d}s_m +$$
$$\frac{1}{4\pi} \iint_{s_m} \mathbf{t}_m(\mathbf{r}) \cdot \iint_{s_n} \mathbf{f}_n(\mathbf{r}') \frac{1}{|\mathbf{r}-\mathbf{r}'|}\mathrm{d}s'_n \mathrm{d}s_m - \tag{C.71}$$
$$\frac{k^2}{8\pi} \iint_{s_m} \mathbf{t}_m(\mathbf{r}) \cdot \iint_{s_n} \mathbf{f}_n(\mathbf{r}')|\mathbf{r}-\mathbf{r}'|\mathrm{d}s'_n \mathrm{d}s_m$$

Replacing the RWG basis function with its definition from (C.17), results in:

$$I2_{mn} = \iint_{s_m} \mathbf{t}_m(\mathbf{r}) \cdot \iint_{s_n} \mathbf{f}_n(\mathbf{r}') \left(\frac{e^{-jk|\mathbf{r}-\mathbf{r}'|}}{4\pi|\mathbf{r}-\mathbf{r}'|} - \frac{1}{4\pi|\mathbf{r}-\mathbf{r}'|} + \frac{k^2}{8\pi}|\mathbf{r}-\mathbf{r}'| \right) \mathrm{d}s'_n \mathrm{d}s_m +$$
$$\frac{l_n}{8\pi A_n} \iint_{s_m} \mathbf{t}_m(\mathbf{r}) \cdot \iint_{s_n} \frac{\mathbf{r}' - \mathbf{p}^{+'}}{|\mathbf{r}-\mathbf{r}'|}\mathrm{d}s'_n \mathrm{d}s_m - \tag{C.72}$$
$$\frac{l_n k^2}{16\pi A_n} \iint_{s_m} \mathbf{t}_m(\mathbf{r}) \cdot \iint_{s_n} (\mathbf{r}' - \mathbf{p}^{+'})|\mathbf{r}-\mathbf{r}'|\mathrm{d}s'_n \mathrm{d}s_m$$

It is assumed that s_n is the positive triangle for the RWG function, and the second and third integrals can simply be multiplied by a negative number when s_n is the negative triangle for the above equation to be valid. Then, the inner integrals of the second and third integrals in the equation above are given by [5]:

$$\iint_{s_n} \frac{\mathbf{r}' - \mathbf{q}}{|\mathbf{r}-\mathbf{r}'|}\mathrm{d}s' = \sum_{i=1}^{3} \hat{m}_i I_i^1 + (\boldsymbol{\rho} - \mathbf{q}) \iint_{s_n} \frac{1}{|\mathbf{r}-\mathbf{r}'|}\mathrm{d}s' \tag{C.73}$$

$$\iint_{s_n} (\mathbf{r}' - \mathbf{q})|\mathbf{r}-\mathbf{r}'|\mathrm{d}s' = \frac{1}{3}\sum_{i=1}^{3} \hat{m}_i I_i^3 + (\boldsymbol{\rho} - \mathbf{q}) \iint_{s_n} |\mathbf{r}-\mathbf{r}'|\mathrm{d}s' \tag{C.74}$$

Where the integrals in equations (C.73) and (C.74), are given by equations (C.56) and (C.57) respectively.

C.6.3 Evaluation of I3

I3 is zero when the $s_m = s_n$, or when they lie on the same plane. This is because:

$$\nabla G(\mathbf{r},\mathbf{r}') = \frac{G(\mathbf{r},\mathbf{r}')}{|\mathbf{r}-\mathbf{r}'|^2}(\mathbf{r}-\mathbf{r}') \tag{C.75}$$

$\mathbf{r} - \mathbf{r}'$ is on the same plane as $\mathbf{f}_n(\mathbf{r}')$, when the s_m and s_n triangles are on the same plane or equal. Therefore, the cross product in equation (C.29) results in a vector that is normal on the surface of s_n. The dot product of $\mathbf{f}_m(\mathbf{r}')$ with the normal vector is zero, if the s_m and s_n are equal or lie on the same plane.

Therefore, even though the inner integral of I3 is singular when $s_m = s_n$, the outer integral is zero. I3 has a singularity of order $1/|\mathbf{r} - \mathbf{r}'|$ and the order cannot be reduced. Since the singularity is of high order, the numerical integration becomes inaccurate when the source and the testing triangles are near each other or when touching but not on a similar plane as in figure C.1 [5].

C.6.3.1 Testing with RWG Function

When $\mathbf{t}_m = \mathbf{f}_m$, equation (C.29) becomes:

$$I3_{mn}^{\text{RWG}} = \iint_{s_m} \mathbf{f}_m(\mathbf{r}) \cdot \iint_{s_n} \nabla G(\mathbf{r}, \mathbf{r}') \times \mathbf{f}(\mathbf{r}') \mathrm{d}s' \mathrm{d}s \tag{C.76}$$

The integral is first simplified, before removing the singular term and integrating it analytically. This is done, by first representing the RWG functions explicitly with primed variables representing parameters on the source triangle.

$$I3_{mn}^{\text{RWG}} = \frac{l_m l_n}{4 A_n A_m} \iint_{s_m} (\mathbf{r} - \mathbf{p}) \cdot \iint_{s_n} \nabla G(\mathbf{r}, \mathbf{r}') \times (\mathbf{r}' - \mathbf{p}') \mathrm{d}s' \mathrm{d}s \tag{C.77}$$

Let:

$$(\mathbf{r}' - \mathbf{p}') = (\mathbf{r}' - \mathbf{r}) + (\mathbf{r} - \mathbf{p}) + (\mathbf{p} - \mathbf{p}') \tag{C.78}$$

Thus:

$$\begin{aligned} I3_{mn}^{\text{RWG}} = &\frac{l_m l_n}{4 A_n A_m} \iint_{s_m} (\mathbf{r} - \mathbf{p}) \cdot \iint_{s_n} \nabla G(\mathbf{r}, \mathbf{r}') \times (\mathbf{r}' - \mathbf{r}) \mathrm{d}s' \mathrm{d}s + \\ &\frac{l_m l_n}{4 A_n A_m} \iint_{s_m} (\mathbf{r} - \mathbf{p}) \cdot \iint_{s_n} \nabla G(\mathbf{r}, \mathbf{r}') \times (\mathbf{r} - \mathbf{p}) \mathrm{d}s' \mathrm{d}s + \\ &\frac{l_m l_n}{4 A_n A_m} \iint_{s_m} (\mathbf{r} - \mathbf{p}) \cdot \iint_{s_n} \nabla G(\mathbf{r}, \mathbf{r}') \times (\mathbf{p} - \mathbf{p}') \mathrm{d}s' \mathrm{d}s \end{aligned} \tag{C.79}$$

The first term in equation (C.79) equals 0, because:

$$\nabla G(\mathbf{r}, \mathbf{r}') \times (\mathbf{r}' - \mathbf{r}) = 0 \tag{C.80}$$

The second term also equals zero, because the source and testing functions are similar; this can be illustrated using the following vector identity:

$$\nabla \times (a\mathbf{b}) = \nabla a \times \mathbf{b} + a(\nabla \times \mathbf{b}) \tag{C.81}$$

On the second term in equation (C.79), and the result is:

$$\begin{aligned} I3_{mn}^{\text{RWG}} = &\frac{l_m l_n}{4 A_n A_m} \iint_{s_m} (\mathbf{r} - \mathbf{p}) \cdot \iint_{s_n} \nabla \times \left(G(\mathbf{r}, \mathbf{r}')(\mathbf{r} - \mathbf{p}) \right) \mathrm{d}s' \mathrm{d}s - \\ &\frac{l_m l_n}{4 A_n A_m} \iint_{s_m} (\mathbf{r} - \mathbf{p}) \cdot \iint_{s_n} G(\mathbf{r}, \mathbf{r}') \left(\nabla \times (\mathbf{r} - \mathbf{p}) \right) \mathrm{d}s' \mathrm{d}s + \\ &\frac{l_m l_n}{4 A_n A_m} \iint_{s_m} (\mathbf{r} - \mathbf{p}) \cdot \iint_{s_n} \nabla G(\mathbf{r}, \mathbf{r}') \times (\mathbf{p} - \mathbf{p}') \mathrm{d}s' \mathrm{d}s \end{aligned} \tag{C.82}$$

Using Leibnitz's integral theorem and the fact that:

$$\nabla \times \mathbf{r} = \vec{0} \tag{C.83}$$

And:

$$\nabla \times \mathbf{p} = \vec{0} \tag{C.84}$$

Equation (C.82) reduces to:

$$\begin{aligned} I3_{mn}^{\text{RWG}} = &\frac{l_m l_n}{4 A_n A_m} \iint_{s_m} (\mathbf{r} - \mathbf{p}) \cdot \nabla \times \iint_{s_n} G(\mathbf{r}, \mathbf{r}')(\mathbf{r} - \mathbf{p}) \mathrm{d}s' \mathrm{d}s + \\ &\frac{l_m l_n}{4 A_n A_m} \iint_{s_m} (\mathbf{r} - \mathbf{p}) \cdot \iint_{s_n} \nabla G(\mathbf{r}, \mathbf{r}') \times (\mathbf{p} - \mathbf{p}') \mathrm{d}s' \mathrm{d}s \end{aligned} \tag{C.85}$$

Again, applying the vector identity:

$$\nabla \cdot (\mathbf{a} \times \mathbf{b}) = \mathbf{b} \cdot (\nabla \times \mathbf{a}) - \mathbf{a} \cdot (\nabla \times \mathbf{b}) \tag{C.86}$$

To the first term of equation (C.85), with:

$$\mathbf{a} = \mathbf{r} - \mathbf{p} \tag{C.87}$$

$$\mathbf{b} = (\mathbf{r} - \mathbf{p}) \iint_{s_n} G(\mathbf{r}, \mathbf{r}') \mathrm{d}s' \tag{C.88}$$

Equation (C.85) becomes:

$$
\begin{aligned}
\mathrm{I3}_{mn}^{\mathrm{RWG}} = & \frac{l_m l_n}{4 A_n A_m} \iint_{s_m} \nabla \cdot \left((\mathbf{r} - \mathbf{p}) \times (\mathbf{r} - \mathbf{p}) \iint_{s_n} G(\mathbf{r}, \mathbf{r}') \mathrm{d}s' \right) \mathrm{d}s + \\
& \frac{l_m l_n}{4 A_n A_m} \iint_{s_m} (\nabla \times (\mathbf{r} - \mathbf{p})) \cdot \left((\mathbf{r} - \mathbf{p}) \iint_{s_n} G(\mathbf{r}, \mathbf{r}') \mathrm{d}s' \right) \mathrm{d}s + \\
& \frac{l_m l_n}{4 A_n A_m} \iint_{s_m} (\mathbf{r} - \mathbf{p}) \cdot \iint_{s_n} \nabla G(\mathbf{r}, \mathbf{r}') \times (\mathbf{p} - \mathbf{p}') \mathrm{d}s' \mathrm{d}s
\end{aligned}
\tag{C.89}
$$

The first and the second terms in the above equation evaluate to zero, and I3 becomes:

$$
\begin{aligned}
\mathrm{I3}_{mn}^{\mathrm{RWG}} &= \frac{l_m l_n}{4 A_n A_m} \iint_{s_m} (\mathbf{r} - \mathbf{p}) \cdot \iint_{s_n} \nabla G(\mathbf{r}, \mathbf{r}') \times (\mathbf{p} - \mathbf{p}') \mathrm{d}s' \mathrm{d}s \tag{C.90} \\
&= \frac{l_m l_n}{4 A_n A_m} \iint_{s_m} (\mathbf{r} - \mathbf{p}) \cdot (\mathbf{p} - \mathbf{p}') \times \iint_{s_n} \nabla' G(\mathbf{r}, \mathbf{r}') \mathrm{d}s' \mathrm{d}s \tag{C.91}
\end{aligned}
$$

Equation (C.91) involves the integral of the gradient of the green's function with reference to the source variables. Using the fact that [7]:

$$\nabla' G(\mathbf{r}, \mathbf{r}') = -\nabla G(\mathbf{r}, \mathbf{r}') \tag{C.92}$$

Equation (C.90) can be written as:

$$\mathrm{I3}_{mn}^{\mathrm{RWG}} = -\frac{l_m l_n}{4 A_n A_m} \iint_{s_m} (\mathbf{r} - \mathbf{p}) \cdot (\mathbf{p} - \mathbf{p}') \times \iint_{s_n} \nabla G(\mathbf{r}, \mathbf{r}') \mathrm{d}s' \mathrm{d}s \tag{C.93}$$

To integrate the above equation for near singular conditions, the Green's function is replaced by that in equation (C.35).

$$
\begin{aligned}
\mathrm{I3}_{mn}^{\mathrm{RWG}} = & -\frac{l_m l_n}{4 A_n A_m} \iint_{s_m} (\mathbf{r} - \mathbf{p}) \cdot (\mathbf{p} - \mathbf{p}') \times \iint_{s_n} \nabla \left(G(\mathbf{r}, \mathbf{r}') - \frac{1}{4\pi |\mathbf{r} - \mathbf{r}'|} + \frac{k^2}{8\pi} |\mathbf{r} - \mathbf{r}'| \right) \mathrm{d}s' \mathrm{d}s - \\
& \frac{l_m l_n}{16 \pi A_n A_m} \iint_{s_m} (\mathbf{r} - \mathbf{p}) \cdot (\mathbf{p} - \mathbf{p}') \times \iint_{s_n} \nabla \left(\frac{1}{|\mathbf{r} - \mathbf{r}'|} \right) \mathrm{d}s' \mathrm{d}s + \\
& \frac{k^2 l_m l_n}{32 \pi A_n A_m} \iint_{s_m} (\mathbf{r} - \mathbf{p}) \cdot (\mathbf{p} - \mathbf{p}') \times \iint_{s_n} \nabla \left(|\mathbf{r} - \mathbf{r}'| \right) \mathrm{d}s' \mathrm{d}s
\end{aligned}
\tag{C.94}
$$

The first integral above is regular and is integrated numerically. The inner integral of the second integral has a logarithmic singularity [5], which causes inaccuracies when the outer integral is evaluated numerically. To avoid this difficulty, the gradient operator is decomposed into the normal and surface components and the terms involving each are evaluated separately; i.e.:

$$\frac{l_m l_n}{16 \pi A_n A_m} \iint_{s_m} (\mathbf{r} - \mathbf{p}) \cdot (\mathbf{p} - \mathbf{p}') \times \iint_{s_n} \left(\nabla_n \left(\frac{1}{|\mathbf{r} - \mathbf{r}'|} \right) + \nabla_s \left(\frac{1}{|\mathbf{r} - \mathbf{r}'|} \right) \right) \mathrm{d}s' \mathrm{d}s \tag{C.95}$$

The normal gradient term evaluates to [8]:

$$
\begin{aligned}
\iint_{s_n} \nabla_n \left(\frac{1}{|\mathbf{r} - \mathbf{r}'|} \right) \mathrm{d}s' \mathrm{d}s &= \mathrm{N_{obs}} \iint_{s_n} \frac{1}{|\mathbf{r} - \mathbf{r}'|^3} \mathrm{d}s' \mathrm{d}s \tag{C.96} \\
&= \mathrm{sgn}(\mathrm{N_{obs}}) \sum_{i=1}^{3} \beta_i \tag{C.97}
\end{aligned}
$$

The integral involving the surface gradient operation, is integrated by using the surface gradient theorem [1] to convert the inner integral into a line integral, and then changing the order of integration. Doing this avoids the logarithmic singularity discussed above [5]. Let:

$$\mathrm{V_{RWG}} = \iint_{s_m} (\mathbf{r} - \mathbf{p}) \cdot (\mathbf{p} - \mathbf{p}') \times \iint_{s_n} \nabla_s \left(\frac{1}{|\mathbf{r} - \mathbf{r}'|} \right) \mathrm{d}s' \mathrm{d}s \tag{C.98}$$

The procedure described above results in:

$$V_{\text{RWG}} = \iint_{s_m} (\mathbf{r} - \mathbf{p}) \cdot (\mathbf{p} - \mathbf{p}') \times \sum_{i=1}^{3} \hat{m}_i \int_{\partial s_n} \left(\frac{1}{|\mathbf{r} - \mathbf{r}'|} \right) \partial s' \, \mathrm{d}s \tag{C.99}$$

$$= \sum_{i=1}^{3} \int_{\partial s_n} ((\mathbf{p} - \mathbf{p}') \times \hat{m}_i) \cdot \iint_{s_m} \frac{(\mathbf{r} - \mathbf{p})}{|\mathbf{r} - \mathbf{r}'|} \mathrm{d}s \partial s' \tag{C.100}$$

The inner integral is given by equation (C.73), and the outer integral is evaluated numerically. And lastly the inner integral of the third integral of equation (C.94) is given by:

$$\iint_{s_n} \nabla \left(|\mathbf{r} - \mathbf{r}'| \right) \mathrm{d}s' = N_{\text{obs}} \hat{n} \iint_{s_n} |\mathbf{r} - \mathbf{r}'| \mathrm{d}s' - \sum_{i=1}^{3} \hat{m}_i I_i^1 \tag{C.101}$$

C.6.3.2 Testing with $\hat{n} \times$ RWG Function

When $\mathbf{t}_m = \hat{n} \times \mathbf{f}_m$, equation (C.29) becomes:

$$\text{I3}_{mn}^{\text{nRWG}} = \iint_{s_m} (\hat{n}(\mathbf{r}) \times \mathbf{f}_m(\mathbf{r})) \cdot \iint_{s_n} \nabla G(\mathbf{r}, \mathbf{r}') \times \mathbf{f}(\mathbf{r}') \mathrm{d}s' \mathrm{d}s \tag{C.102}$$

By representing the testing RWG function explicitly, the above equation becomes:

$$\text{I3}_{mn}^{\text{nRWG}} = \frac{l_m l_n}{4 A_n A_m} \iint_{s_m} (\hat{n} \times (\mathbf{r} - \mathbf{p})) \cdot \iint_{s_n} \nabla G(\mathbf{r}, \mathbf{r}') \times (\mathbf{r}' - \mathbf{p}') \mathrm{d}s' \mathrm{d}s \tag{C.103}$$

The next step is to let:

$$\nabla G(\mathbf{r}, \mathbf{r}') = -\nabla' G(\mathbf{r}, \mathbf{r}') \tag{C.104}$$

$$(\mathbf{r}' - \mathbf{p}') = (\mathbf{r}' - \mathbf{r}) + (\mathbf{r} - \mathbf{p}') \tag{C.105}$$

Then, equation (C.103) becomes:

$$\begin{aligned}
\text{I3}_{mn}^{\text{nRWG}} = & \frac{l_m l_n}{4 A_n A_m} \iint_{s_m} (\hat{n} \times (\mathbf{r} - \mathbf{p})) \cdot \iint_{s_n} (\mathbf{r}' - \mathbf{r}) \times \nabla' G(\mathbf{r}, \mathbf{r}') \mathrm{d}s' \mathrm{d}s + \\
& \frac{l_m l_n}{4 A_n A_m} \iint_{s_m} (\hat{n} \times (\mathbf{r} - \mathbf{p})) \cdot \iint_{s_n} (\mathbf{r}' - \mathbf{p}') \times \nabla' G(\mathbf{r}, \mathbf{r}') \mathrm{d}s' \mathrm{d}s
\end{aligned} \tag{C.106}$$

Where, as shown earlier:

$$(\mathbf{r}' - \mathbf{r}) \times \nabla G(\mathbf{r}, \mathbf{r}') = \vec{0} \tag{C.107}$$

Therefore:

$$\text{I3}_{mn}^{\text{nRWG}} = \frac{l_m l_n}{4 A_n A_m} \iint_{s_m} (\hat{n} \times (\mathbf{r} - \mathbf{p})) \cdot (\mathbf{r} - \mathbf{p}') \times \iint_{s_n} \nabla' G(\mathbf{r}, \mathbf{r}') \mathrm{d}s' \mathrm{d}s \tag{C.108}$$

Substitution of the Green's function definition of equation (C.35) into the equation above results in:

$$\begin{aligned}
\text{I3}_{mn}^{\text{nRWG}} = & \frac{l_m l_n}{4 A_n A_m} \iint_{s_m} (\hat{n} \times (\mathbf{r} - \mathbf{p})) \cdot (\mathbf{r} - \mathbf{p}') \times \iint_{s_n} \nabla' \left(G(\mathbf{r}, \mathbf{r}') - \frac{1}{4\pi |\mathbf{r} - \mathbf{r}'|} + \frac{k^2}{8\pi} |\mathbf{r} - \mathbf{r}'| \right) \mathrm{d}s' \mathrm{d}s \\
& + \frac{l_m l_n}{16\pi A_n A_m} \iint_{s_m} (\hat{n} \times (\mathbf{r} - \mathbf{p})) \cdot (\mathbf{r} - \mathbf{p}') \times \iint_{s_n} \nabla' \left(\frac{1}{|\mathbf{r} - \mathbf{r}'|} \right) \mathrm{d}s' \mathrm{d}s \\
& - \frac{l_m l_n}{32\pi A_n A_m} \iint_{s_m} (\hat{n} \times (\mathbf{r} - \mathbf{p})) \cdot (\mathbf{r} - \mathbf{p}') \times \iint_{s_n} \nabla' \left(|\mathbf{r} - \mathbf{r}'| \right) \mathrm{d}s' \mathrm{d}s
\end{aligned} \tag{C.109}$$

The first integral is regular and is integrated numerically. The second and third integrals are treated as with $\text{I3}_{mn}^{\text{RWG}}$, except for the surface gradient term of the second integral, which is treated as follows. Let:

$$V_{\text{nRWG}} = \frac{1}{4\pi} \iint_{s_m} (\hat{n} \times (\mathbf{r} - \mathbf{p})) \cdot (\mathbf{r} - \mathbf{p}') \times \iint_{s_n} \nabla_s' \left(\frac{1}{|\mathbf{r} - \mathbf{r}'|} \right) \mathrm{d}s' \mathrm{d}s \tag{C.110}$$

Using the surface divergence on the inner integral results in:

$$V_{\text{nRWG}} = \frac{1}{4\pi} \sum_{i=1}^{3} \iint_{s_m} (\hat{n} \times (\mathbf{r} - \mathbf{p})) \cdot (\mathbf{r} - \mathbf{q}) \times \int_{\partial s_n} \hat{m}_i \left(\frac{1}{|\mathbf{r} - \mathbf{r}'|} \right) \partial s' \mathrm{d}s \tag{C.111}$$

To simplify the above equation and to change the order of integration:

$$(\mathbf{r} - \mathbf{p}') = (\mathbf{r} - \mathbf{p}) + (\mathbf{p} - \mathbf{p}') \tag{C.112}$$

This results in:

$$V_{\text{nRWG}} = \frac{1}{4\pi} \sum_{i=1}^{3} \int_{\partial s_n} ((\mathbf{p} - \mathbf{q}) \times \hat{m}_i) \cdot \left(\hat{n}(\mathbf{r}) \times \iint_{s_m} \frac{\mathbf{r} - \mathbf{p}}{|\mathbf{r} - \mathbf{r}'|} ds \right) \partial l' +$$
$$\frac{1}{4\pi} \sum_{i=1}^{3} \int_{\partial s_n} \hat{m}_i \cdot \hat{n}(\mathbf{r}) \iint_{s_m} \frac{|\mathbf{r} - \mathbf{p}|^2}{|\mathbf{r} - \mathbf{r}'|} ds \partial l' \tag{C.113}$$

Where:

$$\frac{|\mathbf{r} - \mathbf{p}|^2}{|\mathbf{r} - \mathbf{r}'|} = |\mathbf{r} - \mathbf{r}'| + 2(\mathbf{r}' - \mathbf{p}) \cdot \frac{(\mathbf{r} - \mathbf{p})}{|\mathbf{r} - \mathbf{r}'|} - |\mathbf{r} - \mathbf{p}|^2 \frac{1}{|\mathbf{r} - \mathbf{r}'|} \tag{C.114}$$

Therefore, the inner integral of the second integral of equation (C.110) becomes:

$$V_{\text{nRWG}} = \frac{1}{4\pi} \sum_{i=1}^{3} \int_{\partial s_n} ((\mathbf{p} - \mathbf{p}') \times \hat{m}_i) \cdot \left(\hat{n}(\mathbf{r}) \times \iint_{s_m} |\mathbf{r} - \mathbf{r}'| ds \right) \partial l' +$$
$$\frac{1}{4\pi} \sum_{i=1}^{3} \int_{\partial s_n} (\hat{m}_i \cdot \hat{n}(\mathbf{r})) \iint_{s_m} |\mathbf{r} - \mathbf{r}'| ds \partial l' +$$
$$\frac{1}{2\pi} \sum_{i=1}^{3} \int_{\partial s_n} (\hat{m}_i \cdot \hat{n}(\mathbf{r}))(\mathbf{r}' - \mathbf{p}) \cdot \iint_{s_m} \frac{\mathbf{r} - \mathbf{p}}{|\mathbf{r} - \mathbf{r}'|} ds \partial l' -$$
$$\frac{1}{4\pi} \sum_{i=1}^{3} \int_{\partial s_n} (\hat{m}_i \cdot \hat{n}(\mathbf{r})) |\mathbf{r}' - \mathbf{p}|^2 \iint_{s_m} \frac{1}{|\mathbf{r} - \mathbf{r}'|} ds \partial l' \tag{C.115}$$

C.6.4 Numerical Integration

Integrals of equations: (C.27), (C.28), (C.29), (C.30), (C.31) and are evaluated numerically, even when the integrand of the inner integrals becomes singular; because the outer integral is not. Therefore, numerical integration plays an important role in the evaluation of the integrals.

The implementation of the line and surface integrals using numerical integration methods is presented.

C.6.4.1 Line Integrals

The line integrals are performed using the 3-point Guassian-Legendre quadrature formula, where the integral is approximated by a sum of weighted integrand values that are evaluated at predetermined points; i.e. [1]:

$$\int_{-1}^{1} h(s) ds = \sum_{i=1}^{3} W_i h(s_i) \tag{C.116}$$

Where: W_i is the ith weight, and s_i the ith predetermined points where the integrand $(h(s))$ is evaluated. The weights and corresponding points for the 3-point Guassian-Legendre formula are shown in table C.1. The line integrals of $I1_{\text{nRWG}}$, $I3_{\text{RWG}}$, and $I3_{\text{nRWG}}$ for singular or nearly singular conditions are of the form:

Table C.1: Weights and points for the 3-point Gaussian-Legendre integration rule [1].

Weight(W_i)	Evaluation Point (s_i)
5/9	$-\sqrt{3/5}$
8/9	0
5/9	$\sqrt{3/5}$

$$\int_{0}^{a} h(\mathbf{r}) ds$$

Where, a is the length of the side of the triangle and:

$$r = (x, y, z) \tag{C.117}$$

To perform the integration r must be represented in terms of s. Before representing r in terms of s, the coordinate system is transformed into one where the one of the coordinate axis is perpendicular to the plane of the triangle. This is the transformation from figure C.3 (a) to figure C.3 (b). This reduces the number of components that are required to represent points on the line segment that represents the side of the triangle to two instead of three to simplify the analysis. The transformation is performed using the following matrix equation:

$$\left\{ \begin{array}{c} u \\ v \\ n \end{array} \right\} = \left[\begin{array}{ccc} \hat{u} \cdot \hat{x} & \hat{u} \cdot \hat{y} & \hat{u} \cdot \hat{z} \\ \hat{v} \cdot \hat{x} & \hat{v} \cdot \hat{y} & \hat{v} \cdot \hat{z} \\ \hat{n} \cdot \hat{x} & \hat{n} \cdot \hat{y} & \hat{n} \cdot \hat{z} \end{array} \right] \left\{ \begin{array}{c} x - x_2 \\ y - y_2 \\ z - z_2 \end{array} \right\} \tag{C.118}$$

Where:

- $\hat{u}$ is the unit vector parallel to the side formed by nodes $\mathbf{n}_2$ and $\mathbf{n}_3$ in figure C.3 (a); pointing from $\mathbf{n}_2$ to $\mathbf{n}_3$
- $\hat{n}$ is the unit vector normal to the plane of the triangle.
- $\hat{v}$ is a unit vector that is parallel to both $\hat{u}$ and $\hat{n}$

Using the new coordinate system:

$$r = (u, v, 0) \tag{C.119}$$

And:

$$s = \sqrt{(v - v_{\text{start}})^2 + (u - u_{\text{start}})^2} \tag{C.120}$$

s is the distance between points (u, v) and $(u_{\text{start}}, v_{\text{start}})$[1]. To represent u and v in terms of s a new parameter α is introduced. It is defined as the angle that is formed by the line segment that represents the side of the triangle and the u-axis, and is given by:

$$\alpha = \arctan \left(\frac{v_{\text{start}} - v_{\text{end}}}{u_{\text{start}} - u_{\text{end}}} \right) \tag{C.121}$$

Then u and v, are represented using s and α as:

$$u = s \cos \alpha + u_{\text{start}} \tag{C.122}$$
$$v = s \sin \alpha + v_{\text{start}} \tag{C.123}$$

Replacing the components of $\mathbf{r}$ in equation (C.119), with those in the equations above permits the representation of the line integrals as:

$$\int_0^a h(\mathbf{r}) \, ds = \int_0^a h(s) \, ds \tag{C.124}$$

The integral of equation (C.116) is from -1 to 1, and can therefore not be used to directly for the evaluation of equation (C.124). The limits of the integral in equation (C.124) are changed from 0 to a to those from -1 to 1. With this alteration, the integration variable is also altered to preserve the meaning of the integral. The new integration variable is s' and is defined as:

$$s' = ms + c \tag{C.125}$$

Where: m accounts for the scaling of the axis, and c accounts for the offset (the limits of integration start from -1 instead of 0). m and s are solved using the following equations:

$$a = m + c \qquad s' = a, \text{ when } s = 1 \tag{C.126}$$
$$0 = c - m \qquad s' = 0, \text{ when } s = -1 \tag{C.127}$$

The solution of m and c from the above equations is:

$$m = c = \frac{a}{2} \tag{C.128}$$

Therefore:

$$s = \frac{2}{a} s' + 1 \tag{C.129}$$

---

[1]The coordinate of one of the ends of the side of the triangle

(a)

(b)

(c)
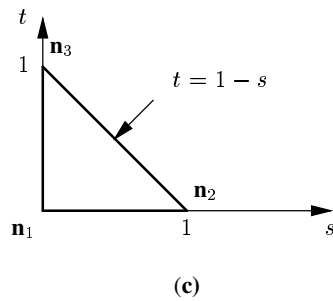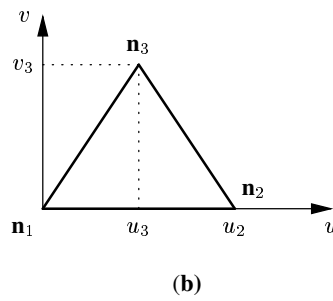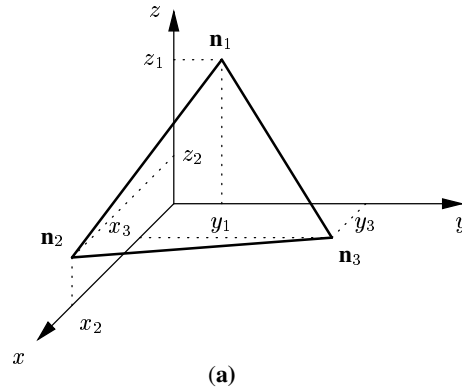
Figure C.3: Triangle in different coordinate systems.

And:

$$\mathrm{d}s = \frac{2}{a}\mathrm{d}s'$$
(C.130)

Substituting s and $\mathrm{d}s$ from the above equations in equation (C.124) results in:

$$
\begin{aligned}
\int_0^a h(s)\mathrm{d}s &= \int_{-1}^1 h\left(\frac{2}{a}s' + 1\right)\frac{2}{a}\mathrm{d}s \\
&= \frac{2}{a}\int_{-1}^1 h\left(\frac{a}{2}s_i' + \frac{a}{2}\right)\mathrm{d}s' \\
&= \frac{2}{a}\sum_{i=1}^3 \mathrm{W}_i h\left(\frac{2}{a}s_i' + 1\right)
\end{aligned}
$$
(C.131)

Where s_i' are the evaluation points in table C.1.

C.6.4.2 Surface Integrals

The surface integral are performed using the 7-point Gaussian quadrature rule. As with the line integral, the integral is replaced by a weighted sum of values of the integrand evaluated at predetermined point in the domain of the triangle (figure C.3 (c)); i.e. [9]:

$$\int_{t=0}^{t=1} \int_{s=0}^{s=1-t} \mathbf{h}(\mathbf{r}) \, \mathrm{d}s \, \mathrm{d}t = \sum_{i=1}^{7} \mathrm{W}_i h(\mathbf{r}_i)(\mathbf{r}_i) \tag{C.132}$$

Where: W_i is defined as in the line integral case, and $\mathbf{r}_i$ are the corresponding inside the triangle domain and are given by:

$$\mathbf{r}_i = (s_i, t_i, 0) \tag{C.133}$$

Values of W_i and $\mathbf{r}_i$ for the 7-point Gaussian quadrature formula are given in table C.2.

Table C.2: Weights and points for the 7-point Gaussian quadrature rule [9].

Weight	s	t
$9/80$	$1/3$	$1/3$
$(155 + \sqrt{15})/2400$	$(6 + \sqrt{15})/21$	$(6 + \sqrt{15})/21$
$(155 + \sqrt{15})/2400$	$(9 - 2\sqrt{15})/21$	$(6 + \sqrt{15})/21$
$(155 + \sqrt{15})/2400$	$(6 + \sqrt{15})/21$	$(9 - 2\sqrt{15})/21$
$(155 - \sqrt{15})/2400$	$(6 - \sqrt{15})/21$	$(6 - \sqrt{15})/21$
$(155 - \sqrt{15})/2400$	$(9 + \sqrt{15})/21$	$(6 - \sqrt{15})/21$
$(155 - \sqrt{15})/2400$	$(6 - \sqrt{15})/21$	$(9 + \sqrt{15})/21$

The triangles that are used for representing the surface that supports the current distributions, are generally not right angled and they are oriented arbitrarily as in figure C.3. This means that points on the triangles will have 3 components, i.e.:

$$\mathbf{r} = (x, y, z) \tag{C.134}$$

Therefore, the triangles must be transformed into a coordinate system where one of the coordinate axis is perpendicular to the plane of the triangle, since the integration points are given for a coordinate system with two component. This transformation is performed using equation (C.118).

Using the new coordinate system:

$$\mathbf{r} = (u, v, 0) \tag{C.135}$$

Surface integral that must be evaluated are of the form:

$$\int_{v_{\mathrm{start}}}^{v_{\mathrm{end}}} \int_{u_{\mathrm{start}}}^{u_{\mathrm{end}}} \mathbf{h}(\mathbf{r}) \, \mathrm{d}u \, \mathrm{d}v$$

The limits of the integration above have to be altered to resemble those of equation (C.132), in order to use the 7-point Gaussian quadrature formula to evaluate the integral. This is performed by transforming the integration domain to one where the integration domain becomes a right angled triangle; this the transformation from figure C.3 (b) to figure C.3 (c).

The transformation is performed using the following eqaution:

$$\left\{ \begin{array}{c} u \\ v \end{array} \right\} = \left[\begin{array}{cc} u_3 & u_1 \\ 0 & v_1 \end{array} \right] \left\{ \begin{array}{c} s \\ t \end{array} \right\} \tag{C.136}$$

Equation (C.136) is obtained by solving the following couple equations:

$$u = \mathrm{A}s + \mathrm{B}t + \mathrm{C} \tag{C.137}$$

$$v = \mathrm{D}s + \mathrm{E}t + \mathrm{F} \tag{C.138}$$

Where A,B,C,D, and E; are computed using the fact the nodes of the triangle in the uv coordinate system transform to the corresponding node in the st coordinate system; see figure C.3 (b) and (c). Using these

conditions, the following equation are generated:

$$
\left\{
\begin{array}{c}
u_1 \\
v_1 \\
0 \\
0 \\
u_3 \\
0
\end{array}
\right\}
=
\left[
\begin{array}{cccccc}
0 & 1 & 1 & 0 & 0 & 0 \\
0 & 0 & 0 & 0 & 1 & 1 \\
0 & 0 & 1 & 0 & 0 & 0 \\
0 & 0 & 0 & 0 & 0 & 1 \\
1 & 0 & 1 & 0 & 0 & 0 \\
0 & 0 & 0 & 1 & 0 & 1
\end{array}
\right]
\left\{
\begin{array}{c}
A \\
B \\
C \\
D \\
E \\
F
\end{array}
\right\}
\tag{C.139}
$$

Which when solved for A, B, C, D, E, and F; yield:

$$
\left\{
\begin{array}{c}
A \\
B \\
C \\
D \\
E \\
F
\end{array}
\right\}
=
\left\{
\begin{array}{c}
u_3 \\
u_1 \\
0 \\
0 \\
v_1 \\
0
\end{array}
\right\}
\tag{C.140}
$$

Therefore, the relation between u, v, s and t is given as:

$$
\begin{aligned}
u &= u_3 s + u_1 t \tag{C.141} \\
v &= v_1 t \tag{C.142}
\end{aligned}
$$

Using the above equations [10]:

$$
\mathrm{d}u\,\mathrm{d}s = u_3 v_1 \,\mathrm{d}s\,\mathrm{d}t \tag{C.143}
$$

Therefore:

$$
\begin{aligned}
\int_{v_{\text{start}}}^{v\,\text{end}} \int_{u_{\text{start}}}^{u\,\text{end}} \mathbf{h}(\mathbf{r})\,\mathrm{d}u\,\mathrm{d}v
&= \int_{t=0}^{t=1} \int_{s=0}^{s=1-t} h(\mathbf{r})\,u_3 v_1 \,\mathrm{d}s\,\mathrm{d}t \\
&= u_3 v_1 \int_{t=0}^{t=1} \int_{s=0}^{s=1-t} h(\mathbf{r})\,\mathrm{d}s\,\mathrm{d}t \tag{C.144} \\
&= u_3 v_1 \sum_{i=1}^{7} \mathbf{W}_i h(\mathbf{r}_i)
\end{aligned}
$$

Where:

$$
\mathbf{r} = (u_3 s + u_1 t, v_1 t) \tag{C.145}
$$

C.7 Conclusion

An overview of MoM procedure for reducing a MoM formulation to a matrix equation is presented, and applied in reducing the MoM formulation part of the FEM-MoM formulation used for analysis of printed antennas to a matrix equation.

The MoM formulation gives the relation between the equivalent electric and magnetic current densities on an arbitrary surface. The arbitrary surface, which supports the current densities is divided into triangles and RWG basis functions are used for expanding both current densities within the triangles. The formulation is then reduced to a matrix equation by testing the EFIE part of the formulation using RWG $+ \hat{n} \times$ RWG function and the MFIE part by $\hat{n} \times$ RWG. Equations for the resulting matrix equations are presented and the detailed instructions for evaluation of integrals terms of the formulation are presented.

References

[1] J. Jin. *The Finite Element Method in Electromagnetics*. New York: John Wiley and Sons, Inc., second ed., 2002.

[2] R. F. Harrington. "Matrix Methods for Field Problems." *Proceedings of the IEEE*, vol. 55, no. 02, pp. 136–149, 02 1967.

[3] S. Rao, D. Wilton, and A. Glisson. "Electromagnetic Scattering by Surfaces of Arbitrary Shape." *IEEE Transactions on Antennas and Propagation*, , no. 30, pp. 409–418, 05 1982.

[4] D. B. Davidson. *Computational Electromagnetics for RF and Microwave Engineering*. Cambridge, first ed., 2005.

[5] P. Ylä-Olijala and M. Taskinen. "Calculation of CFIE Impedance Matrix Elements With RWG and $n \times$RWG Functions." *IEEE Transactions on Antennas and Propagation*, vol. 51, pp. 1837 – 1846, 08 2003.

[6] X. Sheng, J. Jin, J. Song, W. Chew, and C. Lu. "Solution of Combined-Field Integral Equation Using Multilevel Fast Multipole Algorithm for Scattering by Homogeneous Bodies." *IEEE Transactions on Antennas and Propagation*, vol. 46, no. 11, pp. 1718–1726, 11 1998.

[7] C. A. Balanis. *Advanced Engineering Electromagnetics*. John Wiley and Sons, first ed., 1989.

[8] R. D. Graglia. "On the Numerical Integration of the Linear Shape Functions Times the 3-D Green's Function or its Gradient on a Plane Triangle." *IEEE Transactions on Antennas and Propagation*, vol. 41, no. 10, pp. 1448–1455, 10 1993.

[9] Y. Renard and J. Pommier. *GetFEM++, Documentation Part 3: Description of Finite Element and Integration Methods*, 04 2006.

[10] G. James. *Advanced Modern Engineering Mathematics*. Addison-Wesles, second ed., 1999.

Appendix D

Reduction of FEM Formulation into a Matrix Equation

D.1 Introduction

FEM (Finite Element Method) is a numerical technique for obtaining approximate solutions to boundary-value problems [1]. It is used in CEM (Computational Electromagnetics) for solving boundary-value problems that are formulated in terms of partial differential equations. The differential equations are solved by reducing the equation that governs the problem being solved into a matrix equation, which can be solved using a computer.

The reduction of the FEM formulation part of the FEM-MoM (Method of Moments) formulation used for the analysis of probe-fed printed antennas, to a matrix equation is presented. Derivation of the FEM-MoM formulation is presented in section A.3 of appendix A. The analysis is performed by firstly reducing the problem into two coupled problem, using the surface equivalence principle. The antenna structure is enclosed within a fictitious surface, which does not touch conducting regions of the structure. Then the following problems are defined, using the surface equivalence principle:

1) The first problem involves the region enclosed by the fictitious surface defined above with equivalent electric and magnetic current densities on the fictitious surface and fields set to zero everywhere outside the fictitious surface. Analysis of this problem for the electric field inside volume region is performed using FEM, where the FEM formulation relates the electric field within the volume region and the equivalent electric current density on the fictitious surface.
2) The second problem involves the region outside the fictitious surface also with equivalent electric and magnetic current densities on a fictitious surface, fields everywhere inside the fictitious surface set to zero and the region inside the fictitious replaced by free-space material. Analysis of this problem is performed using MoM, where the MoM formulation gives a relation between equivalent electric and magnetic current densities.

The equivalent current densities in the two problems above are defined using the field boundary conditions, where it is found that the magnitudes of the corresponding current densities are equal but the current densities are in opposite directions. Therefore, the FEM and MoM formulations form two coupled equations, which are used for solution of the electric field inside the fictitious surface and the equivalent electric current density on the fictitious surface. The equivalent magnetic current density on the fictitious surface is obtained from the electric field within the region enclosed by the fictitious surface.

The presentation is structured as follows. The FEM formulation, which is derived in appendix A is presented, followed by an overview of the FEM procedure for solution of the boundary value problems. This is followed by implementation of the procedure that is discussed in the overview, in the following sections. Then, the closed form expressions for the integral terms in the formulation are derived.

D.2 Formulation

As indicated in the introduction, the derivation of the FEM formulation for the first problem is presented in section A.3.1 of appendix A. The formulation is derived using the Rayleigh-Ritz method and the required functional is given by:

$$F(\mathbf{E}) = \frac{1}{2} \iiint_V \left(\frac{1}{\mu_r} (\nabla \times \mathbf{E}) \cdot (\nabla \times \mathbf{E}) - k_0^2 \epsilon_r \mathbf{E} \cdot \mathbf{E} \right) dV +$$
$$jk_0 Z_0 \iiint_V \mathbf{E} \cdot \mathbf{J} \, dV + jk_0 Z_0 \oiint_S \mathbf{E} \cdot \mathbf{J}_{\text{eq}} dS \tag{D.1}$$

This is for the following boundary value problem, which requires solution of:

$$\nabla \times \left(\frac{1}{\mu} \nabla \times \mathbf{E}(\mathbf{r}) \right) - \omega^2 \epsilon \mathbf{E}(\mathbf{r}) = -j\omega \mathbf{J}(\mathbf{r}) \qquad \mathbf{r} \in V \tag{D.2}$$

For the electric field within a region (V), given the following boundary conditions:

$$\hat{n} \times \mathbf{E}(\mathbf{r}) = 0 \qquad \mathbf{r} \in S_{\text{cond}} \tag{D.3}$$

And:

$$\hat{n} \times (\nabla \times \mathbf{E}(\mathbf{r})) = -j\omega\mu\hat{n} \times \mathbf{H}(\mathbf{r}) \qquad \mathbf{r} \in S \tag{D.4}$$

Where:

- $\mathbf{J}$ is the impressed electric current density used for modelling the probe feed and is given by:

$$\mathbf{J}(\mathbf{r}) = \mathrm{I}\delta(x - x_s)\delta(y - y_s)\hat{z} \tag{D.5}$$

  Assuming that the filament (see section A.4.3 of appendix A.3), which supports the current is z directed.
- V is the region that encloses the antenna structure such that the enclosing boundary does not touch conducting regions of the antenna structure.
- S_{cond} is the surfaces of conducting regions within V.
- S is the enclosing surface of V (i.e. the fictitious surface).

The boundary condition of equation (D.3) is enforced by setting the tangential field values on the conducting values to zero.

D.3 Overview of the Finite Element Method

Given a boundary problem of the form:

$$\mathcal{L}(f) = g \tag{D.6}$$

Where: $\mathcal{L}$ is a differential operator for FEM problems in CEM, g is a known excitation, f is an unknown function to be determined, and the problem domain is denoted by V. The solution of the above equation for f is obtained using FEM as follows.

V is divided into simpler geometric shapes, which will be assumed to be triangles in this section. Then, f is expanded as a sum of weighted interpolation or basis functions within each of the triangles, i.e.:

$$f^{\mathrm{e}} = \sum_{n=1}^{N} \alpha_n f_n^{\mathrm{e}} \tag{D.7}$$

Where: f^{e} is the unknown function within the eth triangle, f_n^{e} is the nth basis function within e^{th} triangle, α_n is the weight of the nth basis function, and N is the total number of basis functions within a triangle. The weights (α_n) are the numbers and are related to the unknown functions, e.g., they could be the value of the unknown function at a one of the triangle nodes. The unknown function within V becomes:

$$f = \sum_{e=1}^{N_{\mathrm{e}}} f^{\mathrm{e}} \tag{D.8}$$

N_e is the total number of triangles that V has been divided into. Representation of f as above is done to reduce the problem to that of determining numbers instead of a functions, which is a simpler problem.

It is a well known fact that a unique solution for a problem with x unknowns requires x equations or conditions. Solution of the unknown weights also requires equations, which are equal to the number of weights. The required equations are generated using either Garlerkin or Rayleigh-Ritz methods. These two methods are discussed in [1], [2], and only the Rayleigh-Ritz method is discussed here since the formulation in section D.3 is derived using the Rayleigh-Ritz method.

When using the Rayleigh-Ritz method: the problem is represented by a function F, which depends on f. This function is called a variational principle or simply functional and is defined such that it is made stationary by f, which satisfies equation (D.6) under given boundary conditions [1], i.e:

$$\delta F(f) = \frac{\partial F(f)}{\partial f} = 0 \tag{D.9}$$

The above equation states that the first variation of F with respect to f is equal to zero, which is a condition that is required in order to make the functional stationary. This reduces the problem to that of determining f which satisfies equation (D.9). However, f is represented by a weighted sum of known functions and the weights are the unknowns. Therefore, the problem actually reduces to that of determining the weights to satisfy equation (D.9) since the functional is a function of α_n. Equation (D.9) is satisfied by setting the partial derivatives of the functional with respect to each of the unknown weights to zero [3], i.e.:

$$\frac{\partial F(f)}{\partial \alpha_n} = 0, \qquad n = 1, 2, \ldots, N_T \tag{D.10}$$

Where N_T is the total number of weights. The above results in the number of equations that are required for a unique solution of the unknown weights. These equations are then put into matrix form and solved using linear algebra methods.

Following the above presentation and [1]; a finite element analysis of boundary value problems includes the following steps:

- Domain Discretisation.
- Selection of the interpolation or basis functions
- Formulation of the system of equations.
- Solution of the system of equations.

The presentation in this appendix is concerned with the first three points, because the subject of this appendix is, the reduction of equation (D.1) into a matrix equation. The last point is the subject of appendix B.

The presentation above is a simplified version of the FEM solution procedure, and a lot of detail has been left out for brevity. A detailed procedure may be obtained in the [1], [2], [3].

D.4 Domain Discretisation

Tetrahedron are chosen for discretisation of the problem domain (V). An example tetrahedron is shown in figure D.5 (b). These elements are selected for this purpose because of their ability to represent arbitrary domains [1], which means regions an arbitrary composition will be represented accurately. Discretisation of the domain must be done such that electromagnetic properties in each tetrahedron are constant.

Representation of V using a connection of tetrahedrons means that S and S_{cond} are represented by a connection of triangles.
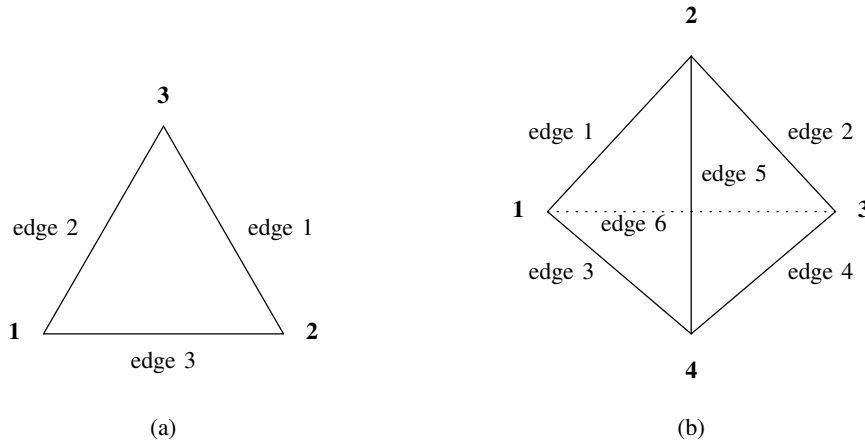
Figure D.1: Enumeration of the edges, and nodes for a triangle and tetrahedron.

D.5 Selection of Interpolation Functions

The electric field within tetrahedrons is represented using Whitney elements or basis functions, which are defined as follows [1, Chapter 8]:

$$\mathbf{N}_i^e = l_i \mathbf{W}_{jk} = l_i \left(L_j^e \nabla L_k^e - L_k^e \nabla L_j^e \right) \tag{D.11}$$

Where:

- L_j and L_k are simplex coordinates and are defined in section D.5.0.3.
- l_i is the length of the ith edge (see figure D.5) of the tetrahedron.
- j and k, are the indices for the start and end nodes of the line segment, which forms edge i of the tetrahedron.

These functions are used for interpolating the electric field within the tetrahedron given the magnitudes of the tangential electric field across the edges of the tetrahedrons. Therefore, the weights are the magnitudes of the tangential electric field across the edges of the tetrahedron.

They are selected for use here because they [4]:

- Are tangentially continuous and normally discontinuous between adjacent tetrahedrons, which are the properties of the electric field at a source free boundary between materials with different electromagnetic properties. This makes for straight forward treatment of inhomogeneous media since tangential continuity is guaranteed.
- Are better at handling field singularities, which may occur for a sharp metal edges. This is particularly important for the application under consideration since V contains metal surfaces.
- Eliminate spurious modes, which are non-physical solutions field solutions with non-zero divergence that may occur in FEM solutions.

The electric field within V, using the above functions is given by:

$$\mathbf{E}(\mathbf{r}) = \sum_{i'=1}^{N_V} E_{i'} \mathbf{N}_{i'}(\mathbf{r}) \tag{D.12}$$

Where: i' is the index for the edges of the structure, $\mathbf{N}_{i'}$ is the corresponding edge basis function whose definition depends on the tetrahedron that $\mathbf{r}$ is in, $E_{i'}$ is the magnitude of the tangential component of $\mathbf{E}$ on edge i', and N_V is the total number of edges in V.

The choice of the basis function is used for interpolating the equivalent electric current density ($\mathbf{J}_{\text{eq}}$) within triangles on S is discussed in section C.4 of appendix C. RWG (Rao-Wilton-Glisson) basis functions are used for this purpose, and they are denoted by $\mathbf{R}$ in this appendix. These functions are used for interpolating

current densities given the magnitude of the normal component of the electric current density through the triangle edges. Therefore, the weights when using these functions is the magnitude of the normal component of the electric current density across the edges.

Therefore, $\mathbf{J}_{eq}$ is written as:

$$\mathbf{J}_{eq}(\mathbf{r}) = \sum_{j'=1}^{N_S} I_{j'} \mathbf{R}_{j'}(\mathbf{r}) \tag{D.13}$$

Where: j' is the index for the edges of the triangles that S is divided into, $\mathbf{R}_{j'}$ is the corresponding RWG basis function whose definition depends on the triangles $\mathbf{r}$ is in, $I_{i'}$ is the magnitude of the normal component of $\mathbf{J}_{eq}$ on edge j', and N_S is the total number of edges on S.

D.5.0.3 Simplex Coordinates
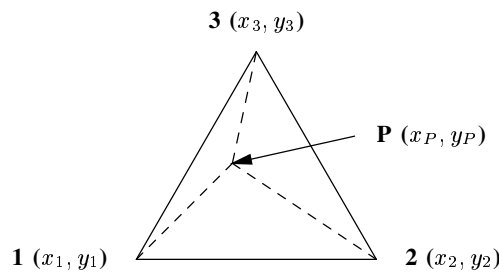
Figure D.2: Triangle.

Simplex coordinates are defined in two and three dimensions over triangular and tetrahedron domains respectively. In two dimensions they are defined with reference to figure D.2 as [2]:

$$L_i^e(x_p, y_p) = \frac{\text{Area } \triangle pjk}{\text{Area } \triangle 123} \tag{D.14}$$

Which is the area of the triangle formed by nodes pjk divided by the area of the element (i.e. triangle), and:

- i is the index used to refer to the subtriangle that is referred to as $\triangle pjk$. i is further defined such that it assumes the number of the node that does not form part of the subtriangle ($\triangle pjk$), i.e. if $j = 1$ and $k = 2$ then $i = 3$.
- j and k are the numbers of the nodes that together with point p form $\triangle pjk$.
- e is the index used to refer to the mesh discretising element.

Therefore:

$$\begin{aligned} L_1^e(x_p, y_p) &= \frac{\text{Area } \triangle p23}{\text{Area } \triangle 123} \\ L_2^e(x_p, y_p) &= \frac{\text{Area } \triangle p13}{\text{Area } \triangle 123} \\ L_3^e(x_p, y_p) &= \frac{\text{Area } \triangle p12}{\text{Area } \triangle 123} \end{aligned} \tag{D.15}$$

Equation (D.14), can be written more compactly as:

$$L_i^e(x_p, y_p) = \frac{1}{2A^e}(a_i + b_i x + c_i y) \tag{D.16}$$

And the symbols in the equation (D.16) are defined as:

$$\begin{pmatrix} 1 & 1 & 1 \\ x_1 & x_2 & x_3 \\ y_1 & y_2 & y_3 \end{pmatrix}^{-1} = \frac{1}{2A^e} \begin{pmatrix} a_1 & b_1 & c_1 \\ a_2 & b_2 & c_2 \\ a_3 & b_3 & c_3 \end{pmatrix} \tag{D.17}$$

$$A^e = \frac{1}{2} \begin{vmatrix} 1 & x_1 & y_1 \\ 1 & x_2 & y_2 \\ 1 & x_3 & y_3 \end{vmatrix} = \frac{1}{2}(b_1 c_2 - b_2 c_1) \tag{D.18}$$

For three dimensional domains, the simplex coordinates are defined with reference to figure D.3 as:

1 (x_1, y_1, z_1)

P (x_P, y_P, z_P)

2 (x_2, y_2, z_2) **4** (x_4, y_4, z_4)

3 (x_3, y_3, z_3)
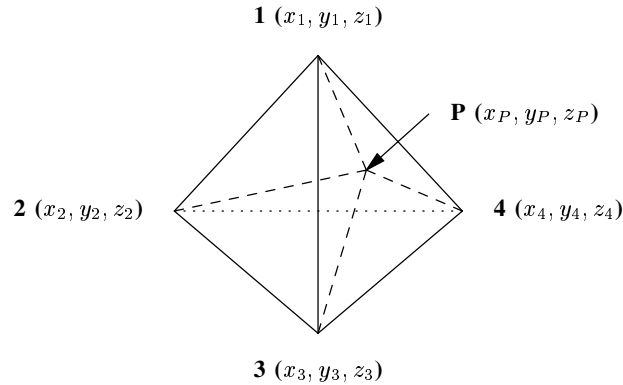
Figure D.3: Tetrahedron.

$$L_i^e(x_p, y_p, z_p) = \frac{\text{Volume } pjkl}{\text{Volume } 1234} \tag{D.19}$$

Which is the volume of the tetrahedron formed by nodes $pjkl$ divided by the volume of the the element (i.e. tetrahedron formed by nodes $ijkl$), and the i, j, k and l are have similar definitions as in the two dimensional case. Thus:

$$\begin{aligned} L_1^e(x_p, y_p, z_p) &= \frac{\text{Volume } p234}{\text{Volume } 1234} \\ L_2^e(x_p, y_p, z_p) &= \frac{\text{Volume } p134}{\text{Volume } 1234} \\ L_3^e(x_p, y_p, z_p) &= \frac{\text{Volume } p124}{\text{Volume } 1234} \\ L_4^e(x_p, y_p, z_p) &= \frac{\text{Volume } p123}{\text{Volume } 1234} \end{aligned} \tag{D.20}$$

As with the two dimensional case equation (D.19), can be written as:

$$L_i^e(x_p, y_p, z_p) = \frac{1}{6V^e}(a_i + b_i x + c_i y + d_i z) \tag{D.21}$$

And the symbols in equation (D.21) are given by:

$$\begin{pmatrix} 1 & 1 & 1 & 1 \\ x_1 & x_2 & x_3 & x_4 \\ y_1 & y_2 & y_3 & y_4 \\ z_1 & z_2 & z_3 & z_4 \end{pmatrix}^{-1} = \frac{1}{6V^e} \begin{pmatrix} a_1 & b_1 & c_1 & d_1 \\ a_2 & b_2 & c_2 & d_2 \\ a_3 & b_3 & c_3 & d_3 \\ a_4 & b_4 & c_4 & d_4 \end{pmatrix} \tag{D.22}$$

$$V^e = \frac{1}{6} \begin{vmatrix} 1 & x_1 & y_1 & z_1 \\ 1 & x_2 & y_2 & z_2 \\ 1 & x_3 & y_3 & z_3 \\ 1 & x_4 & y_4 & z_4 \end{vmatrix} \tag{D.23}$$

The simplex coodinates have the following properties [5]:

- $L_i^e(\boldsymbol{r}) \leq 1$ for $\boldsymbol{r}$ in the domain of the triangle.
- $\sum_{i=1}^{k} L_i^e(\boldsymbol{r}) = 1$, k equals 3 for simplex coordinates over triangular domains and 4 over tetrahedron domains.
- The gradient of each simplex coordinate is constant and normal to the edge/face [1] that is opposite the

[1]Edge in two dimensions and face in three dimensions

node that the simplex coordinate is defined relative to, e.g. $\nabla L_1^e(\boldsymbol{r})$ is normal to the edge formed by nodes 2 and 3 in 2D (see figure D.2), and normal to the face formed by nodes 2, 3 and 4 in 3D (see figure D.3). It can be seen in equations (D.24) and (D.25) that the gradient is constant.

$$\nabla L_i^e = \frac{(b_i, c_i)}{2A} \tag{D.24}$$

$$\nabla L_i^e = \frac{(b_i, c_i, d_i)}{6V} \tag{D.25}$$

D.6 Formulation of the System Matrices

The formulation is reduced to a matrix equation by substituting the electric field and equivalent electric current density from equations (D.12) and (D.13) into the functional of equation (D.1). Then the partial derivative of the functional taken with respect to the unknown weights is set to zero, and that results in the following matrix equation:

$$\sum_{i'=1}^{N} \sum_{j'=1}^{N} \left([K_{i'j'}]\{E_{j'}\} - [B_{i'j'}]\{I_{j'}\} \right) = \sum_{i'=1}^{N} \{C_{i'}\} \tag{D.26}$$

Where:

$$K_{i'j'} = \iiint_V \left(\frac{1}{\mu_r}(\nabla \times \mathbf{N}_{i'}) \cdot (\nabla \times \mathbf{N}_{j'}) - k_0^2 \epsilon_r \mathbf{N}_{i'} \cdot \mathbf{N}_{j'} \right) dV \tag{D.27}$$

$$B_{i'j'} = jk_0 Z_0 \oiint_S \mathbf{N}_{i'} \cdot (\mathbf{R}_{j'}) dS \qquad \text{for edges } i' \text{ and } j' \text{ on S} \tag{D.28}$$

$$C_{i'} = -jk_0 Z_0 \iiint_V \mathbf{N}_{i'} \cdot \mathbf{J} dV \tag{D.29}$$

D.7 Evaluation of Integrals

Integration is a linear operation and since V has been divided into tetrahedrons, the integrals of equations (D.27) and (D.29) are performed per tetrahedron and the resulting integral is the sum of the integrals over each tetrahedron. This also applies to the integrals of equation (D.29), which are performed per triangle that is part of the S and the resulting integral is the sum of the integrals over each of the triangles.

The evaluation of the volume and surface integrals of section D.6 is presented.

D.7.1 Volume Integrals

The volume integrals of equations (D.27) and (D.29) are evaluated. Following the discussion above, the volume integrals are represented as:

$$K_{i'j'} = \sum_{e=1}^{N_{\text{tet}}} \iiint_{V^e} \sum_{i'=1}^{6} \sum_{j'=1}^{6} \left(\frac{1}{\mu_r^e}(\nabla \times \mathbf{N}_{i'}) \cdot (\nabla \times \mathbf{N}_{j'}) - k_0^2 \epsilon_r \mathbf{N}_{i'} \cdot \mathbf{N}_{j'} \right) dV \tag{D.30}$$

$$\text{for edges } i' \text{ and } j' \text{ in } V^e$$

And:

$$C_{i'} = -jk_0 Z_0 \sum_{e=1}^{N_e} \iiint_{V^e} \sum_{i'=1}^{4} \mathbf{N}_{i'} \cdot \mathbf{J} dV \qquad \text{for edge } i' \text{ in } V^e \tag{D.31}$$

Where: V^e is the tetrahedron over which the integral is evaluated, N_{tet} is the total number of tetrahedrons, and μ_r^e is the relative permittivity of the medium that tetrahedron e is part of.

The integral involving the first term of the integrand of equation (D.30) over a tetrahedron is given by:

$$\iiint_{V^e} (\nabla \times \mathbf{N}_i^e) \cdot (\nabla \times \mathbf{N}_{i'}^e) \, dV$$

Where:

$$\nabla \times \mathbf{N}_{i'}^e = \nabla \times l_{i'} (L_{i'1}^e \nabla L_{i'2}^e - L_{i'2}^e \nabla L_{i'1}^e) \tag{D.32}$$

$$= l_{i'} (\nabla \times (L_{i'1}^e \nabla L_{i'2}^e) - \nabla \times (L_{i'2}^e \nabla L_{i'1}^e)) \tag{D.33}$$

$i'1$ and $i'2$ are the indices of the nodes at the ends of edge i. The indices are the numbers assigned to the nodes of the tetrahedrons, i.e., the bold numbers in figure D.5. Using the following vector identity:

$$\nabla \times (\phi \mathbf{A}) = \nabla \phi \times \mathbf{A} + \phi \nabla \times \mathbf{A} \tag{D.34}$$

With: $\mathbf{A} = \nabla L$ and $\phi = L$; equation (D.33) becomes:

$$\nabla \times \mathbf{N}_{i'}^e = l_{i'} (\nabla L_{i'1}^e \times \nabla L_{i'2}^e + L_{i'1}^e \nabla \times \nabla L_{i'2}^e - \nabla L_{i'2}^e \times \nabla L_{i'1}^e - L_{i'2}^e \nabla \times \nabla L_{i'1}^e) \tag{D.35}$$

The curl of the divergence of an arbitrary scalar variable is equal to zero, i.e.:

$$\nabla \times \nabla \phi = 0 \tag{D.36}$$

Where ϕ is an arbitrary scalar variable. Therefore, equation (D.35) becomes:

$$\nabla \times \mathbf{N}_{i'}^e = l_{i'} (\nabla L_{i'1}^e \times \nabla L_{i'2}^e - \nabla L_{i'2}^e \times \nabla L_{i'1}^e) \tag{D.37}$$

$$= 2l_i (\nabla L_{i'1}^e \times \nabla L_{i'2}^e) \tag{D.38}$$

$$= \frac{l_i}{18 (v^e)^2} (c_{i'1} d_{i'2} - c_{i'2} d_{i'1}, \, d_{i'1} b_{i'2} - d_{i'2} b_{i'1}, \, b_{i'1} c_{i'2} - b_{i'2} c_{i'1}) \tag{D.39}$$

If F_{rs}^i is defined as:

$$F_{rs}^i = (c_r d_s - c_s d_r, \, d_r b_s - d_s b_r, \, b_r c_s - b_s c_r) \tag{D.40}$$

Where i is the edge index. Then, it can be shown that:

$$\iiint_{V^e} (\nabla \times \mathbf{N}_{i'}^e) \cdot (\nabla \times \mathbf{N}_{j'}^e) \, dV = \frac{l_{i'} l_{j'}}{324 (v^e)^3} F_{i'1i'2}^{i'} \cdot F_{j'1j'2}^{j'} \tag{D.41}$$

Where v^e is the volume of tetrahedron V^e.

The integral involving the second term of the integrand of equation (D.30) over a tetrahedron is given by:

$$\iiint_{V^e} \mathbf{N}_{i'}^e \cdot \mathbf{N}_{j'}^e \, dV$$

Where:

$$\mathbf{N}_{i'} \cdot \mathbf{N}_{j'}^e = l_{i'} l_{j'} (L_{i'1}^e \nabla L_{i'2}^e - L_{i'2}^e \nabla L_{i'1}^e) \cdot (L_{j'1}^e \nabla L_{j'2}^e - L_{j'2}^e \nabla L_{j'1}^e) \tag{D.42}$$

The above equation is expanded using the distributive property of the vector dot product, into:

$$\mathbf{N}_{i'} \cdot \mathbf{N}_{j'}^e = l_{i'} l_{j'} (L_{i'1}^e L_{j'1}^e (\nabla L_{i'2}^e \cdot \nabla L_{j'2}^e) - L_{i'1}^e L_{j'2}^e (\nabla L_{i'2}^e \cdot \nabla L_{j'1}^e) - \tag{D.43}$$
$$L_{i'2}^e L_{j'1}^e (\nabla L_{1'1}^e \cdot \nabla L_{j'2}^e) + L_{1'2}^e L_{j'2}^e (\nabla L_{i'1}^e \cdot \nabla L_{j'1}^e))$$

If C_{st} is defined as:

$$C_{st} = \nabla L_s \cdot \nabla L_t \tag{D.44}$$

$$= b_s b_t + c_s c_t + d_s d_t \tag{D.45}$$

Then equation (D.43) is written in a more simplified form as:

$$\mathbf{N}_i^e \cdot \mathbf{N}_{i'}^e = l_{i'} l_{j'} \left(C_{i'2j'2} L_{i'1}^e L_{j'1}^e - C_{i'2j'1} L_{i'1}^e L_{j'2}^e - C_{i'1j'2} L_{i'2}^e L_{j'1}^e + C_{i'1j'1} L_{i'2}^e L_{k'2}^e \right) \tag{D.46}$$

Thus:

$$\iiint_{V^e} \mathbf{N}_i^e \cdot \mathbf{N}_{i'}^e \, dV = \iiint_{V^e} l_i^e l_{i'}^e \{ C_{kk'} L_j^e L_{j'}^e - C_{kj'} L_j^e L_{k'}^e - C_{jk'} L_k^e L_{j'}^e + C_{jj'} L_k^e L_{k'}^e \} \, dV \tag{D.47}$$

Where:

$$\iiint_{V^e} L_l^e L_n^e \, dV = \frac{v^e}{20} (1 + \delta_{ln}) \tag{D.48}$$

Using the following equation [1]:

$$\iiint_{V^e} (L_1^e)^k (L_2^e)^l (L_3^e)^m (L_4^e)^n \, dV = \frac{k! l! m! n!}{(k + l + m + n)!} 6 V^e \tag{D.49}$$

l and n in equation (D.48) are the indices of the tetrahedron or triangle nodes, and δ_{ln} is defined as follows:

$$\delta_{ln} = \begin{cases} 1 & \text{if } l = n \\ 0 & \text{otherwise} \end{cases} \tag{D.50}$$

Therefore:

$$\iiint_{V^e} \mathbf{N}_{i'}^e \cdot \mathbf{N}_{j'}^e \mathrm{d}V = \frac{V^e l_{i'}^e l_{j'}^e}{20} \{ C_{i'2j'2}(1 + \delta_{i'1j'1}) - C_{i'2j'1}(1 + \delta_{i'1j'2}) - \tag{D.51}$$
$$C_{i'1j'2}(1 + \delta_{i'2j'1}) + C_{i'1j'1}(1 + \delta_{i'2j'2}) \}$$

The volume integral of equation (D.31) is evaluated as follows. Firstly the definition of the impressed electric current density (equation (D.5)) is substituted into the volume integral part to give:

$$\mathrm{I} \iiint_{V^v} \sum_{i'=1}^{4} \mathbf{N}_{i'} \cdot \hat{z}\delta(x - x_s)\delta(y - y_s)\mathrm{d}V \tag{D.52}$$

The delta functions ($\delta(x - x_s)$ and $\delta(y - y_s)$), reduce the volume integral into a line integral over the z-axis. Where only the basis function, which has a non-zero tangential component in the direction of the z-axis contributes to the integral. This is because of the vector dot product with vector that is tangential to the z-axis, i.e., $\hat{z}$. Therefore, the integral evaluates to:

$$\iiint_{V^e} \sum_{i'=1}^{N} \mathbf{N}_{i'} \cdot (\mathrm{I}\delta(x - x_s)\delta(y - y_s)\hat{z})\mathrm{d}V = \mathrm{I}|z_e - z_s| \tag{D.53}$$

Where z_e and z_s are the z components of the nodes at the start and end points of edge i'.

D.7.2 Surface Integral

Following the discussion in section D.7, the surface integral is represented as:

$$\oiint_S \mathbf{N}_{i'} \cdot \mathbf{R}_{j'} \mathrm{d}S = \sum_{e}^{N_{\text{tri}}} \iint_{S^e} \mathbf{N}_{i'}^e \cdot \mathbf{R}_{j'}^e \mathrm{d}S$$

Where: S_e is one of the triangles that are part of S, and N_{tri} is the number of triangles that S is divided into. The integral over the triangle is evaluated in this section, i.e.:

$$\iint_{S^e} \mathbf{N}_{i'}^e \cdot \mathbf{R}_{j'}^e \mathrm{d}S$$

Using the definition of R from section C.4.1 of appendix C the integral above is expanded as follows:

$$\iint_{S^e} \mathbf{N}_{i'}^e \cdot \mathbf{R}_{j'}^e \mathrm{d}S = \iint_{S^e} \frac{l_{i'}^e l_{j'}^e}{2s^e}(\mathbf{r} - \mathbf{r}_n) \cdot \mathbf{W}_{j'k'}^e \mathrm{d}S \tag{D.54}$$

$$= \iint_{S^e} \frac{l_{i'}^e l_{j'}^e}{2s^e}(\mathbf{r} \cdot \mathbf{W}_{j'k'}^e)\mathrm{d}S - \iint_{S^e} \frac{l_{i'}^e l_{j'}^e}{2s^e}(\mathbf{r}_n \cdot \mathbf{W}_{j'k'}^e)\mathrm{d}S \tag{D.55}$$

$$= \frac{l_{i'}^e l_{j'}^e}{2s_e} \left(\iint_{S^e} \mathbf{r} \cdot \mathbf{W}_{j'k'}^e \mathrm{d}S - \iint_{S^e} \mathbf{r}_n \cdot \mathbf{W}_{j'k'}^e \mathrm{d}S \right) \tag{D.56}$$

Where: s^e is the area of S^e, $\mathbf{r}_n$ is the position vector at the node of the triangles, which is opposite the edge j', and it is assumed that S^e is positive inline with the definition of the RWG basis function. The integral of the first term, of the integrand in equation (D.56) is given by:

$$\iint_{S^e} \mathbf{r} \cdot \mathbf{W}_{i'1i'2}^e \mathrm{d}S = \iint_{S^e} \mathbf{r} \cdot ((\nabla L_{i'2}^e)L_{i'1}^e - (\nabla L_{i'1}^e)L_{i'2}^e)\mathrm{d}S \tag{D.57}$$

$$= \iint_{S^e} (\mathbf{r} \cdot \nabla L_{i'2}^e)L_{i'1}^e \mathrm{d}S - \iint_{S^e} (\mathbf{r} \cdot \nabla L_{i'1}^e)L_{i'2}^e \mathrm{d}S \tag{D.58}$$

Equation (D.58) is then expanded into:

$$\iint_{S^e} \mathbf{r} \cdot \mathbf{W}_{i'1i'2}^e \mathrm{d}S = \frac{1}{4s^{e2}} \iint_{S^e} \left((b_{i'2}u + c_{i'2}v)(a_{i'1} + b_{i'1}u + c_{i'1}v) - \right.$$
$$\left. (b_{i'1}u + c_{i'1}v)(a_{i'2} + b_{i'2}u + c_{i'2}v) \right)\mathrm{d}S \tag{D.59}$$

Simplifying the above equation and adding $a_{i'1}a_{i'2} - a_{i'1}a_{i'2}$ gives:

$$\iint_{S^e} \mathbf{r} \cdot \mathbf{W}^e_{i'1i'2} dS = \frac{1}{4s^{e2}} \iint_{S^e} \Bigg(a_{i'1}(a_{i'2} + b_{i'2}u + c_{i'2}v) - $$
$$a_{i'2}(a_{i'1} + b_{i'1}u + c_{i'1}v) \Bigg) dS \tag{D.60}$$

The above equation can be written in compact form as:

$$\iint_{S^e} \mathbf{r} \cdot \mathbf{W}^e_{i'1i'2} dS = \frac{1}{2s^e} \iint_{S^e} \left(a_{j'} L^e_{k'} - a_{k'} L^e_{j'} \right) dS \tag{D.61}$$

$$= \frac{1}{2s^e} \left(a_{i'1} \iint_{S^e} L^e_{i'2} dS - a_{i'2} \iint_{S^e} L^e_{i'1} dS \right) \tag{D.62}$$

Using the following relation for simplex coordinates on triangles [1]:

$$\iint_{S^e} (L^e_1)^l (L^e_2)^m (L^e_3)^n dS = \frac{l!m!n!}{(l+m+n+2)!} 2s^e \tag{D.63}$$

Equation (D.62) becomes:

$$\iint_{S^e} \mathbf{r} \cdot \mathbf{W}^e_{i'1i'2} d = \frac{(a_{j'} - a_{k'})}{2s^e} \frac{2s^e}{3!} \tag{D.64}$$

$$= \frac{a_{i'1} - a_{i'2}}{6} \tag{D.65}$$

The integrand of the second integral in equation (D.56) is expanded as follows:

$$\iint_{S_e} \mathbf{W}^e_{i'1i'2} dS = \iint_{S_e} \left((\nabla L^e_{i'2}) L^e_{i'1} - (\nabla L^e_{i'1}) L^e_{i'2} \right) dS \tag{D.66}$$

$$= \iint_{S_e} (\nabla L^e_{i'2}) L^e_{i'1} dS - \iint_{S_e} (\nabla L^e_{i'1}) L^e_{i'2} dS \tag{D.67}$$

$$= \nabla L^e_{i'2} \iint_{S_e} L^e_{i'1} dS - \nabla L^e_{i'1} \iint_{S_e} L^e_{i'2} dS \tag{D.68}$$

$$= (\nabla L^e_{i'2} - \nabla L^e_{i'1}) \frac{2s_e}{6} \tag{D.69}$$

$$= \frac{1}{6} (b_{i'2} - b_{i'1}, c_{i'2} - c_{i'1}) \tag{D.70}$$

Therefore:

$$\iint_{S^e} \mathbf{N}^e_{i'} \cdot \mathbf{R}^e_j dS = \frac{l^e_{i'} l^e_j}{12s^e} \left((a_{i'1} - a_{i'2}) - \mathbf{r}_n \cdot (b_{i'2} - b_{i'1}, c_{i'2} - c_{i'1}) \right) \tag{D.71}$$

And if S^e is negative in-line with the definition of the RWG basis function, the integral becomes:

$$\iint_{S^e} \mathbf{N}^e_{i'} \cdot \mathbf{R}^e_{j'} dS = \frac{l_{i'} l_{j'}}{12s^e} \left(\mathbf{r}_n \cdot (b_{i'2} - b_{i'1}, c_{i'2} - c_{i'1}) - (a_{i'1} - a_{i'2}) \right) \tag{D.72}$$

D.8 Conclusion

An overview of the FEM procedure for reducing a FEM formulation to a matrix equation is presented, and applied in reducing the FEM formulation part of the FEM-MoM formulation used for analysis of printed antennas to a matrix equation.

The FEM formulation gives the relation between the electric field within a volume region and the equivalent electric current density on the bounding surface of the volume region. The region where the electric field is computed is represented as a connection of tetrahedrons, and the electric field within each tetrahedron is expanded using vector edge basis functions whose unknowns are the magnitude of the tangential component of the electric field across the edge. Since the tetrahedrons are used for representing the region where the electric field is computed: the enclosing surface is represented by a connection of triangles, which are the faces of the tetrahedrons on the enclosing surface. The RWG basis functions are used for expanding the equivalent electric current density on the enclosing surface. Equations for the resulting matrix equations are presented and the closed form expressions for the integrals are derived.

References

[1] J. Jin. *The Finite Element Method in Electromagnetics*. New York: John Wiley and Sons, Inc., second ed., 2002.

[2] L. K. J.L. Volakis, A. Chatterjee. *Finite Element Method for Electromagnetics: Antennas, Microwave Circuits, and Scattering Applications*. New York: IEEE Press, first ed., 2001.

[3] M. Sadiku. *Numerical Techniques in Electromagnetics*. London: CRC Press, second ed., 2001.

[4] J. Webb. "Edge Elements and What They Can Do for You." *IEEE Transactions on Magnetics*, vol. 29, no. 2, pp. 1460–1465, 3 1993.

[5] D. B. Davidson. *Computational Electromagnetics for RF and Microwave Engineering*. Cambridge, first ed., 2005.

Appendix E

Solution of Matrix Equations

MoM (Method of Moments) and FEM (Finite Element Method) formulations part of the hybrid FEM-MoM formulation derived for the analysis of probe-fed printed antennas in section A.3 of appendix A, were reduced to matrix equations in appendices C and D respectively. The subject of this appendix is the solution of the matrix equations from appendices C and D for the unknown quantities.

The matrix equations that resulted form the reductions are given by equations (E.1) and (E.2), for the FEM and MoM formulations respectively.

$$[K]\{E\} + [B]\{I^{\mathbf{J}_{\mathrm{eq}}}\} = \{C\} \tag{E.1}$$

$$[Z^{\mathbf{M}_{\mathrm{eq}}}]\{I^{\mathbf{M}_{\mathrm{eq}}}\} + [Z^{\mathbf{J}_{\mathrm{eq}}}]\{I^{\mathbf{J}_{\mathrm{eq}}}\} = \{V\} \tag{E.2}$$

Where:

- $[K]$ is a $N_V \times N_V$ sparse matrix.
- $[B]$ is a $N_S \times N_S$ sparse matrix.
- $[Z^{\mathbf{J}_{\mathrm{eq}}}]$ and $[Z^{\mathbf{M}_{\mathrm{eq}}}]$ are $N_S \times N_S$ fully populated matrices.
- $\{E\}$ is an $N_V \times 1$ column vector.
- $\{I^{\mathbf{J}_{\mathrm{eq}}}\}$ and $\{I^{\mathbf{M}_{\mathrm{eq}}}\}$ are $N_S \times 1$ column vectors.

The above equations are solved using a procedure, which is termed the outward looking approach in the literature [1]. Equation (E.2) is written in terms of $\{I^{\mathbf{J}_{\mathrm{eq}}}\}$ as follows:

$$\{I^{\mathbf{J}_{\mathrm{eq}}}\} = [Z^{\mathbf{J}_{\mathrm{eq}}}]^{-1}\left(\{V\} - [Z^{\mathbf{M}_{\mathrm{eq}}}]\{I^{\mathbf{M}_{\mathrm{eq}}}\}\right) \tag{E.3}$$

$\{I^{\mathbf{J}_{\mathrm{eq}}}\}$ in the equation above is then substituted into equation (E.1) and the resulting equation is given by:

$$[K]\{E\} + [B][Z^{\mathbf{J}_{\mathrm{eq}}}]^{-1}\left(\{V\} - [Z^{\mathbf{M}_{\mathrm{eq}}}]\{I^{\mathbf{M}_{\mathrm{eq}}}\}\right) = \{C\} \tag{E.4}$$

Corresponding entries of $\{E\}$ and $\{I^{\mathbf{M}_{\mathrm{eq}}}\}$ are equal in magnitude, but have different signs; i.e. one is positive while the others are negative. This is for the edges on S in $\{E\}$. Therefore, equation (E.4) becomes:

$$\left([K] - [B][Z^{\mathbf{J}_{\mathrm{eq}}}]^{-1}[Z^{\mathbf{M}_{\mathrm{eq}}}]\right)\{E\} = \{C\} - [B][Z^{\mathbf{J}_{\mathrm{eq}}}]^{-1}\{V\} \tag{E.5}$$

Let:

$$[K'] = [K] - [B][Z^{\mathbf{J}_{\mathrm{eq}}}]^{-1}[Z^{\mathbf{M}_{\mathrm{eq}}}] \tag{E.6}$$

$$\{C'\} = \{C\} - [B][Z^{\mathbf{J}_{\mathrm{eq}}}]^{-1}\{V\} \tag{E.7}$$

Substituting the above equations in equation (E.5) gives:

$$[K']\{E\} = \{C'\} \tag{E.8}$$

The above equation can then be used for solution of $\{E\}$. The relevant entries of $\{I^{\mathbf{J}_{\mathrm{eq}}}\}$ are then obtained from $\{E\}$ and used in equation (E.2) for solution of $\{I^{\mathbf{M}_{\mathrm{eq}}}\}$.

$[K']$ is will usually be a large matrix with more that 1000 columns and rows; and this is for small problems. Therefore, it will require a considerable amount of memory if solved using a direct solver and an iterative solver must be used to keep the memory usage low and to take advantage or sparsity of the matrix. An efficient pre-conditioner, which may be used with the iterative solver is presented in [1, p. 471-480].

References

[1] J. Jin. *The Finite Element Method in Electromagnetics*. New York: John Wiley and Sons, Inc., second ed., 2002.

Appendix F

fmsolver User Manual

F.1 Introduction

fmsolver (Finite Element Method - Method of Moments Solver) is a software application for the analysis of probe-fed printed antennas. The analysis is performed using coupled differential and integral equation formulations. The differential equation formulation relates the field within a volumetric region that encloses the antenna structure and the tangential magnetic field on the boundary of the region. The integral equation relates the tangential electric and magnetic fields at the enclosing boundary. Solution of the differential and integral equations are performed numerically using FEM (Finite Element Method) and MoM (Method of Moments) respectively.

Enclosing Boundary

Boundary Separation Distance

Free-Space

Substrate Thickness

Conducting Surface

Boundary Separation Distance

(a)

Boundary Separation Distance

Substrate

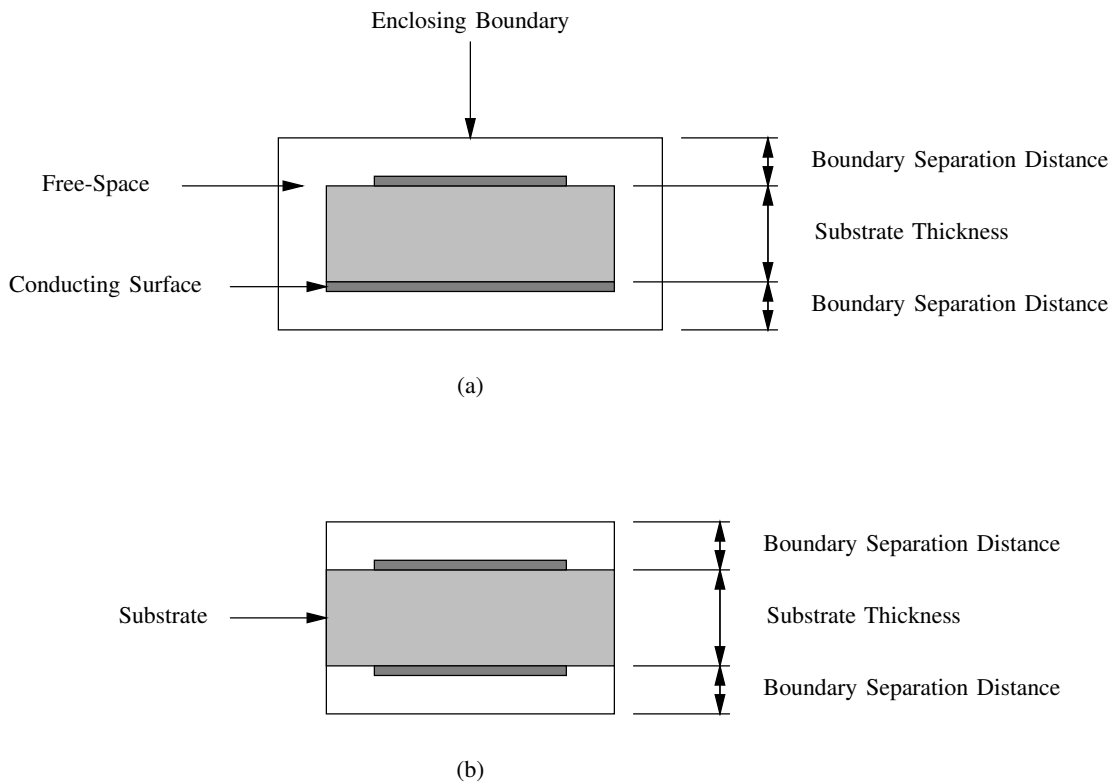Substrate Thickness

Boundary Separation Distance

(b)

Figure F.1: Cross-section of the volumetric region where the electric field distribution is computed.

The volume region where the electric field is computed, is created by enclosing the antenna structure within an enclosure such that the boundary of the enclosure does not touch conducting surface/s of the antenna.

This is because the implementation of the formulation does not account for the case where the boundary of the region touches conducting surface/s within the region. Figure F.1 shows the cross-section of an example region, where it can be seen that the boundary surfaces in both (a) and (b) do not touch any of the conducting surfaces. The boundary of the enclosing region can assume any shape but it must be made conformal to the antenna structure that it encloses for efficiency reasons. The enclosing boundary can also touch the side of the substrate that does not have any conducting surfaces as shown in figure F.1 (b).

Only antenna structures with homogenous substrates can be analysed and antenna parameters that can be computed are:

- Input impedance
- Radiation/Scattering pattern
- Near electric field distribution

The formulation can also be used for the scattering of dielectric structure with/without embedded conducting surfaces. Integral and differential equation formulations can be used separately for the analysis of:

- Conducting surfaces excited by plane wave.
- Eigen-mode solutions of dielectric cavities with conducting outer walls.

Parameters that can be computed for the above structures are:

- Scattering pattern
- Near fields
- Current magnitude distribution
- Resonant frequencies of a cavity

First three parameters for a conducting surface, and the last one for the cavity with conducting walls. The integral equation formulation can only be applied for continuous surfaces with no branches, see figure F.2. Conducting surfaces with branches can be analysed using the hybrid formulation by embedding the surface within a dielectric whose dielectric properties are similar to those of free space.

The information in the manual is presented as follows. The input and output specification of the *fmsolver* are presented in section F.2. Commands that can be used with the *fmsolver* are presented in section F.3. Then, the error messages that are generated by the *fmsolver* are discussed in section F.4 and an example input file is presented in section F.5.

F.2 Program Input and Output

Input into the application is specified via two files, namely: the *input file* and *mesh file/s*. *input file* contains the commands for specifying the required analysis, parameters to be computed, and additional data about the structure that must be analysed. This file must have a ".fm" extension. The *mesh file/s* contains the geometric elements that the structure to be analysed is divided into. This is because structures to be analysed have to be divided into either triangles or tetrahedrons: triangles for surfaces and tetrahedrons for 3D objects. Simulation results from the application are presented in the *output file*. The *output file* has the same name as the *input file* and a ".out" extension.

Details of the files that are discussed above are presented in the following sections.

F.2.1 Mesh File

Structures to be analysed must be divided into either triangles or tetrahedrons, as already indicated. These triangles or tetrahedrons must be specified in a *mesh file*.
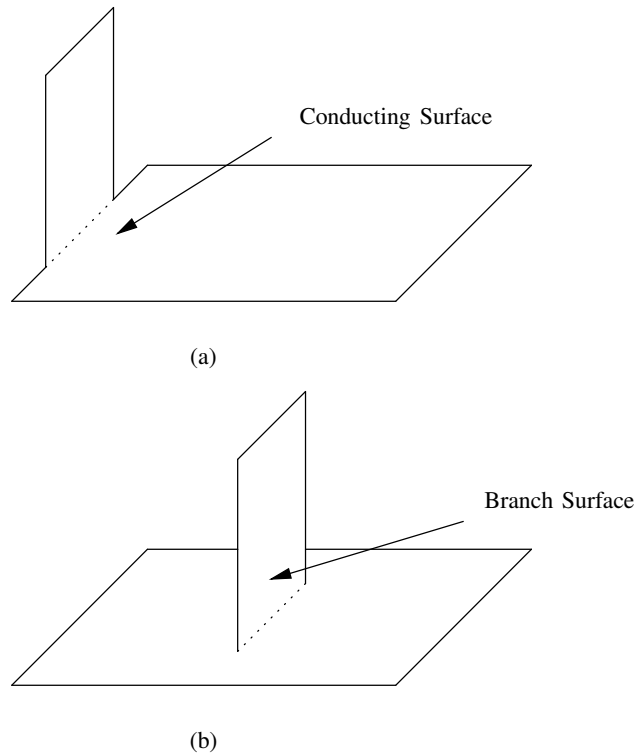
(a)

(b)

Figure F.2: Continuos surface (a), and surface with a branch (b).

Geometric details of all the structures, which can be analysed using *fmsolver* except the probe-fed printed antenna are represented by one mesh file. The geometric details of the probe-fed printed are presented using two mesh files and the format for one of the mesh files is similar to that for the other structures. The specification of the mesh file that is common for all the structures is presented.

(a)

(b)
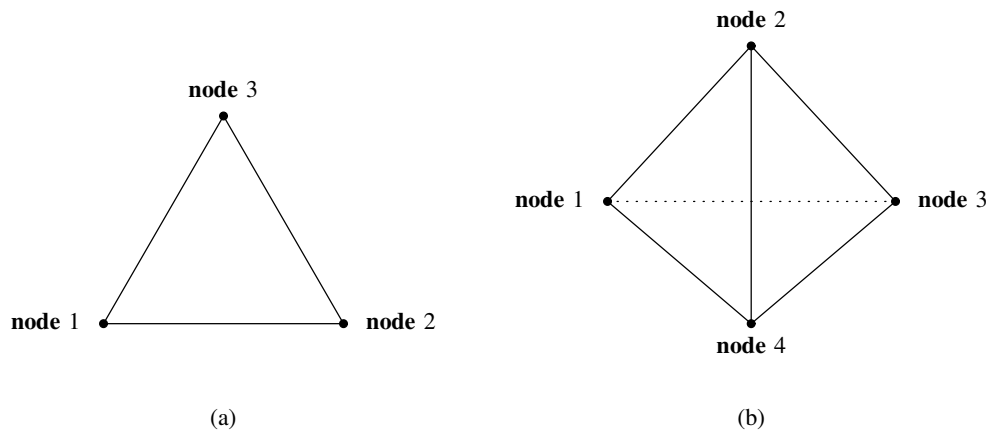
Figure F.3: Triangle (b) and Tetrahedron (b) with node definitions.

The *mesh file* must contain the following data:

- A list of all the nodes that result from the division of the structure into either triangles or tetrahedrons (see figure F.3). The list of the nodes must be ordered, i.e. the position of the node in the list must correspond to the *tag* of the node. A *tag* is the number that is used for identifying the nodes instead of using coordinate values. The following data must be specified: *x*, *y*, and *z* components of the coordinate of the node. The *tag* may be specified as part of the data, but it is not necessary as the position of the

node in the node list is used as a tag. This is the reason why it is important that the nodes be ordered according to *tag* values.

- A list of tetrahedrons and/or triangles. The data that is required for the triangle and the tetrahedron is:
    - *tags* of the nodes that are part of the triangle or tetrahedron (see figure F.3) specified in any order.
    - A *region tag*, which is a number that associates the triangle or tetrahedron with a region of the mesh. Consider a 3D structure made by gluing two dielectric substrates with different electromagnetic properties together. This structure is represented by a mesh of tetrahedrons. In order to analyse the structure; the different substrates are assigned *region tags*, which are assigned to the tetrahedrons that are part of the substrate and will be used for identifying them so they can be assigned the electromagnetic properties of the substrate.

This application can read mesh files that are created using Gmsh. It automatically sorts the nodes in the mesh such that the first node in the list has a *tag* value of 1 and so on. This is done because the nodes of meshes that are created using Gmsh are not sorted in general. Therefore, *mesh files* that are used with this application must use *mesh file* format used in Gmsh (www.guez.org/gmsh).

F.2.1.1 Continous Conducting Surfaces

Continuous conducting surfaces can be used for modeling:

- Conducting surface, which may be open or closed.
- Conducting wires using the strip approximation (see [1, p. 456]).

These structures are represented by a mesh of triangles.

Structures that are made of more than one continuous surface but are not joined can also be analysed. An example of such a structure is two conducting plates placed a distance from one another.

F.2.1.2 Dielectric Volumes

Dielectric volumes can be used for modeling:

- Dielectric bodies that are both homogeneous and inhomogeneous.
- Conducting surfaces, which must be embedded within a dielectric region whose electromagnetic properties are similar to those of free-space unless the conducting surface is actually embedded inside a dielectric.
- Cavities with conducting walls.

These structures are represented by a mesh of tetrahedrons.

If the structure has embedded conducting surfaces, then the triangles that are part of the conducting surface/s must be specified in the *mesh file*. The embedded conducting surfaces can be open or closed and the open surfaces do not have to be continuous. However, it is more efficient to represent continuous conducting surfaces as triangles so that they can be solved using the integral equation formulation.

region tags must be assigned to the different regions of an inhomogeneous dielectric volume, with similar electromagnetic properties. The *region tags* must then be assigned to the tetrahedrons that are part of the different regions of the dielectric volume. Then *region tags* together with the electromagnetic properties of the regions are specified in the *input file*. Triangles that represent embedded conducting surface must also be assigned a *region tag*, which will be used for identifying them when they are available in the *mesh file*. The *region tag* for the triangles must also be specified in the *input file*.

Lastly, the outer surface of a dielectric cavity are assumed to be a PEC (perfect electrical conductor) when computing the resonant frequencies of a dielectric cavity.

F.2.1.3 Probe-Fed Printed Antenna Structure

This structure consists of a dielectric substrate of finite thickness with conducting surfaces on the top and bottom sides of the substrate. An example probe-fed printed antenna structure is shown in figure F.4. The probe feed for this structures is represented by a line of constant current distribution.
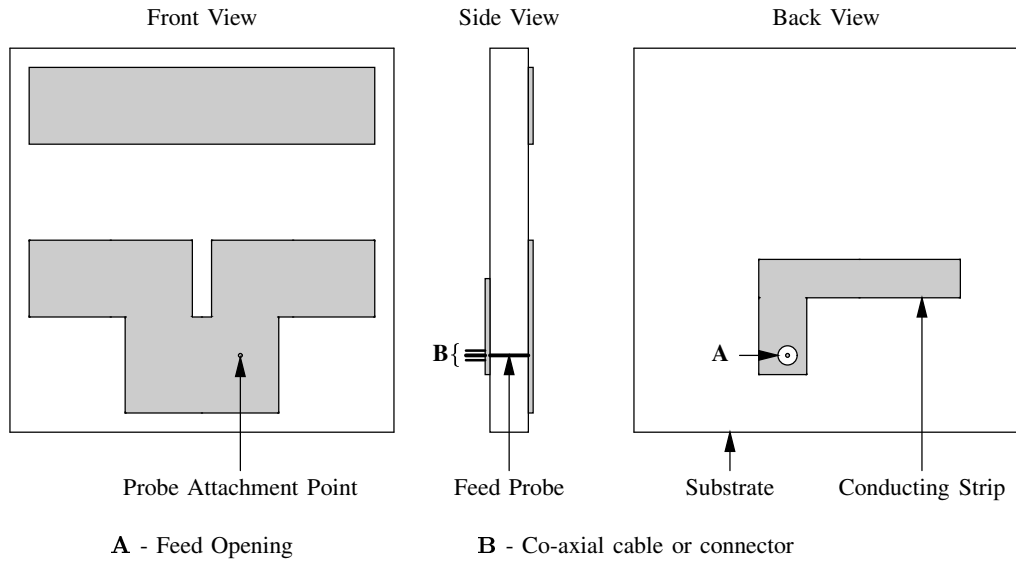
Figure F.4: Example probe-fed printed antenna structure.

These structures are represented by a mesh of tetrahedrons. They are described in this application using two mesh files: one *mesh file* contains the nodes and triangles for the discretisation of the surface that contains the details of the conducting regions of the antenna, and the other *mesh file* contains a listing of the tetrahedrons that the structure is divided into. It is assumed that the antenna structures have conducting surfaces on opposite sides of the substrate.

Figure F.5: Surface with details of the front and back views of the antenna structure in figure F.4.

Meshes for these structures are created as follows:

- Details of the sides of the antenna structure with conducting surfaces are represented on a surface structure that is similar to the one shown in figure F.5. The surface structure must be similar to substrate as shown in figure F.5. This is on condition that the edges of the conducting on neither side of the ant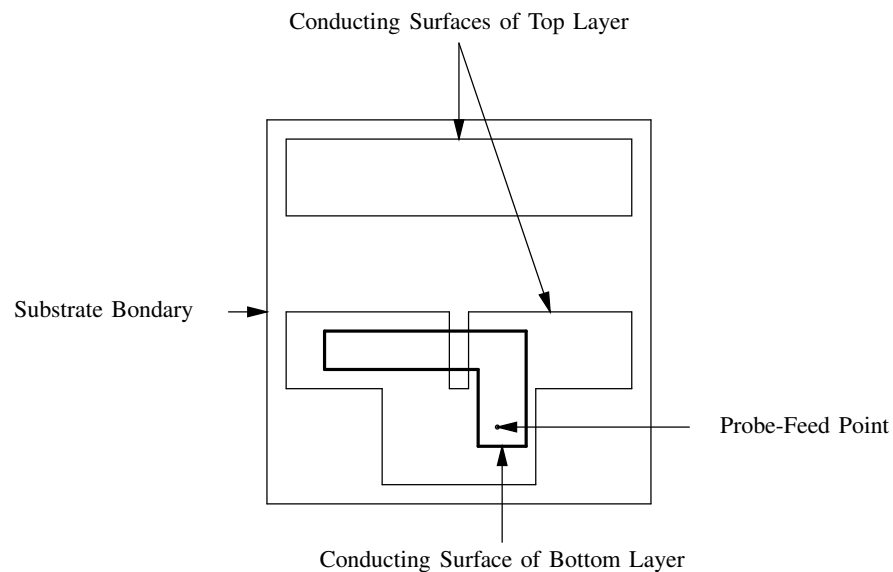enna structure are on the substrate boundary (see figure F.5), otherwise an additional boundary is required to ensure that no part of the boundary touches conducting surfaces of the antenna structure.
- The next step is to create a triangle mesh of the surface from the previous step. The *mesh file* must contain the following:
  - Triangles that are part of the top conducting surface/s, bottom conducting surface/s, substrate, and free-space region with appropriate *region tags*.
  - Triangles that are not part of the top and bottom conducting surfaces, also with appropriate *region tags*.
  - Nodes for feed or shorting pins, which must also be assigned *region tag/s*.

  The *region tags* above are used for identifying the different regions in the mesh and must be specified in the *input file*.
- Then the *mesh file* from the previous step is used as input for the Matlab function *tetmesh*, which uses the node data in the *mesh file* to create tetrahedrons that make up the 3D structure together with the additional tetrahedrons for the free space region that is required to ensure that the boundary of the region does not coincide with conducting surfaces of the structure. The *mesh file* must be sorted before using it as input into the Matlab function, this is done using the *mshsort* application provided with this application. This function produces a file called *tetrahedron.out*, which contain tetrahedron that the structure is divided into. It must be used together with the *mesh file* as input into this application.

F.2.2 Input File

The format of the input file is shown in table F.1. The file is divided into three sections: the problem data, geometry data, and analysis request sections. These three different sections are discussed in the following sections.

Table F.1: Format of the input file

MFP …
STR …
EX …
FR …
GDB
$\vdots$
…*electric and magnetic properties of the tetrahedrons making-up the structure* …
$\vdots$
GDE
ARB
$\vdots$
…*analysis requests* …
$\vdots$
ARE

F.2.2.1 Problem Data

The problem data section of the input file is used for specifying, the following information to the solver:

- Path of the mesh file.

- Type of structure that is represented by the elements in the *mesh file*.
- Information regarding the elements making-up the mesh.
- Excitation for the structure.
- Simulation frequency/frequencies.

The information above is specified using the commands in table F.2, and the commands in this section of the file, must be specified exactly in the order that is shown in table F.1, otherwise the program will give an error.

Table F.2: Commands for the problem data section of input file

Command	Purpose
MFP	For specifying the path of the mesh file
STR	For specifying the type of the structure that is described by the mesh file
EX	For specifying the excitation for the structure
FR	For specifying the simulation frequency/frequencies

F.2.2.2 Geometry Data

The section of the input file between GDB (*Geometry Data Begin*) and GDE (*Geometry Data End*) and contains information regarding the mesh elements that the structure is divided into. This is information such as; the *region tags* used to identify elements that represent different regions of the structure represented by the mesh and the electromagnetic properties (permittivity and permeability) of the regions. The information is specified using the commands shown in table F.3.

Table F.3: Commands for specifying additional information about the mesh elements.

Command	Purpose
DE	For specifying electric and magnetic properties of the tetrahedrons, which compose the dielectric region of the structure.
FS	For identifying the tetrahedrons in the *mesh file*, which compose the free-space region of the structure.

F.2.2.3 Analysis Request

This is the section of the input file between ARB (*Analysis Request Begin*) and ARE (*Analysis Request End*). The following parameters can be requested:

- Near fields for conducting surfaces and probe-fed printed antenna structures.
- Radiation/Scattering pattern for conducting surfaces and probe-fed printed antenna structures.
- Current density distributions: electric current density distributions for all structures except the dielectric volume with no excitation, and magnetic current distributions for all structures except dielectric volume with no excitation and conducting surfaces.
- Electric field within a dielectric volume.

The input impedance of the probe-fed printed antenna that is excited by a probe-feed is computed by default and does not need to be requested.

The commands that are used to request computation of the parameters above are shown in table F.4

Table F.4: Commands for specifying additional information about the mesh elements.

Command	Purpose
NF	Request computation of near fields.
FP	Request computation of the scattering/radiation pattern.
CD	Request computation of current distribution.
EF	Request computation of field inside a dielectric volume.

F.2.3 Output File

The output files contains:

- Information about the structure being simulated. This is: the name of the structure, and the number of elementary geometric elements that are part of the structure.
- Time taken to compute matrices for solution of the different formulations and the solution time.
- Simulation results.

Simulation results are presented in table form. Each table has a title to indicate the data that is presented in the table. Columns of each table are labeled and the labels indicate the data that is presented in the column with the units. The current density data is specified as the magnitude of the current density at the nodes of the triangles that are part of the structure (for conducting surface) or the enclosing boundary of the structure (for dielectric volume and probe-fed printed antenna). This data is specified per triangle, and the entries will be repeated.

F.3 Commands

Detailed specification of the commands that are discussed in section F.2.2 are presented.

F.3.1 MFP Command

The MFP command has the following form:

- MFP *file_path*

Where: *file_path* is the full path of the mesh file. E.g.; *c:\meshes\sphere.msh*, for a mesh file with name *sphere.msh* residing in a folder called *meshes* on the drive with letter *c* on a machine running Microsoft Windows. As stated this command must be the first command in the input file.

F.3.2 STR Command

The STR is used for specifying the type of structure that is represented by the mesh. Structures that can be specified are: metal surface, probe-fed printed antenna, and dielectric volumes. Each of these structures are specified by adding the following strings after the STR command:

- CS: for conducting surface.
- PA: for probe-fed printed antenna.
- DV: for dielectric volume.

Input arguments options change, depending on the structure that is specified. The different command options for different structures are presented in the following sections.

F.3.2.1 Conducting Surface

For conducting surface structures, the command takes the following form:

- STR CS *x_comp y_comp z_comp cs_rgn_tag*

The definitions of the input arguments for the above command are given in table F.5. *x_comp*, *y_comp*, and *z_comp* are the components of the reference point, which is the point that is used as a reference when computing the normals of the triangles. E.g., when the surface is a closed, the reference point is any point inside the structure. This reference point is used to guarantee that the normals of the triangles point towards the outside of the structure. The reference point for open surfaces must be selected such that all the triangles have consistent normals; e.g.: only points $\mathbf{P}_1$ and $\mathbf{P}_2$ will result in consistent normals for the open surface of figure F.6, and points $\mathbf{P}_3$ and $\mathbf{P}_4$ will result in inward pointing normals for one section of the surface and outward pointing normal for the other section of the surface.
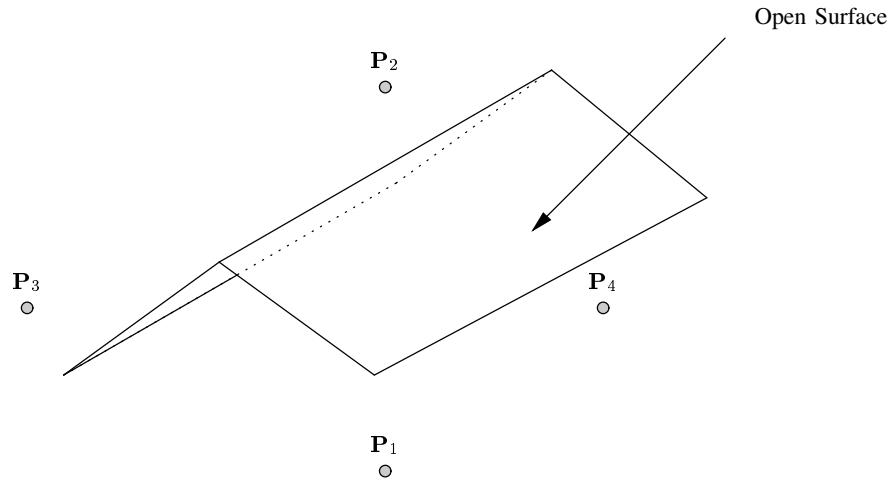

Figure F.6: Open surface with four reference points.

Table F.5: Definition of the arguments of STR CS … command.

Parameter	Type	Function
x_comp	float	X, Y, and Z components of the reference point in meters.
y_comp		
z_comp		
cs_rgn_tag	int	*region tag* for the triangles in the mesh that are part of the conducting surface.

F.3.2.2 Probe-Fed Printed Antenna

The command assumes the following form for a probe-fed printed antenna structure:

- STR PA *no_pins* [*pin_rgn_tag*] *top_cs_tag not_top_cs_tag bot_cs_tag not_bot_cs_tag sbstrt_rgn_tag bndry_rgn_tag bndry_sep_dist sbstrt_thickness*

The definitions of the input arguments for the above command are given in table F.6.

Table F.6: Definition of the arguments of STR PA command ...

Parameter	Type	Function/Options
no_pins	int	Number pins (*for either probe-feed and/or shorting pin*) that are available in the structure. If the excitation is the plane wave and this variable is not set to zero, then all the pins will be assumed to be representing shorting pins.
pin_rgn_tag	int	The *region tag* assigned to the node/s on the mesh for the pin/s. The number of this variables that are available is specified by *no_pins*: e.g., if *no_pins* = 0, then there will be no entry for this field and it must be skipped.
top_cs_tag *bot_cs_tag* *sbstrt_rgn_tag* *bndry_rgn_tag*	int	*region tags* that are assigned to the triangles that are part of the top conducting surface, bottom conducting surface, substrate, and free-space region parts in the mesh of the surface that contains the details of the top and bottom parts of the antenna structure respectively.
not_top_cs_tag *not_bot_cs_tag*	int	*region tags* that are assigned to the triangles on the top and bottom layers of the antenna structure that do not form part of the top or bottom conducting surfaces in the mesh file. This value should be set to zero if no such triangles exist.
sbstrt_thickness *bndry_sep_dist*	float	The thickness of the substrate and the height of outer boundary above and below the top and bottom surfaces of the substrate in meters; see figure F.1.

F.3.2.3 Dielectric Volume

For a dielectric volume, the command takes the following form:

- STR DV *cs_rgn_tag*;

Where: *cs_rgn_tag* is the *region tag* for the triangles that are part of any conducting surface/s that are embedded inside the dielectric volume. If such a surface does not exist then the value of this argument should be set to zero.

F.3.3 EX Command

The EX command is used for specifying the excitation for the problem. Available excitations are: the plane wave and probe-feed (*for probe-fed printed structures only*). This command takes different input arguments depending on the type of excitation used. The general form of the command is:

- EX *type* ...

Where: *type* is used for specifying the type of excitation used. Available excitations are shown in table F.7.

F.3.3.1 Plane Wave

For plane wave excitation the command takes the following form:

- EX 0 *re_x im_x re_y im_y re_z im_z no_phi no_theta strt_phi strt_theta incr_phi incr_theta*

Table F.7: Excitation options for EX command

Option	Function
0	Plane Wave excitation.
1	Probe-Feed excitation.
2	no excitation. This can only be specified for dielectric volume only and the eigenmode solution will be computed, assuming that the structure has perfectly conducting walls.

The input parameter for the above command are defined in table F.8.

Table F.8: Definition of the arguments of EX 0 ... command

Parameter	Type	Function/Options
re_x	float	Real and imaginary parts of the components for the polarisation vector of
im_x		the plane wave in Volts/meter.
re_y		
im_y		
re_z		
im_z		
no_phi	int	Number of azimuth and elevation angles for the direction vector of the
no_theta		plane wave.
strt_phi	float	Start values of the azimuth and elevation angles in degrees.
strt_theta		
incr_phi	float	Incremental values of the azimuth and elevation angles in degrees.
incr_theta		

F.3.3.2 Probe Feed

For probe-feed excitation the command takes the following form:

- EX 1 *no_sources* [*src_tag src_current*]

Definitions of the parameters above are shown in table F.9. *no_sources* values of *src_tag* and *src_current* values must be specified.

Table F.9: Definition of the arguments of EX 1 ... command

Parameter	Type	Function
no_sources	int	The number of probe-feeds in the antenna. This variable indicates the number of *src_edge_tag* and *src_current* variables that have been provided.
src_edge_tag	int	The *region tag* assigned to the node/s on the mesh for the source pin/s. The number of this variables that are available is specified by *no_sources*: e.g., if *no_sources* = 2, then there will be 2 entries of this field and *src_current*. The order of the variables must be preserved.
src_current	float	The magnitude of the current on the source in Amperes. See comment for *src_edge_tag*.

F.3.3.3 No Excitation

No additional parameters are required when no excitation has been specified (i.e. for *type* equal to 2).

F.3.4 FR Command

FR (*Frequency*), used for specifying the simulation frequency or frequencies. The full command with the arguments is:

- FR *freq_incr_mode no_freqs start_freq incr_freq*

The arguments of the command are defined as:

Table F.10: Definition of the arguments of FR ... command

Parameter	Type	Function
incr_mode	int	Specifies the manner in which the frequency must be incremented when a frequency range is specified. - 0 for LINEAR increments, where subsequent frequency values are obtained by adding the incremental frequency to the previous frequencies. - 1 for MULTIPLICATIVE increments, where subsequent frequency values are obtained by multiplying the incremental frequency with the previous frequencies.
no_vals	int	Required number of frequency values.
start	float	Starting frequency value in MHz.
incr	float	Incremental frequency value in MHz.

F.3.5 DE Command

The DE command has the following form:

- DE *rgn_tag real_epsilon imag_epsilon real_mu imag_mu*

The arguments are defined in table F.11.

Table F.11: Definition of the arguments of DE ... command

Parameter	Type	Function
rgn_tag	int	*region_tag* for the tetrahedrons that compose the dielectric region of the structure, whose properties are being specified.
real_mu *real_epsilon* *imag_mu* *imag_epsilon*	float	The real and imaginary components of the relative permittivity and permeability for the dielectric region.

F.3.6 FS Command

The FS command has the following form:

- FS *tag*

Where: *tag* is the number that identifies the tetrahedrons that are part of the free-space region. It is a special case of the DE command with:

- *real_mu* = 1
- *imag_mu* equal = 0
- *real_epsilon* = 1
- *imag_epsilon* = 0

F.3.7 NF Command

As already specified, this command is used for requesting the computation of near fields. It cannot be used for dielectric volume structure with no excitation. It also takes different forms depending on the coordinate system that is used to specify the points where the field values are to be evaluated. The general form of the command is:

- NF *fld crd_sys ...*

Where: *crd_sys* is used for specifying the coordinate system that is used for specifying the points where the near fields are to be computed. The different coordinate system options are shown in table F.12. The input options for the *fld* are shown in table F.13. When the cartesian coordinate system is used for specifying the

Table F.12: Coordinate system options for NF command

Option	Function
0	Rectangular coordinate system.
1	Spherical coordinate system.

input values, the command takes the following form:

- NF *fld* 0 *no_x no_y no_z strt_x strt_y strt_z x_incr y_incr z_incr*

When the sphererical coordinate system is used for specifying the input values, the command takes the following form:

- NF *fld* 1 *no_r no_phi no_theta strt_r strt_phi strt_theta r_incr phi_incr theta_incr*

The input parameters for both forms of the command are defined in table F.13.

F.3.8 FP Command

The FP command takes the following form:

- FP *mode no_theta no_phi strt_theta strt_phi incr_theta incr_phi rad_dist*

Parameters for the command are defined in table F.14.

Table F.13: Definition of the arguments of NF command.

Parameter	Type	Function/Options
no_x no_y no_z no_r no_phi no_theta	int	Required number of *x*, *y*, *z*, *r*, *phi*, and *theta* values.
fld	char	For specifying the type of near field that is required. The options are: • H: for h-field. • E: for e-field.
strt_x strt_y strt_z strt_r strt_phi strt_theta incr_x incr_y incr_z incr_r incr_phi incr_theta	float	For start values of *x*, *y*, *z*, *r*, *phi*, and *theta*. As well as for specifying values that must be used for modifying the values of the different coordinate axes.

Table F.14: Definition of the arguments of FP command.

Parameter	Type	Function/Options
mode	int	Specifies whether the monostatic or bi-static RCS is required. The different options are: • 0: for Monostatic RCS. • 1: for Bi-static RCS.
no_theta no_phi	int	The number of phi and theta values that are required.
strt_theta strt_phi incr_theta incr_phi	float	For specifying start values of *theta* and *phi*. And for specifying values that must be used for modifying the values of *theta* and *phi*.

F.3.9 CD Command

The form of the CD command is:

• CD *current*

The options for *current* are:

• J: for the electric current distribution.
• M: for the magnetic current distribution.

F.3.10 EF Command

The form of the command is:

- EF *rgn_tag*

Where: *rgn_tag* is the tag of the dielectric region for which the electric field must be computed.

F.4 Error Messages

Error messages produced by this application are divided into two categories, and *fmsolver* terminates each time an error condition is encountered. The two categories of error messages are:

- Error messages for errors caused by the user input.
- Error messages for errors caused by invalid data in the application.

Error messages that are caused by user input are self explanatory. These errors are usually caused by incorrect syntax in the *input file*.

The format of the errors that are caused by invalid data is:

- Error in *class name*::*function*: *description*

Where: *class name* is the name of the class where the error originated, *function* is the class method where the error occurred, and *description* is the description of the error that occurred. These types of errors are caused by invalid data in the *mesh file*. The other cause is the specification of a reference point (see section F.3.2.1) that is on the surface of conducting surface for continuous conducting surface structures.

Using surface mesh file with an incorrect *tetrahedron.out* file for a probe-fed printed antenna structure, is a fatal error and causes the application to crash. Specification of *input file*, which does not exist is a fatal error and also causes the application to crash.

F.5 Example Input File

An example mesh file using most of the commands that were presented is shown below.

```
MFP patch_antenna.msh
STR PA 1 1 2 6 3 7 5 4 0.002 0.0016
EX 1 1 1 1
FR 0 8 665 10
GDB
DE 2 4.3 -0.086 1 0
GDE
ARB
FP 1 181 1 0 0 1 0
ARE
```

This is an *input file* for the simulation of a probe-fed printed antenna of a substrate whose: thickness equals 2 mm, and relative permittivity equals $4.3 - 0.086i$. The simulation is performed starting from 665 MHz to 737 MHz in increments of 8 MHz; and the power radiation density and input impedance are computed for each simulation frequency. The power radiation density is computed for $\phi = 0^0$ and $0^0 \leq \theta \leq 180^0$.

References

[1] C. A. Balanis. *Antenna Theory: Analysis and Design*. John Wiley and Sons, second ed., 1997.